Kobe University Repository : Kernel

PDF issue: 2026-08-11

# Aspects of point interaction

Ohya, Satoshi

(Degree)
博士（理学）

(Date of Degree)
2010-03-25

(Date of Publication)
2012-01-20

(Resource Type)
doctoral thesis

(Report Number)
甲4902

(URL)
https://hdl.handle.net/20.500.14094/D1004902

※ 当コンテンツは神戸大学の学術成果です。無断複製・不正使用等を禁じます。著作権法で認められている範囲内で、適切にご利用ください。

# Aspects of point interaction

**Satoshi Ohya**

*Department of Physics*
*Graduate School of Science, Kobe University*
*1-1 Rokkodai, Nada, Kobe 657-8501, Japan*

A Dissertation submitted to
Kobe University
in partial fulfillment of the requirements
for the degree of Doctor of Science

January 2010

# Contents

# Abstract

This dissertation describes theoretical aspects of point interaction in quantum physics on one-dimensional topological graph known as quantum graph. After the precise definition of point interaction on quantum graph, we study the exact renormalization group flow and path integral description of point interaction. As an application we attempt to construct a worldline formalism of perturbative quantum field theory with a single extra compact dimension. Using this formalism, we find the master formulae for scalar one-loop amplitudes with arbitrary number of external gauge bosons in Abelian gauge theory with a single extra dimension compactified on a circle.

# Acknowledgments

I would like to thank my advisor, Makoto Sakamoto, for fruitful discussions and his valuable suggestions without which this dissertation could not be produced in the present form. I am also grateful to Izumi Tsutsui and Taksu Cheon for stimulating me to the subject of quantum graph.

Finally, my thanks go to all the members (past and present) of Particle Theory Group of Kobe University.

# Chapter 1

# Introduction

## 1.1 Why point interaction?

Point interaction, or interaction of zero range, may be the simplest yet ubiquitous interactions in low-energy physics. We naively expect that any short ranged interaction, which may be a defect or impurity or brane, could be approximated by a point interaction in the long-wavelength limit. In order to get detailed information about what the short ranged interaction is, we need to use a probe particle whose de Broglie wavelength is shorter than the size of the range of interaction. In other words, the longer the probe particle's wavelength is, the less information we can get about microscopic details of the short ranged interaction. This is the reason why point interaction appears in such diverse fields as nanoscience, condensed matter physics, as well as modern high energy physics when one limits to consider some appropriate low-energy scale.

This dissertation describes theoretical aspects of point interactions in quantum theory on graph (quantum graph) that is no longer differentiable manifold. The reason why we consider quantum graph is that it is not only a more general setting than a system on one-dimensional manifold such as line or interval or circle, but also provides great insight to an ordinary one-dimensional system. Before going to discuss this point further, we would like to give a brief overview of theoretical and experimental backgrounds relevant to the physics of point interactions on graphs.

## 1.2 Theoretical and experimental background

There are two main motivations for studying quantum systems on graphs. The first is a recent development of manufacturing mesoscopic networks (graphs) of one-dimensional systems. It is known that the most simplest model for such a system is quantum graph [1,2].

The second for this work is to understand worldline formulation of perturbative quantum field theory with a single extra dimension in the presence of defects or boundaries. When extra space is one-dimensional, such defects or boundaries can be viewed as point interactions along the direction of extra dimension.

Apparently, these two fields of quantum physics have nothing in common. However, they actually have a single common point in respect that boundary condition plays a crucial role in quantum dynamics. As we will see throughout of this dissertation, physics of point interaction is nothing but physics of boundary condition. Now let us take a brief look at quantum role of boundary condition/point interaction from nanoscale to high energy

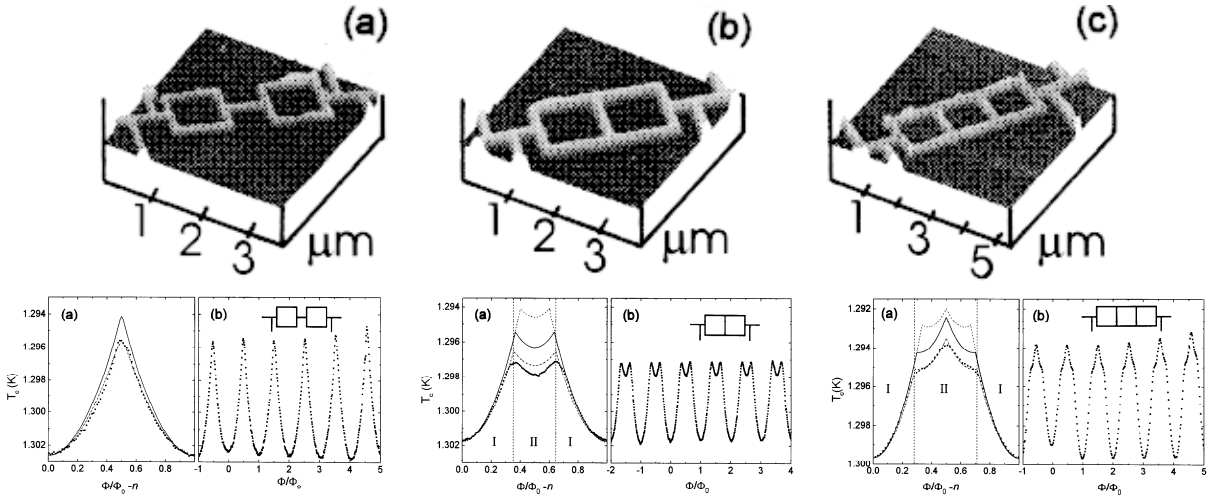


(d) Bola (e) Double loop (f) Triple loop

Figure 1.1: Top: Experimental realization of (a) bola, (b) double loop, and (c) triple loop structures of Al superconducting wire. Bottom: Experimental measurement of critical temperature $T_c(\Phi)$ for (d) the bola, (e) the double loop, and (f) the triple loop with the subtraction of universal parabolic background. The N/S phase boundary exhibits the oscillatory behavior for the magnetic flux $\Phi$ penetrating through the samples. Taken from V. V. Moshchalkov *et al.*, `arXiv:cond-mat/9804267[cond-mat.supr-con]` [3].

physics as well as mathematical physics.

### 1.2.1 N/S phase boundary in mesoscopic systems

Recent development of nanotechnology such as an electron-beam lithography enables us to fabricate mesoscopic networks of one-dimensional superconducting wires [3–5], where sample geometry plays an important role. Such a mesoscopic superconducting system has been studied in different sample topology, e.g., loop, square loop, double square loop and microladders etc. [3–5] (see Figure 1.1 top), with sizes smaller than the temperature-dependent correlation length $\xi(T)$ and the magnetic field penetration depth $\lambda(T)$. The experimentally observed normal/superconducting (N/S) phase boundary exhibits oscillatory behavior in the magnetic field-temperature (so called $H$-$T$) phase diagram (see Figure 1.1 bottom), which is different from the ordinary parabolic behavior of non-mesoscopic superconductors. Those oscillatory behaviors are in excellent agreement with calculations based on the Ginzburg-Landau theory. Near the phase boundary, it is known that the quartic term of the Ginzburg-Landau Lagrangian can be neglected such that the N/S phase boundary is well-described by the following linearized differential equation (see for textbook description [6])

$$-\frac{\hbar^2}{2m}\left(\vec{\nabla}-i\frac{e^*}{\hbar c}\vec{A}\right)^2\psi_s=-\alpha(T)\psi_s, \tag{1.1}$$

with

$$-\alpha(T)=\frac{\hbar^2}{2m\xi^2(T)} \quad \text{and} \quad \xi(T)=\frac{\xi(0)}{\sqrt{1-T/T_c}}. \tag{1.2}$$

Eq.(1.1) is nothing but the Schrödinger equation for a particle of mass $m$ and charge $e^* = 2e$ in the presence of a magnetic field $\vec{H} = \vec{\nabla} \times \vec{A}$ by identifying $-\alpha(T)$ as the energy eigenvalue $E(H)$. The lowest energy eigenvalue $E_{\text{lowest}}(H)$ corresponds to the highest possible temperature $T_c(H)$ for the nucleation of the superconducting order parameter $\psi_s$ (whose modulus is proportional to the density of Cooper pair). Thus, the N/S phase boundary in the $H$-$T$ phase diagram can be found by using the following simple procedure [4]:

1. solve the Schrödinger equation (1.1) by identifying $E(H) = -\alpha(T)$;
2. take the lowest energy eigenvalue $E_{\text{lowest}}(H)$ and calculate the critical temperature $T_c(H)$ by the relation $E_{\text{lowest}}(H) = -\alpha(T_c(H))$.

To get the glimpse of the procedure, let us consider a mesoscopic superconducting ring of radius $R$ in the presence of a constant magnetic field $\vec{H}$ penetrating through the sample. The Schrödinger equation is easily solved with the result[1]

$$E_n(\Phi) = \frac{\hbar^2}{2m}\left(\frac{n - \Phi/\Phi_0}{R}\right)^2, \quad n \in \mathbb{Z}, \tag{1.3}$$

where $\Phi = (e^*/\hbar c)\pi R^2 H$ is the magnetic flux and $\Phi_0 = hc/e^*$ is the flux quantum. The relation $-\alpha(T_c(\Phi)) = E_{\text{lowest}}(\Phi)$ enables us to find the $H$-$T$ phase boundary from the equation

$$1 - \frac{T_c(\Phi)}{T_c} = \left(\frac{\xi(0)}{R}\right)^2 \left(n - \frac{\Phi}{\Phi_0}\right)^2. \tag{1.4}$$

Notice that for a given $\Phi$, $n$ must be chosen to minimize $(n - \Phi/\Phi_0)^2$. Consequently, the N/S phase boundary in the $H$-$T$ phase diagram exhibits oscillatory behavior with a period $\Phi_0$ (see Figure 1.2), which is indeed observed in the Little-Parks experiment [7]. As is well known (and as we will see in chapter 4) the magnetic flux contribution $\Phi/\Phi_0$ in the energy spectrum (1.3) can be introduced by twisted boundary condition of wavefunction such that it belongs to the notion of point interactions on a circle (or, more general, quantum graph). Consequently, we can say that the N/S phase boundary is determined by only the spectrum of Laplace operator (or free Hamiltonian) defined on a sample with appropriate boundary conditions.

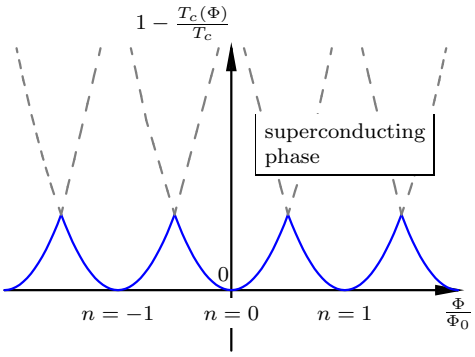


Figure 1.2: N/S phase boundary (blue curve) in mesoscopic superconducting ring with $\xi(0)/R = 1$.

In general, spectrum (especially low energy spectrum) of Laplace operator is very sensitive to the geometry and boundary conditions. Now it it evident that by changing the actual sample topology, we can strongly modify the lowest energy level $E_{\text{lowest}}(H)$ and thus the N/S phase boundary. Although there exist some attempts [8, 9], a systematic description of N/S phase boundaries for mesoscopic samples of different topology, made from the same material under the same conditions, has not yet been fully understood. This is mainly due to the complexity and difficulty to analyze the spectrum of arbitrary sample geometry. We believe that systematic study for the spectrum of (compact) quantum graphs will gain insight into these problems.

[1] We here ignore the parabolic background $E(H) \propto (\text{sample area}) \times H^2$ because it is a universal contribution that always appears when a magnetic field penetrates through the sample.

### 1.2.2 Exact trace formulae

Quantum graphs has also been attracted much attention to mathematical physicists due to its exact solvability. One of the exact mathematical results relevant for our physical interests (especially for path integral and its application to perturbative quantum field theory with extra compact dimensions) is the *exact trace formulae* given by [10]. Generally speaking, trace formulae are *duality* relations between quantum energy spectrum and classical length spectrum (or periodic orbits), which can be schematically expressed as follows:

$$\sum (\text{classical length spectrum}) = \sum (\text{quantum energy spectrum}). \tag{1.5}$$

By 'classical length spectrum' we mean the physically (or topologically) distinct closed trajectories for a classical particle on a given background space. By 'quantum energy spectrum', on the other hand, we mean the eigenvalues of the Laplace operator defined on a given background space. One of the simplest examples of exact trace formulae is the Poisson summation formula, usually referred to as the Poisson resummation formula for particle theorists. The Poisson summation formula is an exact trace formula on a smooth circle, or flat tori, and based on the Fourier analysis.

Now, in a view point of perturbative quantum field theory with extra compact dimensions, Eq.(1.6) can be re-expressed as follows:

$$\sum \left( \begin{array}{l} \text{physically distinct closed loop} \\ \text{winding around extra dim.} \end{array} \right) = \sum (\text{Kaluza-Klein mode}). \tag{1.6}$$

If one considers a smooth circle of radius $R$ as an extra dimension, then the left hand side is given by the summation over the trajectories for a free particle (free because a circle is smooth) distinguished by the winding number $w \in \mathbb{Z}$, and the right hand side is given by the summation over Kaluka-Klein mass $n/R$, $n \in \mathbb{Z}$; that is,

$$\frac{1}{2\pi} \sum_{w \in \mathbb{Z}} \mathrm{e}^{ip \cdot 2\pi w R} = \frac{1}{2\pi R} \sum_{n \in \mathbb{Z}} \delta(p - n/R), \tag{1.7}$$

where $p$ is a parameter variable. This is nothing but the Poisson summation formula. If one considers as an extra dimension a circle in the presence of point-like defect such as $\delta$-function potential, however, the Poisson summation formula is no longer available: it is limited to the case where the spectrum is distributed in equidistance.

As we will see in chapter 4, systematic study of quantum graph shows that it is possible to derive the trace formulae exactly even if a system admits nontrivial point-like defects such as $\delta$-function potentials and we can no longer find the Kaluza-Klein mass spectrum analytically.

### 1.2.3 Quantum field theory with extra dimensions

In the previous section we have seen that trace formulae can be re-expressed as (1.6), which seems to be almost handmade for loop calculations in perturbative quantum field theory with extra compact dimensions. In the following let us take a look at the long-distance IR structure of extra dimensional models from the view point of winding number.

A fluctuation of quantum fields winding around the extra compact dimensions is the long-distance contribution in nature so that it is irrelevant for the far UV behavior of the theory. Thus, as far as we concern the nonzero winding sector, high-energy physics could be

well separated from low-energy physics. This infrared structure of extra-dimensional field theory has opened up a new vista for the gauge hierarchy problem in particle physics in the context of gauge-Higgs unification [11], where the Standard Model Higgs fields are identified as the extra spatial components of higher-dimensional gauge field. A local operator corresponding to the Higgs mass is forbidden by the higher-dimensional gauge symmetry. However, it is radiatively generated via the nonlocal operator of Wilson line phase, which is induced by quantum fluctuations of matter fields winding around the extra compact dimensions and thus totally independent of the UV cutoff and predictable.

The standard approach to perturbative extra dimensional field theory consists of momentum space Feynman rules in terms of Kaluza-Klein modes provided by the dimensional reduction. In this approach it is far from obvious whether virtual particles, or internal lines of given Feynman diagrams, wind around the extra compact dimensions or not without turning into position-space Feynman rules by using the trace formula. Since winding number naturally arises in the path integral description from the beginning as a sum over all possible paths, it is more desirable to reformulate extra-dimensional field theory into the path-integral oriented way, at least for practical computational level. This will be achieved by translating extra-dimensional models into the worldline formalism. Worldline formalism is a mapping of field theoretic problems onto quantum mechanical path integrals, identifying the trajectory of a fluctuation in coordinate space with the path of a quantum mechanical particle in the presence of a given background field. In four-dimensional perturbative field theory it is known that the worldline formalism is powerful enough to compute the effective action and amplitudes at least for one-loop order. In higher-dimensional field theory with extra compact dimensions, however, it is very difficult to formulate perturbative field theory into the worldline formalism when extra dimensions admit nontrivial defects or boundaries in spite of the existence of exact trace formulae. This is a problem of single-particle quantum mechanical path integral rather than field theoretical one. Although there exist some attempts [12–14], until now it is not yet fully understood how to incorporate such a point interaction into the worldline formalism.

## 1.3 Outline of the dissertation

This dissertation is organized as follows. In chapter 2 we give a precise definition of how to treat point interactions in quantum theory on a graph. In chapter 3 we investigate the renormalization group flow of point interaction, which can be derived exactly. In chapter 4 we derive the path integral description of point interaction on a rose graph. In chapter 5 we study the worldline formalism of gauge theory with a single extra dimension conpactified on a circle. We derive the one-loop master formulae for general $N$-point gauge theory amplitudes as Feynman parameter integral representations. Chapter 6 is devoted to summary and outlook.

# Chapter 2

# Point interaction in quantum graph

In this chapter we give a precise definition of point interaction at the vertex of star graph with $N$ bonds as a set of boundary conditions provided by the self-adjoint extension of the Laplace operator on the graph. The resultant boundary conditions are characterized by an $N \times N$ unitary matrix. We also study symmetry classes of $U(N)$ family of point interactions.

## 2.1 Introduction

Quantum graph, also known as quantum wire or quantum network or quantum circuit, is an idealized one-dimensional quantum mechanical system where the configuration space is a graph, i.e. a set of finite and/or semi-infinite lines that are connected at some vertices by certain relations. The simplest quantum graph is a star graph, which consists of several half-lines joining at the single vertex (see Figure 2.1). Such a quantum system on a graph provides a testing ground for theoretical laboratory of rapidly developing one-dimensional mesoscopic systems, whose typical sizes are of nanometer order.

A natural question first comes into mind is how do we define a quantum mechanics on such a graph which is no longer differentiable manifold (because at the vertex it is not locally $\mathbb{R}$). An important observation is that quantum graph can be viewed as a system constructed by joining (or sewing) each quantum system defined on each finite/semi-infinite line at a single vertex. Then the problem is reduced to a problem how should we sew each quantum mechanical system consistently. This sewing quantum mechanics problem is solved by requiring that the probability current density should be conserved even at the vertices. This requirement is usually referred to as the *Kirrchhoff's law of probability current*, just as an analogue of that for electric circuits, and ends up with boundary conditions for wavefunctions at the vertex. It is not an exaggeration to say that all the problems of quantum graphs are just reduced to a single problem how to specify the boundary conditions at the vertex.

Another important point to note is that quantum graph is essentially a topological object; that is, we do not need to concern how a graph is embedded into our real world. A graph may be planar as well as non-planar and be bent when it is realized as a subset of our three-dimensional Euclidean space $\mathbb{R}^3$.

The rest of this chapter is organized as follows. In section 2.2 we define a quantum system for a free particle on a star graph with $N$ bonds by requiring the conservation of probability current density at the vertex. It turns out that point interaction at the vertex

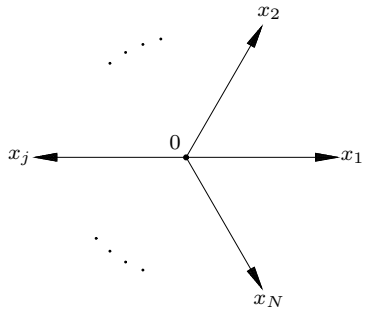


Figure 2.1: Star graph with $N$ bonds. Arrows represent the directions of each bond. The vertex is located at $x_1 = x_2 = \cdots = x_N = 0$.

is characterized by an $N \times N$ unitary matrix $U \in U(N)$. In section 2.3 we derive the one-particle scattering matrix exactly. In section 2.4 we try to classify symmetry classes of $U(N)$ point interactions. After a brief review for the case of $U(2)$, we give a classification of symmetry classes of $U(3)$ family of point interactions. Section 2.5 is devoted to conclusions and discussions.

## 2.2 $U(N)$ family of point interaction

Let us consider a free particle on a star graph which consists of $N$ half-lines joining at the single vertex; see Figure 2.1. Each half-line is assigned a number $j$ ($j = 1, 2, \cdots, N$) and introduced a coordinate $x_j \in (0, \infty)$. The junction point $x_1 = x_2 = \cdots = x_N = 0$ and the $j$th half-line are usually referred to as the *vertex* and the $j$th *bond*, respectively.

Now let $\psi_j(x_j)$ be the square-integrable wavefunction on the $j$th bond. The Schrödinger equation for a free particle on the star graph is given by

$$H\psi_j(x_j) = E\psi_j(x_j), \quad j = 1, 2, \cdots, N, \tag{2.1}$$

where the Hamiltonian $H$ is defined as

$$H = -\frac{\mathrm{d}^2}{\mathrm{d}x_j^2}. \tag{2.2}$$

(Here as in the following we will use the units where $\hbar = 2m = 1$.) Notice that Eq.(2.2) is only the formal definition of the Hamiltonian operator unless we specify its self-adjoint domain or boundary conditions at the vertex. The self-adjointness of $H$ indicates the conservation of probability in the whole quantum system and leads to the *Kirchhoff's law of probability current* [1]:

$$\sum_{j=1}^{N} j_j(0) = 0, \tag{2.3}$$

where the probability current density on the $j$th bond is defined by

$$j_j(x_j) := -i(\psi_j'^*(x_j)\psi_j(x_j) - \psi_j^*(x_j)\psi_j'(x_j)), \quad ' := \frac{\mathrm{d}}{\mathrm{d}x_j}. \tag{2.4}$$

For the following discussions it is convenient to introduce the $N$-component column vector $\vec{\Psi}$ and its derivative $\vec{\Psi}'$ as

$$\vec{\Psi}(x_1, x_2, \cdots, x_N) := (\psi_1(x_1), \psi_2(x_2), \cdots, \psi_N(x_N))^T, \tag{2.5a}$$

$$\vec{\Psi}'(x_1, x_2, \cdots, x_N) := (\psi_1'(x_1), \psi_2'(x_2), \cdots, \psi_N'(x_N))^T, \tag{2.5b}$$

where $T$ stands for the transposition of matrix. Then the requirement for the probability conservation (2.3) can be written as $\vec{\Psi}(0)^\dagger \cdot \vec{\Psi}'(0) = \vec{\Psi}'(0)^\dagger \cdot \vec{\Psi}(0)$, or, equivalently,

$$\left|\vec{\Psi}(0) - iL_0\vec{\Psi}'(0)\right|^2 = \left|\vec{\Psi}(0) + iL_0\vec{\Psi}'(0)\right|^2, \tag{2.6}$$

where $\vec{\Psi}(0)$ is the shorthand notation for $\vec{\Psi}(0, 0, \cdots, 0)$ and $L_0$ is an *arbitrary* non-vanishing real length scale, which is just introduced to adjust the length dimension of the equation (2.6). Since our Hamiltonian is characterized by lack of any scale parameters, we immediately see that any dimensionful quantities, such as momentum or energy of a particle, must be scaled by this arbitrary parameter $L_0$. As we will see in section 3.2, $L_0$ turns out to play a role of a renormalization scale if we require any physical quantities such as scattering amplitudes or bound state energies should not depend on the choice of $L_0$. The dependence of the theory on this scale parameter will be described by the renormalization group.

Eq.(2.6) shows that the squared length of the $N$-dimensional complex column vector $\vec{\Psi}(0) - iL_0\vec{\Psi}'(0)$ is equal to that of $\vec{\Psi}(0) + iL_0\vec{\Psi}'(0)$, which implies that these two vectors must be related by an $N$-dimensional unitary transformation. Thus we can write

$$\vec{\Psi}(0) - iL_0\vec{\Psi}'(0) = U\left[\vec{\Psi}(0) + iL_0\vec{\Psi}'(0)\right], \quad U \in U(N). \tag{2.7}$$

For the following discussions it is more convenient to parameterize the matrix $U$ into the spectral decomposition form:

$$U = \sum_{j=1}^{N} \mathrm{e}^{i\alpha_j} P_j, \tag{2.8a}$$

$$P_j = \frac{1}{N}\mathbb{1}_N + 2\vec{e}_j \cdot \vec{T}, \tag{2.8b}$$

where $0 \leq \alpha_j < 2\pi$ $(j = 1, 2, \cdots, N)$ and $\vec{e}_j$ is an $N^2 - 1$-dimensional real vector, which can be constructed by $N(N-1)$ successive adjoint rotations of $SU(N)$ weight vector $\vec{w}_j$ in the fundamental representation. $\vec{T} = (T^1, T^2, \cdots, T^{N^2-1})$ is the hermitian traceless generator of $SU(N)$ and $P_j$ is the hermitian projection operator fulfilling $\sum_{j=1}^{N} P_j = \mathbb{1}_N$, $P_i P_j = \delta_{ij} P_j$ and $P_j^\dagger = P_j$, where $\mathbb{1}_N$ is the $N \times N$ unit matrix and $\dagger$ indicates the hermitian conjugate. As an example, for the case of $N = 2$ the projection operator $P_j$ can be parameterized as follows:

$$P_1 = \frac{\mathbb{1}_2 + \vec{e} \cdot \vec{\sigma}}{2}, \tag{2.9a}$$

$$P_2 = \frac{\mathbb{1}_2 - \vec{e} \cdot \vec{\sigma}}{2}, \tag{2.9b}$$

where $\vec{e} = (e_x, e_y, e_z)^T$ is a unit vector fulfilling $e_x^2 + e_y^2 + e_z^2 = 1$ and $\vec{\sigma} = (\sigma_1, \sigma_2, \sigma_3)^T$ is the Pauli matrix.

Plugging back into the equation, the boundary conditions (2.7) boil down to the following $N$ independent equations

$$P_j\big[\vec{\Psi}(0) + L_j\vec{\Psi}'(0)\big] = \vec{0}, \quad j = 1, 2, \cdots, N, \tag{2.10}$$

where

$$L_j := L_0 \cot(\alpha_j/2). \tag{2.11}$$

Notice that when $\alpha_j = 0$ or $\pi$ the scale parameters $L_j$ drop out from (2.10):

$$P_j\vec{\Psi}'(0) = \vec{0}, \quad \text{for } \alpha_j = 0, \tag{2.12a}$$
$$P_j\vec{\Psi}(0) = \vec{0}, \quad \text{for } \alpha_j = \pi. \tag{2.12b}$$

In section 3.2, we will see that these scale-independent boundary conditions describe the vertex at the fixed points of RG flow.

## 2.3 Exact S-matrix

Although particle production and annihilation process are absent in a system of one-particle quantum mechanics on a star graph, the scattering matrix (S-matrix) in this system becomes nontrivial due to the presence of a point interaction, which acts as a point scatter. In this section we derive an *exact* one-particle S-matrix whose components are reflection and transmission coefficients for a continuum state once scattered from the point scatter located at the vertex. As we will see below, S-matrix completely determines the dynamics of the system not only for scattering states but also for nontrivial bound states.

The general solution to the Schrödinger equation (2.1) for positive energy $E > 0$ is the linear combination of the plain waves

$$\psi_j(x_j; k) = A_j^{\text{in}}(k)\mathrm{e}^{-ikx_j} + A_j^{\text{out}}(k)\mathrm{e}^{ikx_j}, \quad j = 1, \cdots, N, \tag{2.13}$$

where $k = \sqrt{E} > 0$. Notice that the coefficients $A_j^{\text{in}}(k)$ and $A_j^{\text{out}}(k)$ may depend on $k$. The superscripts 'in' and 'out' mean the incoming/outgoing waves toward/against the vertex, respectively (see Figure 2.2).

The boundary value vectors are

$$\vec{\Psi}(0) = \vec{A}^{\text{in}}(k) + \vec{A}^{\text{out}}(k), \tag{2.14a}$$
$$\vec{\Psi}'(0) = ik\big[-\vec{A}^{\text{in}}(k) + \vec{A}^{\text{out}}(k)\big], \tag{2.14b}$$

where $\vec{A}^{\text{in}}(k)$ and $\vec{A}^{\text{out}}(k)$ are $N$-component column vectors defined as

$$\vec{A}^{\text{in}}(k) := \big(A_1^{\text{in}}(k), A_2^{\text{in}}(k), \cdots, A_N^{\text{in}}(k)\big)^T, \tag{2.15a}$$
$$\vec{A}^{\text{out}}(k) := \big(A_1^{\text{out}}(k), A_2^{\text{out}}(k), \cdots, A_N^{\text{out}}(k)\big)^T. \tag{2.15b}$$

Substituting these into the boundary conditions (2.10) we get

$$\vec{0} = P_j\big[\vec{\Psi}(0) + L_j\vec{\Psi}'(0)\big] = (1 + ikL_j)P_j\left(\vec{A}^{\text{out}}(k) - \frac{ikL_j - 1}{ikL_j + 1}\vec{A}^{\text{in}}(k)\right). \tag{2.16}$$

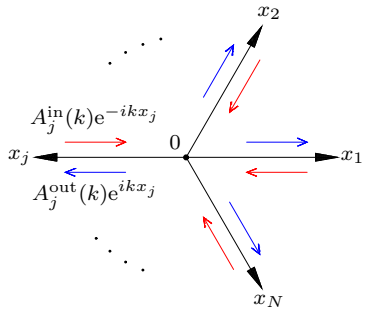


Figure 2.2: One-particle scattering from the vertex. Red arrow on the $j$th bond represents the incoming wave $A_j^{\rm in}(k)e^{-ikx_j}$ toward the vertex and blue one the outgoing wave $A_j^{\rm out}(k)e^{ikx_j}$ against the vertex.

Since the factor $(1+ikL_j)$ cannot be zero for real $k>0$, we have

$$P_j\left(\vec{A}^{\rm out}(k)-\frac{ikL_j-1}{ikL_j+1}\vec{A}^{\rm in}(k)\right)=\vec{0},\quad j=1,2,\cdots,N. \tag{2.17}$$

Since Eq.(2.17) with different $j$ is orthogonal to each other, they can be combined into the following form

$$\vec{0}=\sum_{j=1}^{N}P_j\left(\vec{A}^{\rm out}(k)-\frac{ikL_j-1}{ikL_j+1}\vec{A}^{\rm in}(k)\right)=\vec{A}^{\rm out}(k)-\sum_{j=1}^{N}\frac{ikL_j-1}{ikL_j+1}P_j\vec{A}^{\rm in}(k), \tag{2.18}$$

where the second equality follows from $\sum_{j=1}^{N}P_j=\mathbb{1}_N$. Thus,

$$\vec{A}^{\rm out}(k)=S(kL_0)\vec{A}^{\rm in}(k), \tag{2.19}$$

where $S(kL_0)$ is an $N\times N$ matrix defined as

$$S(kL_0):=\sum_{j=1}^{N}\frac{ikL_j-1}{ikL_j+1}P_j=\mathbb{1}_N-2\sum_{j=1}^{N}\frac{1}{1+ikL_j}P_j. \tag{2.20}$$

Eq.(2.19) shows that the matrix $S(kL_0)$ plays a role of an evolution map between the "in-state" $\vec{A}^{\rm in}(k)$ and the "out-state" $\vec{A}^{\rm out}(k)$. The $ij$-component of the matrix $S(kL_0)$ is nothing but the transition amplitude for a particle traveling from the $j$th bond to the $i$th bond. Thus, the diagonal element $S_{jj}$ should be interpreted as the reflection coefficient $R_j(kL_0)$ for a particle of momentum $k$ on the $j$th bond. Similarly, the off-diagonal element $S_{ij}$ $(j\neq i)$ should be interpreted as the transmission coefficient $T_{ij}(kL_0)$ for a particle traveling from the $j$th bond and scattered to the $i$th bond. Hence we write

$$S(kL_0)=\begin{pmatrix}R_1(kL_0) & T_{12}(kL_0) & \cdots & T_{1,N}(kL_0)\\ T_{21}(kL_0) & R_2(kL_0) & \cdots & T_{2,N}(kL_0)\\ \vdots & \vdots & \ddots & \vdots\\ T_{N,1}(kL_0) & T_{N,N-1}(kL_0) & \cdots & R_N(kL_0)\end{pmatrix}. \tag{2.21}$$

In the literature [2] the matrix $S(kL_0)$ is refereed to as the (on-shell) vertex scattering matrix. In this dissertation I will call $S(kL_0)$ the S-matrix.

Here let us summarize several important properties of the S-matrix:

1. *Unitarity.*
From Eq.(2.20) it is obvious that the S-matrix $S(kL_0)$ is unitary, $S^\dagger(kL_0)S(kL_0) = S(kL_0)S^\dagger(kL_0) = \mathbb{1}_N$, and has the modulus unity eigenvalues $(ikL_j-1)/(ikL_j+1)$, $j = 1, 2, \cdots, N$. Note that at $kL_0 = 1$ the S-matrix satisfies the following normalization condition

$$S(1) = U. \tag{2.22}$$

2. *Hermitian analyticity.*
Since the eigenvalues $(ikL_j - 1)/(ikL_j + 1)$ are meromorphic function of $k$, it can be analytically continued to the entire complex $k$-plain. Then the S-matrix $S(z)$ for $z = kL_0 \in \mathbb{C}$ satisfies the following relation

$$S^\dagger(z) = S(-z^*), \tag{2.23}$$

from which we find

$$R_j^*(z) = R_j(-z^*), \tag{2.24a}$$
$$T_{ij}^*(z) = T_{ji}(-z^*). \tag{2.24b}$$

3. *Bound states.*
The negative energy or bound state solution is obtained by just replacing $ik$ to $\kappa(> 0)$ in Eq.(2.13). The square integrability of the wavefunction on the star graph requires $A_j^{\rm out}(-i\kappa) = 0$ for all $j$ and hence from Eq.(2.16) the nontrivial bound state solutions can exist if and only if $\kappa = 1/L_j$ with $L_j > 0$, in which case the bound state wavefunction is given by

$$\psi_j(x) \propto \exp\left(-\frac{x_j}{L_j}\right), \quad 0 < x_j < \infty. \tag{2.25}$$

The corresponding energy eigenvalue is

$$E_j = -\frac{1}{L_j^2}. \tag{2.26}$$

Without any loss of generality, we can assume that $L_0 > 0$. With this assumption, the number of bound states on the star graph is determined by the number of eigenphases lying on the region $0 < \alpha_j < \pi$. Now it is clear that in the star graph with $N$ bonds there exist at most $N$ bound states.

Whether the bound states exist or not can also be explained from the scattering theory point of view. It follows from the boundary conditions (2.16) that at $k = i/L_j$, which is a simple pole in the S-matrix, the general solution (2.13) with $\vec{A}^{\rm out}(i/L_j) = \vec{0}$ behaves as $\psi_j(x_j; k = i/L_j) \propto \exp(-x_j/L_j)$ with negative energy eigenvalue $E_j = (i/L_j)^2 = -1/L_j^2$. When $k$ is in the upper half $k$-plain (i.e. $L_j > 0$), the wavefunction at the pole exhibits an exponentially damping behavior asymptotically and hence is normalizable. This shows that if a simple pole in the S-matrix lie on the positive imaginary $k$-axis, it corresponds to a bound state. When $k$ is in the lower half $k$-plain (i.e. $L_j < 0$), on the other hand, the wavefunction has an exponentially growing behavior asymptotically and thus cannot be normalizable. Such a real- and finite-energy yet non-normalizable solution is referred to as an *antibound* (or *virtual*) *state*.

As the simplest example, possible distributions of bound and antibound state poles for the case of $N = 2$ are depicted in Figure 2.3.

We here note that if there is no bound state pole the following relation holds:

$$\int_{-\infty}^{\infty} \frac{\mathrm{d}k}{2\pi}\, \mathrm{e}^{ikx} S(kL_0) = \delta(x)\mathbb{1}_N, \quad x > 0, \tag{2.27}$$

which follows from Eq.(2.20).

4. *Logarithmic derivative.*
The logarithmic derivative of the S-matrix satisfies the following relation

$$\frac{1}{i}\frac{\mathrm{d}}{\mathrm{d}k}\log S(kL_0) = \frac{S^\dagger(kL_0) - S(kL_0)}{2ik} \left( = -\sum_{j=1}^{N} \frac{2L_j}{1+(kL_j)^2} P_j \right), \tag{2.28}$$

which will be important for the path integral representation of the Feynman kernel on a rose graph; see chapter 4.

5. *Power series expansion.*
Although one-particle S-matrix can be derived exactly, it also admits perturbative expansions. Noting that the elementary identities

$$\frac{1}{1+ikL_j} = \begin{cases} \displaystyle\sum_{n=0}^{\infty} (-ikL_j)^n, & \text{for } |kL_j| < 1, \\ \displaystyle -\sum_{n=1}^{\infty} \left(\frac{i}{kL_j}\right)^n, & \text{for } |kL_j| > 1, \end{cases} \tag{2.29}$$

we can expand the S-matrix into the following infinite series

$$S(kL_0) = \begin{cases} \displaystyle -\mathbb{1}_N - 2\sum_{n=1}^{\infty}\sum_{j=1}^{N} (-ikL_j)^n P_j, & \text{for } |kL_j| < 1, \\ \displaystyle \mathbb{1}_N + 2\sum_{n=1}^{\infty}\sum_{j=1}^{N} \left(\frac{i}{kL_j}\right)^n P_j, & \text{for } |kL_j| > 1. \end{cases} \tag{2.30}$$

In chapter 3 we will use these power series expansions for the renormalization group analysis.

6. *Duality.*
Noting that the elementary identity $[\cot(\alpha_j/2)]^{-1} = \tan(\alpha_j/2) = -\cot((\alpha_j \pm \pi)/2)$, we see that the eigenvalue of the S-matrix has the following remarkable property

$$\frac{ikL_0\cot(\alpha_j/2) - 1}{ikL_0\cot(\alpha_j/2) + 1} = -\frac{i(kL_0)^{-1}\cot((\alpha_j \pm \pi)/2) - 1}{i(kL_0)^{-1}\cot((\alpha_j \pm \pi)/2) + 1}, \tag{2.31}$$

from which we conclude that

$$S(kL_0; \alpha_j, e_j^a) = -S((kL_0)^{-1}; \alpha_j \pm \pi, e_j^a), \tag{2.32}$$

where '+' sign for $0 \le \alpha_j < \pi$ and '−' sign for $\pi \le \alpha_j < 2\pi$. This identity indicates that the high-energy regime of the theory characterized by the parameters $\{\alpha_j, e_j^a\}$

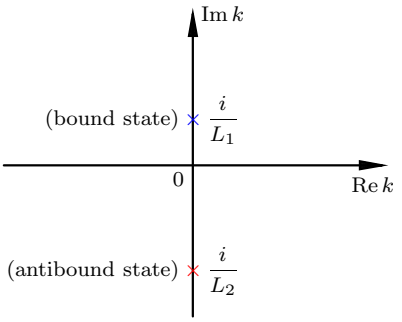


(a) Case $(0,\pi) < (\alpha_1,\alpha_2) < (\pi,2\pi)$.

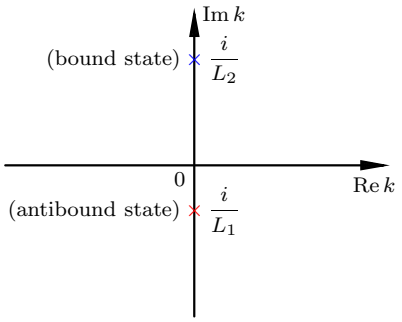


(b) Case $(\pi,0) < (\alpha_1,\alpha_2) < (2\pi,\pi)$.

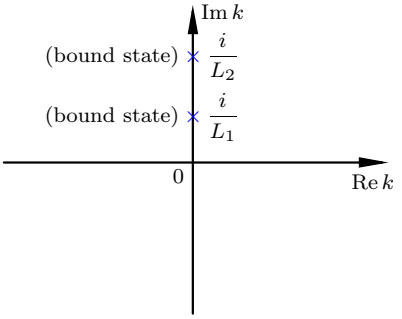


(c) Case $(0,0) < (\alpha_1,\alpha_2) < (\pi,\pi)$.

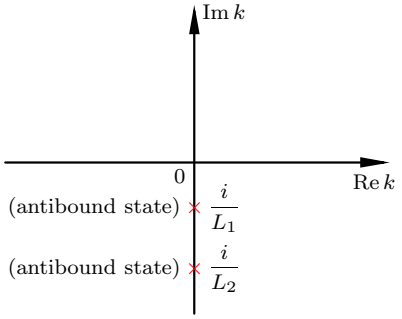


(d) Case $(\pi,\pi) < (\alpha_1,\alpha_2) < (2\pi,2\pi)$.

Figure 2.3: Possible distributions of poles of $S(kL_0)$ in the complex $k$-plain for $N = 2$. A simple pole lying on the positive (negative) imaginary axis corresponds to a bound (antibound or virtual) state.

is equivalent, or *dual*, to the (opposite sign of) low-energy regime of the theory characterized by the parameters $\{\alpha_j \pm \pi, e_j^a\}$. This duality of S-matrix has been studied and emphasized by many authors. Notice that Eq.(2.32) implies that the transformation $\alpha_j \mapsto \alpha_j \pm \pi$ interchanges the ultraviolet (UV) and infrared (IR) regions of scattering states and further a normalizable bound state and a non-normalizable antibound state. In section 3.4 we will briefly discuss this duality transformation from the renormalization group point of view.

## 2.4 Symmetry classes of point interactions

As discussed in Introduction, physics of point interactions is essentially low-energy one. In a philosophy of renormalization group theory, low-energy physics will be well captured by *relevant interactions* and *symmetries*, the former requires an analysis of renormalization group flow in a space of all possible point interactions allowed for a given system, which is a main subject of chapter 3 and will be studied in great detail there. In this respect, it is very important to classify the symmetry classes of $U(N)$ family of point interaction in a general footing.

Before embarking on the classification of symmetries for the system of star graph, it is wise to remember first what we mean by a symmetry. To this end, we here trace the argument given in [15] by rewriting it suitable for the following discussions.

Given a system with point interaction at the vertex described by $U$, we call a unitary or an antiunitary transformation $\mathcal{V}$ of the wavefunctions on each bond, $\psi_j \overset{\mathcal{V}}{\mapsto} \tilde{\psi}_j = \mathcal{V}_j\psi_j$, symmetry if it commutes with the differential operator $H$ and further $\tilde{\psi}_j$ also satisfies the same boundary conditions that $\psi_j$ fulfills.

To be more precise, let us suppose that a transformation $\mathcal{W}$ of the wavefunction, $\psi_j \overset{\mathcal{W}}{\mapsto} \tilde{\psi}_j = \mathcal{W}_j\psi_j$, commutes with $H$ and induces transformations on the boundary value vectors as

$$\vec{\Psi}(0) \overset{\mathcal{W}}{\mapsto} \vec{\tilde{\Psi}}(0) = W\vec{\Psi}(0), \quad \vec{\Psi}'(0) \overset{\mathcal{W}}{\mapsto} \vec{\tilde{\Psi}}'(0) = W'\vec{\Psi}'(0), \tag{2.33}$$

with some $N \times N$ matrices $W$ and $W'$. As we will see below, in most cases $W = W'$ and further $W(= W')$ is either a unitary or an antiunitary matrix. So let us first consider the unitary case $W = W' \in U(N)$. In this case the boundary condition (2.7) changes, under the transformations (2.33), as

$$(\mathbb{1}_N - U)W\vec{\Psi}(0) - iL_0(\mathbb{1}_N + U)W\vec{\Psi}'(0) = \vec{0}. \tag{2.34}$$

Multiplying the inverse $W^{-1} = W^\dagger$ by the left we have

$$(\mathbb{1}_N - W^\dagger UW)\vec{\Psi}(0) - iL_0(\mathbb{1}_N + W^\dagger UW)\vec{\Psi}'(0) = \vec{0}. \tag{2.35}$$

Thus, we see that $\mathcal{W}$ induces a map

$$U \overset{\mathcal{W}}{\mapsto} U_{\mathcal{W}} = W^\dagger UW. \tag{2.36}$$

If $U_{\mathcal{W}} = U$, or, equivalently, $[U, W] = 0$, such a transformation $\mathcal{W}$ becomes a symmetry[1]. Notice that in such a case $U$ and $W$ are simultaneously diagonalizable so that they have eigenvectors in common with each other and thus also projection operators. This fact provides us an alternative way to construct the projection operator of $U$ by $P_{\mathcal{W}j} = \vec{w}_j \cdot \vec{w}_j^\dagger$ with $\{\vec{w}_j\}_{j=1}^N$ being a set of orthonormal eigenvectors of $W$. We will use this method in section 2.4.2. Note also that since $\det(\lambda\mathbb{1}_N - U_{\mathcal{W}}) = \det(\lambda\mathbb{1}_N - U)$, any symmetry transformation provided by a unitary matrix $W$ cannot change eigenvalues of $U$. This implies that such a symmetry $\mathcal{W}$ does not impose any restrictions on the parameter space spanned by the eigenphases $\alpha_j$, $j = 1, 2, \cdots, N$.

Let us next consider an antiunitary case, that appears when one considers a symmetry transformation related to the time-reversal. Note that any antiunitary matrix $W$ can be written as $W = XK$ where $X$ is some unitary matrix and $K$ complex conjugates everything to its right. Note further that $K$ satisfies $K^2 = 1$.

Then, in an antiunitary case $W = XK$, the boundary condition (2.7) changes, under (2.33), as

$$(\mathbb{1}_N - U)XK\vec{\Psi}(0) - iL_0(\mathbb{1}_N + U)XK\vec{\Psi}'(0) = \vec{0}. \tag{2.37}$$

Successive multiplication of $U^{-1} = U^\dagger$ and $(XK)^{-1} = KX^\dagger$ by the left yields

$$-(\mathbb{1}_N - KX^\dagger U^\dagger XK)\vec{\Psi}(0) + iL_0(\mathbb{1}_N + KX^\dagger U^\dagger XK)\vec{\Psi}'(0) = \vec{0}, \tag{2.38}$$

[1] Since, by assumption, $\mathcal{W}$ commutes with $H$, the transformation $U \overset{\mathcal{W}}{\mapsto} U_{\mathcal{W}}$ does not change the spectrum of the two systems, one characterized by $U$ and the other by $U_{\mathcal{W}}$, even if $U \neq U_{\mathcal{W}}$. In the literature [15] such a spectrum-preserving transformation is referred to as the *generalized symmetry*.

where we have used $K(-i) = iK$ in the second term of the left hand side. Noting that $KX^\dagger U^\dagger XK = X^T U^T X^* KK = X^T U^T X^*$, we see that $\mathcal{W}$ induces a map

$$U \overset{\mathcal{W}}{\mapsto} U_{\mathcal{W}} = X^T U^T X^*. \tag{2.39}$$

If $U_{\mathcal{W}} = U$, $\mathcal{W}$ becomes a symmetry of the system. It should be noted here that since, just as in the unitary case, $\det(\lambda \mathbb{1}_N - U_{\mathcal{W}}) = \det(\lambda \mathbb{1}_N - U^T)$, any symmetry transformation provided by an antiunitary matrix $W = XK$ cannot change eigenvalues of $U$, which implies that the parameter space of $\alpha_j$ $(j = 1, 2, \cdots, N)$ is free from restrictions under any symmetry characterized by a unitary as well as an antiunitary matrix.

The above argument is easily translated into the symmetry of an (on-shell) S-matrix. Since the "in-state" and "out-state" vectors can be written as $\vec{A}^{\text{in/out}}(k) = \frac{1}{2}[\vec{\Psi}(0) \pm \frac{1}{ik}\vec{\Psi}'(0)]$, which follows from (2.14a) and (2.14b), the above introduced $\mathcal{W}$ induces transformations on these vectors as

$$\vec{A}^{\text{in/out}}(k) \overset{\mathcal{W}}{\mapsto} \vec{\tilde{A}}^{\text{in/out}}(k) = \begin{cases} W\vec{A}^{\text{in/out}}(k) & \text{for } W \text{ unitary,} \\ W\vec{A}^{\text{out/in}}(k) & \text{for } W \text{ antiunitary,} \end{cases} \tag{2.40}$$

where we have used $\pm\frac{1}{ik}K = K(\mp\frac{1}{ik})$. Notice that for the case of $W$ antiunitary, "in-state" and "out-state" are interchanged, as they should in a respect of time-reversal. Then, the defining equation of an S-matrix (2.19) changes as $W\vec{A}^{\text{out/in}}(k) = S(kL_0)W\vec{A}^{\text{in/out}}(k)$ for $W$ unitary/antiunitary. Hence the transformation $\mathcal{W}$ induces the following map:

$$S(kL_0) \overset{\mathcal{W}}{\mapsto} S_{\mathcal{W}}(kL_0) = \begin{cases} W^\dagger S(kL_0)W & \text{for } W \text{ unitary,} \\ X^T S^T(kL_0)X^* & \text{for } W \text{ antiunitary.} \end{cases} \tag{2.41}$$

If $S_{\mathcal{W}}(kL_0) = S(kL_0)$ we can also say that such a $\mathcal{W}$ is a symmetry of an S-matrix.

Using this general discussion, in the subsequent sections we will try to reveal possible symmetry classes of point interaction in star graphs. For the sake of simplicity, however, in what follows we will restrict ourselves to $U(2)$ and $U(3)$ family of point interactions.

### 2.4.1 I-junction

Let us first consider the symmetry classes of $U(2)$ family of point interactions in an I-junction of two half lines, i.e. a single line; see Figure 2.4. We note that symmetries and invariant subfamilies of point interaction on a line have already been studied in the literature [16, 17] and completely classified (see Table 2.1). It should be emphasized that this section is just a review and does not contain any new results: it is aimed to make this dissertation self-contained.

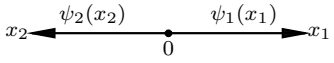


Figure 2.4: I-junction of two half-lines.

#### 2.4.1.1 Parity

Let us first consider the *parity* transformation $\mathscr{P} : x_{1,2} \mapsto x_{2,1}$, which acts on the vector $\vec{\Psi}(x_1, x_2) = (\psi_1(x_1), \psi_2(x_2))^T$ as

$$\mathscr{P} : \vec{\Psi}(x_1, x_2) \mapsto (\mathscr{P}\vec{\Psi})(x_1, x_2) := \sigma_1 \vec{\Psi}(x_1, x_2). \tag{2.42}$$

Table 2.1: Subfamily for $U(2)$ family of point interactions [15, 18].

| subfamily of point interactions | constraints on $U$ | constraints on parameter space | |
|---|---|---|---|
| | | $T^2$: $(\alpha_1, \alpha_2)$ | $S^2$: $(e_x, e_y, e_z)$ |
| reflectionless subfamily<br>(smooth subfamily) | $\det(U \pm \mathbb{1}_2) = 0$<br>& $U = \sigma_1 U^T \sigma_1$ | $(0, \pi)$, $(\pi, 0)$ | $(e_x, e_y, 0)$ |
| scale-independent subfamily | $U = \pm\mathbb{1}_2$<br>$\det(U \pm \mathbb{1}_2) = 0$ | $(0, 0)$, $(\pi, \pi)$<br>$(0, \pi)$, $(\pi, 0)$ | –<br>$(e_x, e_y, e_z)$ |
| transmissionless subfamily<br>(separated subfamily) | $U = \sigma_3 U \sigma_3$ | $(\alpha_1, \alpha_2)$ | $(0, 0, \pm 1)$ |
| $\mathscr{P}$-symmetric subfamily | $U = \sigma_1 U \sigma_1$ | $(\alpha_1, \alpha_2)$ | $(\pm 1, 0, 0)$ |
| $\mathscr{T}$-symmetric subfamily | $U = U^T$ | $(\alpha_1, \alpha_2)$ | $(e_x, 0, e_z)$ |
| $\mathscr{P}\mathscr{T}$-symmetric subfamily | $U = \sigma_1 U^T \sigma_1$ | $(\alpha_1, \alpha_2)$ | $(e_x, e_y, 0)$ |

Thus, under $\mathscr{P}$ the boundary value vectors are changed as $\vec{\Psi}(0) \overset{\mathscr{P}}{\mapsto} \sigma_1 \vec{\Psi}(0)$ and $\vec{\Psi}'(0) \overset{\mathscr{P}}{\mapsto} \sigma_1 \vec{\Psi}'(0)$. Since $\sigma_1$ is unitary as well as hermitian, according to the formula the parity transformation $\mathscr{P}$ induces the following map:

$$U \overset{\mathscr{P}}{\mapsto} U_{\mathscr{P}} = \sigma_1 U \sigma_1. \tag{2.43}$$

Since $\sigma_1 \sigma_j \sigma_1 = \sigma_j$ only for the case $j = 1$, it is obvious that in our parameterization the parity invariant subfamily ($U_{\mathscr{P}} = U$) is specified by the condition $e_y = e_z = 0$.

#### 2.4.1.2 Time-reversal

Let us next consider the *time-reversal* transformation $\mathscr{T}$, which is an antiunitary operation and given by

$$\mathscr{T} : \vec{\Psi}(x_1, x_2) \mapsto (\mathscr{T}\vec{\Psi})(x_1, x_2) := K\vec{\Psi}(x_1, x_2) = \vec{\Psi}^*(x_1, x_2). \tag{2.44}$$

Then the boundary value vectors are changed as $\vec{\Psi}(0) \overset{\mathscr{T}}{\mapsto} K\vec{\Psi}(0)$ and $\vec{\Psi}'(0) \overset{\mathscr{T}}{\mapsto} K\vec{\Psi}'(0)$. It follows from the formula that $\mathscr{T}$ induces the map

$$U \overset{\mathscr{T}}{\mapsto} U_{\mathscr{T}} = U^T. \tag{2.45}$$

Since symmetric Pauli matrices are $\sigma_1$ and $\sigma_3$, the time-reversal invariant subfamily ($U_{\mathscr{T}} = U$) is specified by the condition $e_y = 0$.

#### 2.4.1.3 $\mathscr{P}\mathscr{T}$ symmetry

Let us next consider the $\mathscr{P}\mathscr{T}$ transformation. $\mathscr{P}\mathscr{T}$ symmetry plays an important role for a system in the presence of an applied magnetic field, where the parity and time-reversal invariance are broken yet the $\mathscr{P}\mathscr{T}$ symmetry holds. It should be emphasized that the $U(2)$ family of point interaction is also responsible for a system with an external constant magnetic field: when one considers a quantum mechanical system on a circle of circumference $L$

with a single point interaction at the origin, an Aharonov-Bohm phase, which appears when an external magnetic field penetrates through the circle, can be represented as transmission coefficients for a particle once winds around the circle. In terms of the boundary conditions, it can be expressed as a twisted boundary conditions $\psi(L) = \mathrm{e}^{i\theta}\psi(0)$ and $\psi'(L) = \mathrm{e}^{i\theta}\psi'(0)$ by choosing $\theta$ to be (proportional to) the applied magnetic flux.

Now let us move on to the analysis of $\mathscr{P}\mathscr{T}$ transformation, which is defined by the successive transformation of $\mathscr{P}$ and $\mathscr{T}$:

$$\mathscr{P}\mathscr{T} : \vec{\Psi}(x_1, x_2) \mapsto (\mathscr{P}\mathscr{T}\vec{\Psi})(x_1, x_2) := (\mathscr{P}(\mathscr{T}\vec{\Psi}))(x_1, x_2) = \sigma_1 K\vec{\Psi}(x_1, x_2). \tag{2.46}$$

Under this antiunitary transformation, the boundary value vectors are changed as $\vec{\Psi}(0) \overset{\mathscr{P}\mathscr{T}}{\mapsto} \sigma_1 K\vec{\Psi}(0)$ and $\vec{\Psi}'(0) \overset{\mathscr{P}\mathscr{T}}{\mapsto} \sigma_1 K\vec{\Psi}'(0)$ so that the $\mathscr{P}\mathscr{T}$ transformation induces the map

$$U \overset{\mathscr{P}\mathscr{T}}{\mapsto} U_{\mathscr{P}\mathscr{T}} = \sigma_1 U^T \sigma_1. \tag{2.47}$$

Noting that the identity $\sigma_1\sigma_{1,2}^T\sigma_1 = \sigma_{1,2}$, we see that the $\mathscr{P}\mathscr{T}$-symmetric subfamily ($U = U_{\mathscr{P}\mathscr{T}}$) is specified by the condition $e_z = 0$.

#### 2.4.1.4 Weyl scaling

Let us next consider the *Weyl scaling* $\mathscr{W}_\lambda$, which is a continuous transformation with a real parameter $\lambda > 0$. This acts on the vector $\vec{\Psi}$ as

$$\mathscr{W}_\lambda : \vec{\Psi}(x_1, x_2) \mapsto (\mathscr{W}_\lambda\vec{\Psi})(x_1, x_2) := \lambda^{-1/2}\vec{\Psi}(\lambda x_1, \lambda x_2). \tag{2.48}$$

Under this, the S-matrix is mapped as

$$S(kL_0) \overset{\mathscr{W}_\lambda}{\mapsto} S(\lambda k L_0). \tag{2.49}$$

Thus the scale-independent subfamily is specified by the constraints $(\alpha_1, \alpha_2) = (0, 0)$, $(\pi, \pi)$, $(0, \pi)$, $(\pi, 0)$. As we will see in chapter 3, these scale-invariant subfamily becomes the fixed points of renormalization group flow.

#### 2.4.1.5 Half-reflection ($\mathbb{Z}_2$-reflection)

Let us finally consider the *half-reflction* transformation $\mathscr{R}$ which acts on the vector $\vec{\Psi}$ as

$$\mathscr{R} : \vec{\Psi}(x_1, x_2) \mapsto (\mathscr{R}\vec{\Psi})(x_1, x_2) := \sigma_3\vec{\Psi}(x_1, x_2). \tag{2.50}$$

Then the boundary value vectors are changed as $\vec{\Psi}(0) \overset{\mathscr{R}}{\mapsto} \sigma_3\vec{\Psi}(0)$ and $\vec{\Psi}'(0) \overset{\mathscr{R}}{\mapsto} \sigma_3\vec{\Psi}'(0)$ so that $\mathscr{R}$ induces the map

$$U \overset{\mathscr{R}}{\mapsto} U_{\mathscr{R}} = \sigma_3 U \sigma_3. \tag{2.51}$$

Thus, the invariant subfamily under the half-reflection transformation is specified by the conditions $e_x = e_y = 0$. It should be noted that in this subfamily the S-matrix becomes diagonal, that is, the transmission coefficients identically vanish. This implies a particle cannot penetrate through the origin so that the system is physically equivalent to that of two decoupled half lines. In this sense the half-reflection invariant subfamily is dubbed as the separated subfamily [18].

#### 2.4.1.6 Spectrum-preserving $\mathfrak{su}(2)$

We have seen that the parity and half-reflection transformations induce maps given by the Pauli matrices $\sigma_1$ and $\sigma_3$. It is then quite natural to consider a map given by $\sigma_2$, which is induced by a transformation $\mathscr{Q} = -i\mathscr{R}\mathscr{P}$:

$$\mathscr{Q} : \vec{\Psi}(x_1, x_2) \mapsto (\mathscr{Q}\vec{\Psi})(x_1, x_2) := -i(\mathscr{R}(\mathscr{P}\vec{\Psi}))(x_1, x_2) = \sigma_2\vec{\Psi}(x_1, x_2). \tag{2.52}$$

Then the boundary value vectors are changed as $\vec{\Psi}(0) \overset{\mathscr{Q}}{\mapsto} \sigma_2\vec{\Psi}(0)$ and $\vec{\Psi}'(0) \overset{\mathscr{Q}}{\mapsto} \sigma_2\vec{\Psi}'(0)$ such that $\mathscr{Q}$ induces a map

$$U \overset{\mathscr{Q}}{\mapsto} U_{\mathscr{Q}} = \sigma_2 U \sigma_2. \tag{2.53}$$

Concerning the fact that a set $\{\sigma_1, \sigma_2, \sigma_3\}$ spans the Lie algebra $\mathfrak{su}(2)$ of the special unitary group $SU(2)$, the set of following three discrete transformations also spans the algebra $\mathfrak{su}(2)$:

$$\mathfrak{su}(2) = \mathrm{span}\{\mathscr{P}, \mathscr{Q}, \mathscr{R}\}. \tag{2.54}$$

Since these three discrete transformations obviously commute with the free Hamiltonian $H$, a quantum system on I-junction of two half-lines with a point interaction at the vertex characterized by $U$ has the same spectrum to that characterized by $U_{\mathscr{W}}$ with $\mathscr{W}$ being any elements of the algebra (2.54). As discussed in [17], if a system is invariant under $\mathscr{P}$ and $\mathscr{R}$, that is, characterized by $U$ satisfying (2.43) and (2.51) simultaneously, which is realized by the matrix of the form $U = \mathrm{e}^{i\alpha}\mathbb{1}_2$ $(0 \leq \alpha < 2\pi)$, the Lie algebra $\mathfrak{su}(2)$ becomes symmetries of the system and hence energy eigenstates are categorized by the irreducible representation of $\mathfrak{su}(2)$.

### 2.4.2 Y-junction

Let us next consider the symmetry classes of $U(3)$ family of point interactions in a Y-junction of three half-lines (see Figure 2.5). Although the Y-junction of three quantum wires has been extensively discussed by many authors as the simplest but nontrivial topological space which does not manifold, its symmetry classes have not yet been uncovered. This is mainly due to the highly nontrivial structure of parameter space for the unitary group $U(3)$. In this section we would like to try to address this issue. Notice that the maps of $U \in U(3)$ induced by the time-reversal and Weyl scaling transformations are the same for those obtained in the previous section because they do not depend on the geometrical structure of space. The nontrivial point is that the generalization of parity. Noting that the parity transformation is nothing but the permutation of two half-lines, it is quite reasonable to consider as the generalization of parity in a system of Y-junction all possible permutations of three half-lines, which obviously consist of the symmetric group of order three $S_3$. It is well known that $S_3$ is isomorphic to the dihedral group of order three $D_3$, which is the symmetry group of rotations of an equilateral triangle with undirected sides and consists of the six elements: identity transformation, 2 rotations through angles $2\pi/3$ and $4\pi/3$, and 3 distinct transpositions of two of

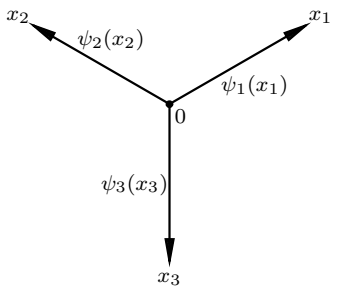


Figure 2.5: Y-junction of three half-lines.

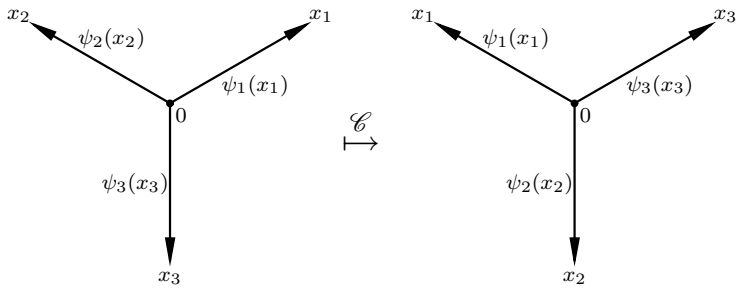


Figure 2.6: Counterclockwise rotation $\mathscr{C}$ through an angle $2\pi/3$.

three vertices. Note that the first three elements form a subgroup, a cyclic group of order three $C_3$.

In the following sections we will study the action of the group $D_3$ on a system of Y-junction of three half-lines.

#### 2.4.2.1 Cyclic group $C_3$

Let us first study the action of *cyclic group* $C_3$ (or $\mathbb{Z}_3$) on a system of Y-junction of three half-lines. The cyclic group $C_3$ can be generated by a single element $\mathscr{C}$ of a counterclockwise rotation through an angle $2\pi/3$ (see Figure 2.6), and it consists of three elements: $C_3 = \{\mathscr{C}, \mathscr{C}^2, \mathscr{C}^3 = \mathbb{1}\}$. The action of $\mathscr{C}$ on the vector $\vec{\Psi}(x_1, x_2, x_3) = (\psi_1(x_1), \psi_2(x_2), \psi_3(x_3))^T$ is as follows:

$$\mathscr{C} : \vec{\Psi}(x_1, x_2, x_3) \mapsto (\mathscr{C}\vec{\Psi})(x_1, x_2, x_3) := C\vec{\Psi}(x_1, x_2, x_3), \tag{2.55}$$

where $C$ is a $3 \times 3$ traceless unitary matrix given by

$$C = \begin{pmatrix} 0 & 0 & 1 \\ 1 & 0 & 0 \\ 0 & 1 & 0 \end{pmatrix}. \tag{2.56}$$

It should be noted that $C^2 = C^\dagger = C^{-1}$ and $C^3 = \mathbb{1}_3$. Under the rotation $\mathscr{C}$, the boundary value vectors are changed as $\vec{\Psi}(0) \overset{\mathscr{C}}{\mapsto} C\vec{\Psi}(0)$ and $\vec{\Psi}'(0) \overset{\mathscr{C}}{\mapsto} C\vec{\Psi}'(0)$ so that $\mathscr{C}$ induces the map

$$U \overset{\mathscr{C}}{\mapsto} U_{\mathscr{C}} = C^\dagger U C. \tag{2.57}$$

Next consider the parameterization of $U$ satisfying $[U, C] = 0$. To this end we first note that the unitary matrix $C$ has three distinct eigenvalues $c_1 = \omega$, $c_2 = \omega^2$, $c_3 = \omega^3 = 1$ with $\omega = \mathrm{e}^{i2\pi/3}$ being the 3rd root of unity fulfilling $\omega^2 + \omega + 1 = 0$ and $\omega^* = \omega^2$. The corresponding orthonormal eigenvectors are, respectively,

$$\vec{c}_1 = \tfrac{1}{\sqrt{3}}(1, \omega^2, \omega)^T, \tag{2.58a}$$

$$\vec{c}_2 = \tfrac{1}{\sqrt{3}}(1, \omega, \omega^2)^T, \tag{2.58b}$$

$$\vec{c}_3 = \tfrac{1}{\sqrt{3}}(1, 1, 1)^T. \tag{2.58c}$$

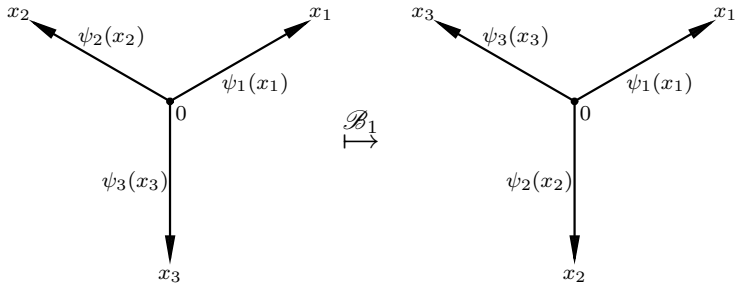


Figure 2.7: Transposition $\mathscr{B}_1$ of $x_2$- and $x_3$-axis.

As noted in section 2.4, the projection operator of $U$ can be constructed as $P_{\mathscr{C}j} = \vec{c}_j \cdot \vec{c}_j^{\dagger}$ $(j = 1, 2, 3)$. A straightforward calculation yields

$$P_{\mathscr{C}1} = \frac{1}{3}\begin{pmatrix} 1 & \omega & \omega^2 \\ \omega^2 & 1 & \omega \\ \omega & \omega^2 & 1 \end{pmatrix} = \frac{\mathbb{1}_3 + \omega C + \omega^2 C^2}{3}, \tag{2.59a}$$

$$P_{\mathscr{C}2} = \frac{1}{3}\begin{pmatrix} 1 & \omega^2 & \omega \\ \omega & 1 & \omega^2 \\ \omega^2 & \omega & 1 \end{pmatrix} = \frac{\mathbb{1}_3 + \omega^2 C + \omega C^2}{3}, \tag{2.59b}$$

$$P_{\mathscr{C}3} = \frac{1}{3}\begin{pmatrix} 1 & 1 & 1 \\ 1 & 1 & 1 \\ 1 & 1 & 1 \end{pmatrix} = \frac{\mathbb{1}_3 + C + C^2}{3}. \tag{2.59c}$$

Thus the $\mathscr{C}$-invariant subfamily of $U(3)$ family of point interactions is a three parameter family described by the three eigenphases $\alpha_1$, $\alpha_2$ and $\alpha_3$.

#### 2.4.2.2 Transposition

Let us next consider the *transposition* of two of three half-lines (see Figure 2.7). The transposition of Y-junction consists of the three elements $\mathscr{B}_j$ $(j = 1, 2, 3)$ and acts on the vector $\vec{\Psi}$ as

$$\mathscr{B}_j : \vec{\Psi}(x_1, x_2, x_3) \overset{\mathscr{B}_j}{\mapsto} (\mathscr{B}_j\vec{\Psi})(x_1, x_2, x_3) := B_j\vec{\Psi}(x_1, x_2, x_3), \tag{2.60}$$

where $B_j$ is a $3 \times 3$ symmetric unitary matrix given by

$$B_1 = \begin{pmatrix} 1 & 0 & 0 \\ 0 & 0 & 1 \\ 0 & 1 & 0 \end{pmatrix}, \quad B_2 = \begin{pmatrix} 0 & 0 & 1 \\ 0 & 1 & 0 \\ 1 & 0 & 0 \end{pmatrix}, \quad B_3 = \begin{pmatrix} 0 & 1 & 0 \\ 1 & 0 & 0 \\ 0 & 0 & 1 \end{pmatrix}. \tag{2.61}$$

It should be noted that $B_2 = B_1C = C^2B_1$ and $B_3 = B_1C^2 = CB_1$ because the rotations $\mathscr{C}$ $(\mathscr{C}^2)$ followed by the reflection $\mathscr{B}_1$ and the reflection $\mathscr{B}_1$ followed by the rotation $\mathscr{C}^2$ $(\mathscr{C})$ both result in the reflection across the $x_2$- and $x_3$-axis, respectively. Note further that a set of three matrices $\{B_1, B_2, B_3\}$ does not form any group under the multiplication rule of matrices, however, a set of six unitary matrices $\{\mathbb{1}_3, C, C^2; B_1, B_2, B_3\}$ does form a symmetric group of order three $S_3$, or, equivalently, dihedral group of order three $D_3$, as it should.

Under the transposition $\mathscr{B}_j$, the boundary value vectors are changed as $\vec{\Psi}(0) \overset{\mathscr{B}_j}{\mapsto} B_j\vec{\Psi}(0)$ and $\vec{\Psi}'(0) \overset{\mathscr{B}_j}{\mapsto} B_j\vec{\Psi}'(0)$ such that $\mathscr{B}_j$ induces the map

$$U \overset{\mathscr{B}_j}{\mapsto} U_{\mathscr{B}_j} = B_j U B_j. \tag{2.62}$$

Next consider the $\mathscr{B}_1$-invariant subfamily of point interactions characterized by the condition $[U, B_1] = 0$. The unitary matrix $B_1$ has the eigenvalues $b_1^{(1)} = 1$, $b_1^{(2)} = 1$, $b_1^{(3)} = -1$ so that the corresponding eigenvectors enjoy the following parameterizations

$$\vec{b}_1^{(1)} = (\mathrm{e}^{-i\phi}\cos\theta, \tfrac{1}{\sqrt{2}}\sin\theta, \tfrac{1}{\sqrt{2}}\sin\theta)^T, \tag{2.63a}$$

$$\vec{b}_1^{(2)} = (-\mathrm{e}^{-i\phi}\sin\theta, \tfrac{1}{\sqrt{2}}\cos\theta, \tfrac{1}{\sqrt{2}}\cos\theta)^T, \tag{2.63b}$$

$$\vec{b}_1^{(3)} = \tfrac{1}{\sqrt{2}}(0, 1, -1)^T. \tag{2.63c}$$

Using these orthonormal eigenvectors, the projection operators are easily constructed as $P_{\mathscr{B}_1 j} = \vec{b}_1^{(j)} \cdot [\vec{b}_1^{(j)}]^\dagger$, or, more explicitly,

$$P_{\mathscr{B}_1 1} = \begin{pmatrix} \cos^2\theta & \frac{1}{\sqrt{2}}\mathrm{e}^{-i\phi}\sin\theta\cos\theta & \frac{1}{\sqrt{2}}\mathrm{e}^{-i\phi}\sin\theta\cos\theta \\ \frac{1}{\sqrt{2}}\mathrm{e}^{i\phi}\sin\theta\cos\theta & \frac{1}{2}\sin^2\theta & \frac{1}{2}\sin^2\theta \\ \frac{1}{\sqrt{2}}\mathrm{e}^{i\phi}\sin\theta\cos\theta & \frac{1}{2}\sin^2\theta & \frac{1}{2}\sin^2\theta \end{pmatrix}, \tag{2.64a}$$

$$P_{\mathscr{B}_1 2} = \begin{pmatrix} \sin^2\theta & -\frac{1}{\sqrt{2}}\mathrm{e}^{-i\phi}\sin\theta\cos\theta & -\frac{1}{\sqrt{2}}\mathrm{e}^{-i\phi}\sin\theta\cos\theta \\ -\frac{1}{\sqrt{2}}\mathrm{e}^{i\phi}\sin\theta\cos\theta & \frac{1}{2}\cos^2\theta & \frac{1}{2}\cos^2\theta \\ -\frac{1}{\sqrt{2}}\mathrm{e}^{i\phi}\sin\theta\cos\theta & \frac{1}{2}\cos^2\theta & \frac{1}{2}\cos^2\theta \end{pmatrix}, \tag{2.64b}$$

$$P_{\mathscr{B}_1 3} = \frac{1}{2}\begin{pmatrix} 0 & 0 & 0 \\ 0 & 1 & -1 \\ 0 & -1 & 1 \end{pmatrix}. \tag{2.64c}$$

Since the eigenvalue equation $B_1\vec{b}_1^{(j)} = b_1^{(j)}\vec{b}_1^{(j)}$ implies that $B_2(C\vec{b}_1^{(j)}) = b_1^{(j)}(C\vec{b}_1^{(j)})$ and $B_3(C^2\vec{b}_1^{(j)}) = b_1^{(j)}(C^2\vec{b}_1^{(j)})$, the projection operators of $U$ for $\mathscr{B}_2$- and $\mathscr{B}_3$-invariant subfamily are given by $P_{\mathscr{B}_2 j} = C\vec{b}_1^{(j)} \cdot [\vec{b}_1^{(j)}]^\dagger C^\dagger = C P_{\mathscr{B}_1 j} C^2$ and $P_{\mathscr{B}_3 j} = C^2\vec{b}_1^{(j)} \cdot [\vec{b}_1^{(j)}]^\dagger C^{2\dagger} = C^2 P_{\mathscr{B}_1 j} C$. Consequently, the $\mathscr{B}_j$-invariant subfamily is a five parameter family of point interactions described by $\alpha_1$, $\alpha_2$, $\alpha_3$, $\theta$ and $\phi$.

#### 2.4.2.3 $\mathbb{Z}_3$-reflection

As a generalization of the half-reflection, let us finally consider a $\mathbb{Z}_3$-*reflection* $\mathscr{Z}$ which can be defined as an action on the vector $\vec{\Psi}$ as

$$\mathscr{Z} : \vec{\Psi}(x_1, x_2, x_3) \mapsto (\mathscr{Z}\vec{\Psi})(x_1, x_2, x_3) := Z\vec{\Psi}(x_1, x_2, x_3), \tag{2.65}$$

where $Z$ is a $3 \times 3$ unitary matrix given by

$$Z = \begin{pmatrix} 1 & 0 & 0 \\ 0 & \omega & 0 \\ 0 & 0 & \omega^2 \end{pmatrix}. \tag{2.66}$$

Notice that a set $\{Z, Z^2 = Z^\dagger, Z^3 = \mathbb{1}_3\}$ forms an Abelian group $\mathbb{Z}_3$ (or $C_3$). Under the transformation $\mathscr{Z}$ the boundary value vectors are changed as $\vec{\Psi}(0) \overset{\mathscr{Z}}{\mapsto} Z\vec{\Psi}(0)$ and $\vec{\Psi}'(0) \overset{\mathscr{Z}}{\mapsto} Z\vec{\Psi}'(0)$ such that $\mathscr{Z}$ induces the map

$$U \overset{\mathscr{Z}}{\mapsto} U_{\mathscr{Z}} = Z^\dagger U Z. \tag{2.67}$$

If $U_{\mathscr{Z}} = U$, the transformation $\mathscr{Z}$ becomes a symmetry.

Next consider the parameterization of $U$ for the $\mathscr{Z}$-invariant subfamily. Since the eigenvectors of $Z$ are simply given by $\vec{z}_1 = (0,0,1)^T$, $\vec{z}_2 = (0,1,0)^T$ and $\vec{z}_2 = (1,0,0)$, the projection operators of $U$ are given by $P_{\mathscr{Z}j} = \vec{z}_j \cdot \vec{z}_j^\dagger$:

$$P_{\mathscr{Z}1} = \begin{pmatrix} 0 & 0 & 0 \\ 0 & 0 & 0 \\ 0 & 0 & 1 \end{pmatrix} = \frac{\mathbb{1}_3 + \omega Z + \omega^2 Z^2}{3}, \tag{2.68a}$$

$$P_{\mathscr{Z}2} = \begin{pmatrix} 0 & 0 & 0 \\ 0 & 1 & 0 \\ 0 & 0 & 0 \end{pmatrix} = \frac{\mathbb{1}_3 + \omega^2 Z + \omega Z^2}{3}, \tag{2.68b}$$

$$P_{\mathscr{Z}3} = \begin{pmatrix} 1 & 0 & 0 \\ 0 & 0 & 0 \\ 0 & 0 & 0 \end{pmatrix} = \frac{\mathbb{1}_3 + Z + Z^2}{3}. \tag{2.68c}$$

Thus, a unitary matrix fulfilling the condition $U_{\mathscr{Z}} = U$ is diagonal, $U = \mathrm{diag}(\mathrm{e}^{i\alpha_1}, \mathrm{e}^{i\alpha_2}, \mathrm{e}^{i\alpha_3})$. An important physical implication of this is that, just as in the case of half-reflection, $\mathbb{Z}_3$-reflection invariant subfamily of point interaction does not admit any particle transmissions at the vertex. Thus, the resultant system of Y-junciton is physically equivalent to that of three decoupled half-lines.

#### 2.4.2.4 Spectrum-preserving $\mathfrak{su}(3)$

So far we have introduced several discrete transformations on a system of Y-junction of three half-lines. It should be emphasized that a set of eight traceless unitary matrices plus unit matrix

$$\mathbb{1}_3 = \begin{pmatrix} 1 & 0 & 0 \\ 0 & 1 & 0 \\ 0 & 0 & 1 \end{pmatrix}, \qquad C = \begin{pmatrix} 0 & 0 & 1 \\ 1 & 0 & 0 \\ 0 & 1 & 0 \end{pmatrix}, \qquad C^2 = \begin{pmatrix} 0 & 1 & 0 \\ 0 & 0 & 1 \\ 1 & 0 & 0 \end{pmatrix}, \tag{2.69a}$$

$$Z = \begin{pmatrix} 1 & 0 & 0 \\ 0 & \omega & 0 \\ 0 & 0 & \omega^2 \end{pmatrix}, \quad CZ = \begin{pmatrix} 0 & 0 & \omega^2 \\ 1 & 0 & 0 \\ 0 & \omega & 0 \end{pmatrix}, \quad C^2Z = \begin{pmatrix} 0 & \omega & 0 \\ 0 & 0 & \omega^2 \\ 1 & 0 & 0 \end{pmatrix}, \tag{2.69b}$$

$$Z^2 = \begin{pmatrix} 1 & 0 & 0 \\ 0 & \omega^2 & 0 \\ 0 & 0 & \omega \end{pmatrix}, \quad CZ^2 = \begin{pmatrix} 0 & 0 & \omega \\ 1 & 0 & 0 \\ 0 & \omega^2 & 0 \end{pmatrix}, \quad C^2Z^2 = \begin{pmatrix} 0 & \omega^2 & 0 \\ 0 & 0 & \omega \\ 1 & 0 & 0 \end{pmatrix}, \tag{2.69c}$$

is known to form a basis for the Lie algebra $\mathfrak{u}(3)$ of the unitary group $U(3)$ (see for review [19] and references therein)[2]. It is also known that its subset obtained by excluding the unit matrix $\mathbb{1}_3$ spans the Lie algebra $\mathfrak{su}(3)$ of the special unitary group $SU(3)$, and is named as the *generalized Pauli matrices* [19]. These generalized Pauli matrices differ from the ordinary (hermitian but non-unitary) Gell-Mann matrices used for describing the $SU(3)$ uds flavor symmetry in the standard quark model. One of the advantages to concern the generalized Pauli matrices is its unitarity and cyclic symmetry, which is now obvious.

A remarkable point concerning the fact that the set of eight distinct traceless unitary matrices $\{C, C^2; Z, Z^2; CZ, C^2Z; CZ^2, C^2Z^2\}$ provides a basis for $\mathfrak{su}(3)$ is that corresponding set of eight discrete transformations also spans the algebra $\mathfrak{su}(3)$:

$$\mathfrak{su}(3) = \mathrm{span}\{\mathscr{C}, \mathscr{C}^2; \mathscr{Z}, \mathscr{Z}^2; \mathscr{C}\mathscr{Z}, \mathscr{C}^2\mathscr{Z}; \mathscr{C}\mathscr{Z}^2, \mathscr{C}^2\mathscr{Z}^2\}. \tag{2.70}$$

Since these eight discrete transformations obviously commute with the free Hamiltonian $H$, a quantum system of Y-junction characterized by $U$ has the same spectrum to that characterized by $U_{\mathscr{W}}$ with $\mathscr{W}$ being any elements of the algebra (2.70), even if $\mathscr{W}$ is *not* a symmetry of the system described by $U$. Furthermore, if a system is invariant under both $\mathscr{C}$ and $\mathscr{Z}$, which is realized by a unitary matrix of the form $U = \mathrm{e}^{i\alpha}\mathbb{1}_3$ $(0 \le \alpha < 2\pi)$, the algebra $\mathfrak{su}(3)$ becomes symmetries of the system. Hence, just as in the case of I-junction, in this case energy eigenstates are categorized by the irreducible representation of $\mathfrak{su}(3)$.

## 2.5 Conclusions and discussions

In this chapter we have defined a one-particle quantum mechanical system on a star graph with $N$ bonds consistent with the conservation of probability current density at the vertex. The system is characterized by a unitary matrix $U \in U(N)$. Its dynamics is governed by the one-particle S-matrix which can be derived exactly. We also give a classification of symmetries and invariant subfamily of $U(3)$ family of point interactions in a system of Y-junction of three half-lines. We find that the set of eight distinct discrete transformations (2.70) generated by the counterclockwise rotation $\mathscr{C}$ and $\mathbb{Z}_3$-reflection $\mathscr{Z}$ spans the Lie algebra $\mathfrak{su}(3)$. Now it is easy to generalize this spectrum-preserving $\mathfrak{su}(3)$ to $\mathfrak{su}(N)$. To this end, fist observe that the basis for the Lie algebra $\mathfrak{u}(3)$ is given by $\{C^aZ^b \mid a, b = 0, 1, 2\}$,

[2] One can easily check that the following linear combinations certainly yield the standard hermitian traceless Gell-Mann matrices $\lambda_j$ $(j = 1, 2, \cdots, 8)$:

$$\lambda_1 = E_{21} + E_{12}, \quad \lambda_2 = iE_{21} - iE_{12}, \quad \lambda_4 = E_{31} + E_{13}, \quad \lambda_5 = iE_{31} - iE_{13}, \tag{f2.1a}$$

$$\lambda_6 = E_{32} + E_{23}, \quad \lambda_7 = iE_{32} - iE_{23}, \quad \lambda_3 = \frac{(1-\omega^2)Z + (1-\omega)Z^2}{3}, \quad \lambda_8 = \frac{-\omega Z + (1+\omega)Z^2}{\sqrt{3}}, \tag{f2.1b}$$

where

$$E_{21} := \frac{C + CZ + CZ^2}{3} = \begin{pmatrix} 0 & 0 & 0 \\ 1 & 0 & 0 \\ 0 & 0 & 0 \end{pmatrix}, \qquad E_{31} := \frac{C^2 + C^2Z + C^2Z^2}{3} = \begin{pmatrix} 0 & 0 & 0 \\ 0 & 0 & 0 \\ 1 & 0 & 0 \end{pmatrix}, \tag{f2.2a}$$

$$E_{13} := \frac{C + \omega CZ + \omega^2 CZ^2}{3} = \begin{pmatrix} 0 & 0 & 1 \\ 0 & 0 & 0 \\ 0 & 0 & 0 \end{pmatrix}, \quad E_{23} := \frac{C^2 + \omega C^2Z + \omega^2 C^2Z^2}{3} = \begin{pmatrix} 0 & 0 & 0 \\ 0 & 0 & 1 \\ 0 & 0 & 0 \end{pmatrix}, \tag{f2.2b}$$

$$E_{32} := \frac{C + \omega^2 CZ + \omega CZ^2}{3} = \begin{pmatrix} 0 & 0 & 0 \\ 0 & 0 & 0 \\ 0 & 1 & 0 \end{pmatrix}, \quad E_{12} := \frac{C^2 + \omega^2 C^2Z + \omega C^2Z^2}{3} = \begin{pmatrix} 0 & 1 & 0 \\ 0 & 0 & 0 \\ 0 & 0 & 0 \end{pmatrix}. \tag{f2.2c}$$

which is generated by only two distinct unitary matrices $C$ and $Z$. Thus, in order to study the spectrum preserving $\mathfrak{su}(N)$, it is natural to expect that it would be sufficient to consider the counterclockwise rotation $\mathscr{C}$ through an angle $2\pi/N$ and $\mathbb{Z}_N$-reflection $\mathscr{Z}$. As we will see soon, this observation is indeed true.

In a star graph with $N$ bonds the discrete transformations $\mathscr{C}$ and $\mathscr{Z}$ are defined by

$$\mathscr{C} : \vec{\Psi}(x_1, \cdots, x_N) \mapsto (\mathscr{C}\vec{\Psi})(x_1, \cdots, x_N) := C\vec{\Psi}(x_1, \cdots, x_N), \tag{2.71a}$$

$$\mathscr{Z} : \vec{\Psi}(x_1, \cdots, x_N) \mapsto (\mathscr{Z}\vec{\Psi})(x_1, \cdots, x_N) := Z\vec{\Psi}(x_1, \cdots, x_N), \tag{2.71b}$$

where $C$ and $Z$ are $N \times N$ traceless unitary matrices given by

$$C = \begin{pmatrix} 0 & 0 & 0 & \cdots & 0 & 1 \\ 1 & 0 & 0 & \cdots & 0 & 0 \\ 0 & 1 & 0 & \cdots & 0 & 0 \\ \vdots & \vdots & \vdots & \ddots & \vdots & \vdots \\ 0 & 0 & 0 & \cdots & 0 & 0 \\ 0 & 0 & 0 & \cdots & 1 & 0 \end{pmatrix}, \quad Z = \begin{pmatrix} 1 & 0 & 0 & \cdots & 0 & 0 \\ 0 & \omega & 0 & \cdots & 0 & 0 \\ 0 & 0 & \omega^2 & \cdots & 0 & 0 \\ \vdots & \vdots & \vdots & \ddots & \vdots & \vdots \\ 0 & 0 & 0 & \cdots & \omega^{N-2} & 0 \\ 0 & 0 & 0 & \cdots & 0 & \omega^{N-1} \end{pmatrix}, \tag{2.72}$$

with $\omega = \mathrm{e}^{i2\pi/N}$ being the $N$th root of unity fulfilling $\omega^N = 1$, $1 + \omega + \cdots + \omega^{N-1} = 0$ and $\omega^* = \omega^{N-1}$. It is known that a set of $N^2$ unitary matrices $\{C^a Z^b \mid a, b = 0, 1, \cdots, N-1\}$ forms a basis for the Lie algebra $\mathfrak{u}(N)$ of the unitary group $U(N)$ [19]. Then, the subset $\{C^a Z^b \mid a, b = 0, 1, \cdots, N-1\} \setminus \{C^0 Z^0 = \mathbb{1}_N\}$ spans the Lie algebra $\mathfrak{su}(N)$ of the special unitary group $SU(N)$. As a direct consequence, the following set of $N^2 - 1$ distinct discrete transformations also spans the algebra $\mathfrak{su}(N)$:

$$\mathfrak{su}(N) = \mathrm{span}\{\mathscr{C}^a \mathscr{Z}^b \mid a, b = 0, 1, \cdots, N-1\} \setminus \{\mathscr{C}^0 \mathscr{Z}^0 = \mathbb{1}\}. \tag{2.73}$$

Since these $N^2 - 1$ discrete transformations commute with the free Hamiltonian $H$, they are intrinsically spectrum-preserving. Now it is easy to see that the invariant subfamilies under the transformations $\mathscr{C}$ and $\mathscr{Z}$ are, respectively, characterized by the $N$-parameter families of unitary matrix $U = \sum_{j=1}^{N} \mathrm{e}^{i\alpha_j} P_j$ $(0 \le \alpha_j < 2\pi)$, where $P_j$ $(j = 1, 2, \cdots, N)$ is a hermitian projection operator given by

$$P_j = \begin{cases} \dfrac{\mathbb{1}_N + \omega^j C + \omega^{2j} C^2 + \cdots + \omega^{(N-1)j} C^{N-1}}{N}, & \text{for } \mathscr{C}\text{-invariant subfamily,} \\ \dfrac{\mathbb{1}_N + \omega^j Z + \omega^{2j} Z^2 + \cdots + \omega^{(N-1)j} Z^{N-1}}{N}, & \text{for } \mathscr{Z}\text{-invariant subfamily.} \end{cases} \tag{2.74}$$

If the system is invariant under both $\mathscr{C}$ and $\mathscr{Z}$, then the algebra $\mathfrak{su}(N)$ becomes the symmetry of the system. Since $\mathscr{C}$- and $\mathscr{Z}$-invariance become compatible with each other only when $\alpha_1 = \alpha_2 = \cdots = \alpha_N$, such a system is characterized by the one-parameter family of unitary matrix $U = \mathrm{e}^{i\alpha}\mathbb{1}_N$ $(0 \le \alpha < 2\pi)$, which is nothing but the *center* of the unitary group $U(N)$. In such an $\mathfrak{su}(N)$-invariant system every energy eigenstates fall into the irreducible representations of $\mathfrak{su}(N)$.

# Chapter 3

# Exact RG flow of point interaction

In this chapter we study a renormalization group flow of $U(N)$ family of point interactions for a quantum particle on a star graph. We derive the renormalization group flow of point interactions *exactly* and show that the scale-independent subfamily of point interactions introduced in chapter 2 are realized as nontrivial fixed points.

## 3.1 Introduction

When a slow particle scatters off a short ranged scatterer it cannot resolve the structure of the object since its de Broglie wavelength is very long: In order to get detailed information about what the short ranged scatter is, we need to use a probe particle whose de Broglie wavelength is shorter than the size of the scatter. In other words, the longer the probe particle's wavelength is, the less information we can get about the short ranged scatter. The idea for describing low energy physics is that then it should not be important what precise potential one scatters off, but only how the potential looks at long length scales. The concept behind describing low energy properties in terms of a few (relevant) parameters and symmetries is the idea of renormalization group theory.

Renormalization group approach to quantum mechanics with short ranged or singular potential has a long history. It has been provided a powerful method for analyzing bound state energies and/or scattering amplitudes. Most of the literature concern the $\delta$-function potential in two dimensions [20–28] described by the Hamiltonian

$$H = -\frac{\partial^2}{\partial \vec{r}^2} - 2g\delta^{(2)}(\vec{r}), \quad \vec{r} \in \mathbb{R}^2, \tag{3.1}$$

and the inverse square potential in one dimension (as known as conformal mechanics [29]) described by the Hamiltonian [30–37]

$$H = -\frac{\mathrm{d}^2}{\mathrm{d}r^2} + \frac{\alpha}{r^2}, \quad r > 0, \tag{3.2}$$

where $g$ and $\alpha$ are both dimensionless coupling constants. These two Hamiltonians are characterized by lack of any scale parameters. However, strongly singular behaviors of these potentials at the origin require regularizations in order to make the energy eigenvalue problems well-defined so that it is inevitable to introduce a new scale through this regularization procedure, just as in the case of perturbative quantum field theories. By interpreting this new scale as a renormalization scale, the original ill-defined problem can be put into

a well-posed problem of regularization and renormalization, without use of any knowledge of short-distance physics behind the singularity. This is the reason why renormalization group theory is also powerful enough for analyzing one-particle (or one degree of freedom) quantum mechanics with strongly singular potentials.

It should be noted that both regularization and self-adjoint extension are aimed to define the spectrum of Hamiltonian to be real and lower-bounded, and introduce in common new scales, the former is renormalization scale (or cutoff) and the latter is $L_0$ that we are already familiar with. Indeed, it has been shown that the self-adjoint extension of (3.2) is equivalent to regularization and renormalization procedures [38].

The rest of this chapter is organized as follows. In section 3.2 we derive the exact $\beta$-function and exact renormalization group flow of $U(N)$ family of point interactions. We find $2^N$ fixed points in the parameter space spanned by the eigenphases of unitary matrix $U \in U(N)$. We also discuss the stability of given fixed point. Section 3.3 is devoted to explicit examples of renormalization group flow of $U(2)$ and $U(3)$ family of point interactions. In section 3.4 we briefly discuss the duality found in the previous chapter from the renormalization group point of view. We conclude in section 3.5.

## 3.2 Exact RG flow of point interaction

In this section we study the renormalization group flow of point interactions, which can be derived exactly thanks to the exactness of S-matrix. Before going to discuss the RG flow it may be instructive to investigate the UV ($k \to \infty$) and IR ($k \to 0$) behaviors of the S-matrix and give an observation to what the point interactions at the fixed points of RG flow are.

For the sake of concreteness, let us consider the case of $N = 2$ described by $U$. When $\alpha_{1,2} \neq 0$ or $\pi$ (i.e. $L_{1,2} \neq \infty$ or 0), the S-matrix $S(kL_0)$ flows into the unit matrix $\mathbb{1}_2$ in the UV regime ($k \to \infty$), while in the IR regime ($k \to 0$) it flows into $-\mathbb{1}_2$. Since $S(kL_0) = \pm\mathbb{1}_2$ means $U = \pm\mathbb{1}_2$, we see that in this case the point interactions flow into the infinite walls described by the Dirichlet and Neumann boundary conditions $\vec{\Psi}(0) = \vec{0}$ and $\vec{\Psi}'(0) = \vec{0}$ in the IR and UV limits, respectively; see Eq.(2.7). Note further that the diagonal S-matrix means the transmissionless point interactions, in this case particles cannot penetrate through the origin both in the UV and IR limits. This is physically equivalent to the situation where a single line splits into two disconnected half lines in the UV and IR limits. This is very interesting because it suggests that the *topology change* of space(-time) may be realized as the fixed points of RG flow.

The above situation will be changed when $\alpha_{1,2} = 0$ or $\pi$. Let us first consider the case where $\alpha_1 = 0$ and $\alpha_2 \neq 0$. In this case the S-matrix flows as $S(kL_0) \overset{k\to\infty}{\to} \mathbb{1}_2$ and $S(kL_0) \overset{k\to 0}{\to} P_1 - P_2 = \vec{e}\cdot\vec{\sigma}$, which means that while in the IR regime particles can penetrate through the origin, it is impossible in the UV regime. As a next example let us consider the case where $\alpha_1 = \pi$ and $\alpha_2 \neq \pi$. In this case the S-matrix flows as $S(kL_0) \overset{k\to\infty}{\to} -P_1 + P_2 = -\vec{e}\cdot\vec{\sigma}$ and $S(kL_0) \overset{k\to 0}{\to} -\mathbb{1}_2$. As contrast to the previous case, in this case particles can penetrate through the origin in the UV regime but it is impossible in the IR regime. All of the different behaviors of the S-matrix are summarized in Table 3.1. Different flows of the S-matrix in the IR limit implies that there exist nontrivial fixed points in the $U(2)$ parameter space (theory space).

In what follows we will confirm that this observation is indeed true for generic $N$.

Table 3.1: Flow of the S-matrix $S(kL_0)$ for $N = 2$. $\vec{e} = (e_x, e_y, e_z)^T$ is a unit vector fulfilling $e_x^2 + e_y^2 + e_z^2 = 1$. The third row represents the scale-independent S-matrices.

| $\alpha_1$ | $\alpha_2$ | IR limit ($k \to 0$) | UV limit ($k \to \infty$) |
|---|---|---|---|
| $\alpha_1 \neq 0, \pi$ | $\alpha_2 \neq 0, \pi$ | $S(kL_0) \to -\mathbb{1}_2$ | $S(kL_0) \to \mathbb{1}_2$ |
| $\alpha_1 = 0$ | $\alpha_2 \neq 0, \pi$ | $S(kL_0) \to P_1 - P_2 = \vec{e} \cdot \vec{\sigma}$ | $S(kL_0) \to \mathbb{1}_2$ |
| $\alpha_1 \neq 0, \pi$ | $\alpha_2 = 0$ | $S(kL_0) \to -P_1 + P_2 = -\vec{e} \cdot \vec{\sigma}$ | $S(kL_0) \to \mathbb{1}_2$ |
| $\alpha_1 = \pi$ | $\alpha_2 \neq 0, \pi$ | $S(kL_0) \to -\mathbb{1}_2$ | $S(kL_0) \to -P_1 + P_2 = -\vec{e} \cdot \vec{\sigma}$ |
| $\alpha_1 \neq 0, \pi$ | $\alpha_2 = \pi$ | $S(kL_0) \to -\mathbb{1}_2$ | $S(kL_0) \to P_1 - P_2 = \vec{e} \cdot \vec{\sigma}$ |
| $\alpha_1 = 0$ | $\alpha_2 = 0$ | $S(kL_0) = \mathbb{1}_2$ | $S(kL_0) = \mathbb{1}_2$ |
| $\alpha_1 = \pi$ | $\alpha_2 = \pi$ | $S(kL_0) = -\mathbb{1}_2$ | $S(kL_0) = -\mathbb{1}_2$ |
| $\alpha_1 = 0$ | $\alpha_2 = \pi$ | $S(kL_0) = \vec{e} \cdot \vec{\sigma}$ | $S(kL_0) = \vec{e} \cdot \vec{\sigma}$ |
| $\alpha_1 = \pi$ | $\alpha_2 = 0$ | $S(kL_0) = -\vec{e} \cdot \vec{\sigma}$ | $S(kL_0) = -\vec{e} \cdot \vec{\sigma}$ |

### 3.2.1 Exact $\beta$-functions

As noted before, $L_0$ is just an arbitrary reference scale so that the physical quantities, such as an S-matrix element or a bound-state energy, must be independent of the choice of $L_0$. The lack of dependence of $L_0$ can be expressed as an invariance of the theory under the renormalization group transformation

$$R_t : L_0 \mapsto \bar{L}(t) := L_0 \mathrm{e}^{-t}, \quad -\infty < t < \infty. \tag{3.3}$$

Any change of $L_0$ must be equivalent to changes in the $U(N)$ parameters $g_i = \{\alpha_j, e_j^a\}$. This requirement is expressed as

$$S(kL_0; g_j) = S(k\bar{L}(t); \bar{g}_j(t)), \tag{3.4a}$$
$$E_j(\alpha_j, L_0) = E_j(\bar{\alpha}_j(t), \bar{L}(t)), \tag{3.4b}$$

where $\bar{g}_j(t) = \{\bar{\alpha}_j(t), \bar{e}_j^a(t)\}$ are the running $U(N)$ parameters, which will be determined by the following two equivalent ways:

1. Before embarking on a standard renormalization group approach, it is wise to consider first the S-matrix evaluated at momentum $k\mathrm{e}^t$. Dimensional analysis and the invariance of S-matrix under the RG transformation allow us to relate it to the S-matrix at momentum $k$:

$$S((k\mathrm{e}^t)L_0; g_j) = S(k(L_0\mathrm{e}^t); g_j) = S(k((L_0\mathrm{e}^t)\mathrm{e}^{-t}); \bar{g}_j(t)) = S(kL_0; \bar{g}_j(t)), \tag{3.5}$$

   where the first equality follows from the dimensional analysis: the S-matrix is a dimensionless quantity and hence its momentum dependence must be encoded with the combination $kL_0$. The second equality, on the other hand, follows from Eq.(3.4a). Since momentum $k$ appears only in the combination $kL_j = kL_0 \cot(\alpha_j/2)$, the rescaling of $k$ must be adjusted by the running of $\alpha_j$:

$$kL_j \overset{k \mapsto k\mathrm{e}^t}{\mapsto} (k\mathrm{e}^t)L_j = k(L_j\mathrm{e}^t) = k\left(L_0\mathrm{e}^t \cot\frac{\alpha_j}{2}\right) = k\left(L_0 \cot\frac{\bar{\alpha}_j(t)}{2}\right), \tag{3.6}$$

   where the last equality follows from the requirement (3.4a). Thus, in order for the invariance of the theory under the RG transformation we must have

$$\cot\frac{\bar{\alpha}_j(t)}{2} = \mathrm{e}^t \cot\frac{\alpha_j}{2}, \tag{3.7}$$

from which we obtain

$$\bar{\alpha}_j(t) = 2\arctan\left(\mathrm{e}^{-t}\tan\frac{\alpha_j}{2}\right) = \frac{1}{i}\log\left(\frac{1+i\mathrm{e}^{-t}\tan(\alpha_j/2)}{1-i\mathrm{e}^{-t}\tan(\alpha_j/2)}\right). \tag{3.8}$$

The running of $e_j^a$, on the other hand, must be trivial:

$$\bar{e}_j^a(t) = e_j^a, \tag{3.9}$$

which implies that $e_j^a$ is a *truly marginal* parameter against the RG.

The running of $\bar{\alpha}_j(t)$ for several initial values $\alpha_j$ is depicted in Figure 3.1.

2. Let us next rederive the above results (3.7) and (3.9) by using the renormalization group techniques. Since $S(kL_0; g_i)$ dose not have $t$ in any way, from Eq.(3.4a) we must have

$$\frac{\partial}{\partial t}S(kL_0;g_i)\Big|_{g_i,L_0} = 0 = \frac{\partial}{\partial t}S(k\bar{L}(t);\bar{g}_i(t))\Big|_{g_i,L_0}. \tag{3.10}$$

The first equality is trivial, but the the second one leads to the following homogeneous renormalization group equation

$$\left(-\bar{L}\frac{\partial}{\partial\bar{L}} + \sum_{\bar{g}_i=\bar{\alpha}_i,\bar{e}_i}\beta_{g_i}(\bar{g}_i(t))\frac{\partial}{\partial\bar{g}_i}\right)S(k\bar{L}(t);\bar{g}_i(t)) = 0, \tag{3.11}$$

where the $\beta$-functions are defined by

$$\beta_{g_i}(\bar{g}_i(t)) := \frac{\partial\bar{g}_i(t)}{\partial t}\Big|_{g_i,L_0} \quad \text{with} \quad \bar{g}_i(0) = g_i, \tag{3.12}$$

which determines the running of $U(N)$ parameters.

In order to extract the $\beta$-functions we can differentiate the S-matrix in terms of $t$ explicitly:

$$\begin{aligned}\frac{\partial}{\partial t}S(k\bar{L}(t);\bar{g}_i(t))\Big|_{g_i,L_0} &= \frac{\partial}{\partial t}\left[-\mathbb{1}_N - 2\sum_{n=1}^{\infty}\sum_{j=1}^{N}\big(-ik\bar{L}_j(t)\big)^n\bar{P}_j(t)\right]_{g_i,L_0}\\ &= -2\sum_{n=1}^{\infty}(-ik)^n\sum_{j=1}^{N}\left(n\big(\bar{L}_j(t)\big)^{n-1}\frac{\partial\bar{L}_j(t)}{\partial t}\Big|_{g_i,L_0}\bar{P}_j(t) + \big(\bar{L}_j(t)\big)^n\frac{\partial\bar{P}_j(t)}{\partial t}\Big|_{g_i,L_0}\right),\end{aligned} \tag{3.13}$$

where $\bar{L}_j(t) := \bar{L}(t)\cot(\bar{\alpha}_j(t)/2)$. In the first line we have assumed $|kL_j| < 1$ for any $j$ and used the power series expansion (2.30). In order to implement the requirement (3.10), the coefficient of $k^n$ must vanish for all $n$:

$$\sum_{j=1}^{N}\left(n\big(\bar{L}_j(t)\big)^{n-1}\frac{\partial\bar{L}_j(t)}{\partial t}\Big|_{g_i,L_0}\bar{P}_j(t) + \big(\bar{L}_j(t)\big)^n\frac{\partial\bar{P}_j(t)}{\partial t}\Big|_{g_i,L_0}\right) = 0 \quad \text{for } {}^\forall n. \tag{3.14}$$

Since $\bar{P}_j(t)$ are orthogonal to each other, we see that Eq.(3.14) will be accomplished if and only if

$$0 = \frac{\partial \bar{L}_j(t)}{\partial t}\bigg|_{g_i,L_0} = -\bar{L}_j(t)\left(1 + \frac{1}{\sin\bar{\alpha}_j(t)}\frac{\partial\bar{\alpha}_j(t)}{\partial t}\bigg|_{g_i,L_0}\right), \tag{3.15a}$$

$$0 = \frac{\partial \bar{P}_j(t)}{\partial t}\bigg|_{g_i,L_0} = 2\sum_{a=1}^{N^2-1}\frac{\partial\bar{e}_j^a(t)}{\partial t}\bigg|_{g_i,L_0} T^a. \tag{3.15b}$$

Thus we arrive at the *exact* $\beta$-functions:

$$\beta_{\alpha_j}(\bar{\alpha}_j(t)) = -\sin\bar{\alpha}_j(t) \quad \text{with} \quad \bar{\alpha}_j(0) = \alpha_j, \tag{3.16a}$$

$$\beta_{e_j^a}(\bar{e}_j^a(t)) = 0 \quad \text{with} \quad \bar{e}_j^a(0) = e_j^a. \tag{3.16b}$$

From Eq.(3.16a) we see that $\bar{\alpha}_j(t) = 0$ and $\pi$ are a UV and an IR fixed point, respectively; see Figure 3.2.

Let us next derive the running $U(N)$ parameters by using the above exact $\beta$-functions. To this end we integrate $\mathrm{d}t = \mathrm{d}\alpha_j/\beta_{\alpha_j}$ over the range $(0,t)$. Noting $\bar{\alpha}_j(0) = \alpha_j$ we get

$$\int_0^t \mathrm{d}\tau = -\int_{\alpha_j}^{\bar{\alpha}_j(t)}\frac{\mathrm{d}\alpha}{\sin\alpha}. \tag{3.17}$$

With the help of the integral formula $\int\frac{\mathrm{d}x}{\sin x} = \log|\tan\frac{x}{2}|$ we get

$$t = -\log\left|\frac{\tan(\bar{\alpha}_j(t)/2)}{\tan(\alpha_j/2)}\right|, \tag{3.18}$$

from which we find $|\tan(\bar{\alpha}_j(t)/2)| = |\tan(\alpha_j/2)|\,\mathrm{e}^{-t}$, or, equivalently,

$$\bar{\alpha}_j(t) = 2\arctan\left(\mathrm{e}^{-t}\tan\frac{\alpha_j}{2}\right). \tag{3.19}$$

Since the $\beta$-function for $e_j^a$ identically vanishes, its running becomes trivial:

$$\bar{e}_j^a(t) = e_j^a. \tag{3.20}$$

All of the above results are consistent with those obtained in the previous discussions.

### 3.2.2 Stability of fixed points

Let us next discuss the *exact* RG flow in the $(\alpha_1,\alpha_2,\cdots,\alpha_N)$-space, which is an $N$-dimensional torus $T^N$, by looking at the fixed points at which $\beta_{\alpha_j} = 0$ and analyze their stabilities. To this end, let us first study the stability of a given fixed point. As is well known, flow near a given fixed point follows from the linearized RG equations

$$\frac{\partial}{\partial t}\begin{pmatrix}\bar{\alpha}_1(t)-\alpha_1^*\\ \bar{\alpha}_2(t)-\alpha_2^*\\ \vdots\\ \bar{\alpha}_N(t)-\alpha_N^*\end{pmatrix}\bigg|_{\alpha_j,L_0} = M\begin{pmatrix}\bar{\alpha}_1(t)-\alpha_1^*\\ \bar{\alpha}_2(t)-\alpha_2^*\\ \vdots\\ \bar{\alpha}_N(t)-\alpha_N^*\end{pmatrix} + O\big(\bar{\alpha}_j(t)-\alpha_j^*\big)^2, \tag{3.21}$$

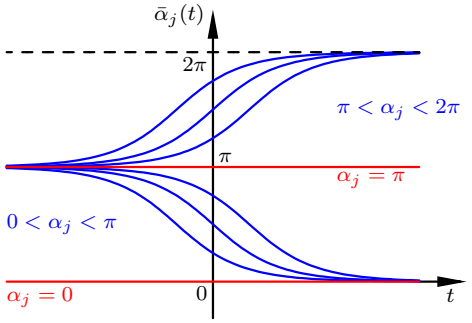


Figure 3.1: Running eigenphases $\bar{\alpha}_j(t)$ with initial values $\alpha_j = 0, \frac{\pi}{4}, \frac{\pi}{2}, \frac{3\pi}{4}, \pi, \frac{5\pi}{4}, \frac{3\pi}{2}, \frac{7\pi}{4}$.

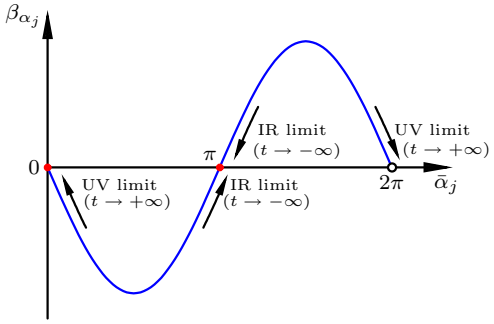


Figure 3.2: Exact $\beta$-function for $\bar{\alpha}_j$. $\bar{\alpha}_j = 0$ ($\pi$) is the UV(IR) fixed point.

where $\alpha_j^* = 0$ or $\pi$, and $M$ is the *stability matrix* given by

$$M = \left( \left. \frac{\partial \beta_{\alpha_i}}{\partial \bar{\alpha}_j} \right|_{\bar{\alpha}_i = \alpha_i^*} \right)_{1 \le i,j \le N} = \begin{pmatrix} -\cos\alpha_1^* & 0 & \dots & 0 \\ 0 & -\cos\alpha_2^* & \dots & 0 \\ \vdots & \vdots & \ddots & \vdots \\ 0 & 0 & \dots & -\cos\alpha_N^* \end{pmatrix}. \tag{3.22}$$

The eigenvectors of $M$ with negative eigenvalues determine the relevant (IR unstable) directions at the given fixed point, and those with positive eigenvalues the irrelevant (IR stable) directions. Since in our present case the stability matrix $M$ is already diagonal, we can easily check the stability of a given fixed point by looking at the explicit solution to the linearized equation

$$\begin{pmatrix} \bar{\alpha}_1(t) \\ \bar{\alpha}_2(t) \\ \vdots \\ \bar{\alpha}_N(t) \end{pmatrix} = \begin{pmatrix} \alpha_1^* \\ \alpha_2^* \\ \vdots \\ \alpha_N^* \end{pmatrix} + \begin{pmatrix} (\alpha_1 - \alpha_1^*)\exp(-\cos\alpha_1^* t) \\ (\alpha_2 - \alpha_2^*)\exp(-\cos\alpha_2^* t) \\ \vdots \\ (\alpha_N - \alpha_N^*)\exp(-\cos\alpha_N^* t) \end{pmatrix} + O(\alpha_j - \alpha_j^*)^2, \tag{3.23}$$

where we have imposed $\bar{\alpha}_j(0) = \alpha_j$. Now it is easy to see the relevancy or irrelevancy of a given fixed point $(\alpha_1^*, \alpha_2^*, \cdots, \alpha_N^*)$:

- If $\alpha_j^* = 0$, $\alpha_j$-direction is *relevant*: as lower the energy scale $t \to -\infty$, the running eigenphase $\bar{\alpha}_j(t)$ moves away from its fixed point value $\alpha_j^*$ exponentially.
- If $\alpha_j^* = \pi$, $\alpha_j$-direction is *irrelevant*: as lower the energy scale $t \to -\infty$, the running eigenphase $\bar{\alpha}_j(t)$ moves towards its fixed point value $\alpha_j^*$ exponentially.

We may distinguish $2^N$ fixed points by the number of relevant parameters:

1. *$N$ relevant parameters (UV stable fixed point).*
   There is a ultraviolet stable fixed point at $(\alpha_1^*, \alpha_2^*, \cdots, \alpha_N^*) = (0, 0, \cdots, 0)$. At this point the unitary matrix becomes the identity matrix, $U = \sum_{j=1}^N P_j = \mathbb{1}$. Thus, by referring to the equation (2.7), we see that this fixed point corresponds to the Neumann boundary conditions at the vertex:

$$\psi_1'(0) = \psi_2'(0) = \cdots = \psi_N'(0) = 0. \tag{3.24}$$

2. *Zero relevant parameter (IR stable fixed point).*
   There is an infrared stable fixed point at $(\alpha_1^*, \alpha_2^*, \cdots, \alpha_N^*) = (\pi, \pi, \cdots, \pi)$. At this point the unitary matrix is $U = \sum_{j=1}^{N}(-1)P_j = -\mathbb{1}$. Thus, from Eq.(2.7) we see that this fixed point corresponds to the Dirichlet boundary conditions:
   $$\psi_1(0) = \psi_2(0) = \cdots = \psi_N(0) = 0. \tag{3.25}$$
   At this stage it should be noted that at the UV and IR fixed points the S-matrix becomes diagonal, which means that the vertex flows into a transmissionless infinite wall both in the UV and IR regimes. This is equivalent to the situation where the star graph with $N$ bonds splits into $N$ independent half-lines because particles cannot penetrate through the vertex at those fixed points. This is one of the simplest example of *topology change* of space discussed in [39, 40].

3. *$n$ relevant parameters with $0 < n < N$.*
   There are $\binom{N}{n} = \frac{N!}{n!(N-n)!}$ fixed points at which they have $n$ relevant directions. To be precise, let us consider a fixed point $(\alpha_1^*, \cdots, \alpha_n^*, \alpha_{n+1}^*, \cdots, \alpha_N^*) = (0, \cdots, 0, \pi, \cdots, \pi)$. At this point the unitary matrix becomes $U = \sum_{j=1}^{n} P_j - \sum_{j=n+1}^{N} P_j = \mathbb{1}_N - 2\sum_{j=n+1}^{N} P_j$. This fixed point corresponds to the following $N$ independent boundary conditions
   $$P_j\vec{\Psi}'(0) = 0, \quad j = 1, \cdots, n, \tag{3.26a}$$
   $$P_j\vec{\Psi}(0) = 0, \quad j = n+1, \cdots, N. \tag{3.26b}$$

## 3.3 Examples

As explicit examples, in the subsequent sections we will study the renormalization group flow of $U(2)$ and $U(3)$ family of point interactions. We also study the boundary conditions realized at the fixed points for the case of $U(2)$.

### 3.3.1 I-junction

As an explicit example let us first consider the case $N = 2$, i.e. the I-junction of two quantum wires at the origin, which is just the line $\mathbb{R}$ (see Figure 2.4). The vertex of I-junction is known to admit the $U(2)$ family of point interactions and there exist the following $2^2 = 4$ distinct fixed points (see Figure 3.3):

$$(\alpha_1^*, \alpha_2^*) = \begin{cases} (0,0): & S = U = \mathbb{1}_2, \\ (\pi,0): & S = U = -P_1 + P_2 = \mathbb{1}_2 - 2P_1, \\ (0,\pi): & S = U = P_1 - P_2 = -\mathbb{1}_2 + 2P_1, \\ (\pi,\pi): & S = U = -\mathbb{1}_2. \end{cases} \tag{3.27}$$

Conformal field theories on these fixed points are discussed by various authors; see, for example, ref. [41, 42]. The exact RG flow of I-junction is depicted in Figure 3.3. According to the discussion given in section 2.3, there exist the following three distinct phases:

(i) zero bound state phase: $(\pi, \pi) < (\alpha_1, \alpha_2) < (2\pi, 2\pi)$,

(ii) single bound state phase: $(\pi, 0) < (\alpha_1, \alpha_2) < (2\pi, \pi)$,
$(0, \pi) < (\alpha_1, \alpha_2) < (\pi, 2\pi)$,

(iii) two bound states phase: $(0, 0) < (\alpha_1, \alpha_2) < (\pi, \pi)$,

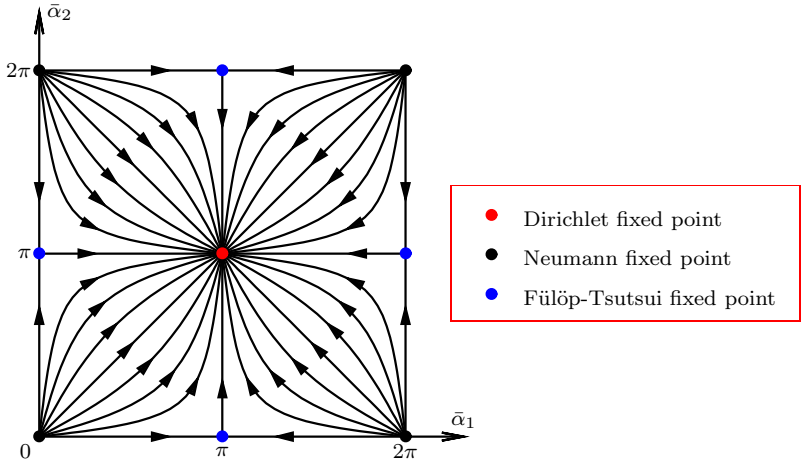


Figure 3.3: Exact RG flow of $(\alpha_1, \alpha_2)$. Arrows denote the directions toward infrared.

where we have assumed $L_0 > 0$.

Let us next study the boundary conditions at the fixed points by parameterizing the projection operators explicitly. There are various ways of parameterizing the projection operators (2.9a) and (2.9b). In this chapter we will use the following convention

$$\vec{e} = (\sin\theta\cos\phi, \sin\theta\sin\phi, \cos\theta)^T, \quad 0 \le \theta < 2\pi, \quad 0 \le \phi \le \pi, \tag{3.28}$$

so that the projection operator becomes

$$P_1 = \frac{1}{2}\begin{pmatrix} 1+\cos\theta & \mathrm{e}^{-i\phi}\sin\theta \\ \mathrm{e}^{i\phi}\sin\theta & 1-\cos\theta \end{pmatrix} = \begin{pmatrix} \cos^2\frac{\theta}{2} & \mathrm{e}^{-i\phi}\sin\frac{\theta}{2}\cos\frac{\theta}{2} \\ \mathrm{e}^{i\phi}\sin\frac{\theta}{2}\cos\frac{\theta}{2} & \sin^2\frac{\theta}{2} \end{pmatrix}, \tag{3.29a}$$

$$P_2 = \frac{1}{2}\begin{pmatrix} 1-\cos\theta & -\mathrm{e}^{-i\phi}\sin\theta \\ -\mathrm{e}^{i\phi}\sin\phi & 1+\cos\theta \end{pmatrix} = \begin{pmatrix} \sin^2\frac{\theta}{2} & -\mathrm{e}^{-i\phi}\sin\frac{\theta}{2}\cos\frac{\theta}{2} \\ -\mathrm{e}^{i\phi}\sin\frac{\theta}{2}\cos\frac{\theta}{2} & \cos^2\frac{\theta}{2} \end{pmatrix}. \tag{3.29b}$$

With this parameterization the boundary conditions at the fixed points $(\alpha_1^*, \alpha_2^*) = (\pi, 0)$ and $(0, \pi)$ are given by

$$(\alpha_1^*, \alpha_2^*) = (\pi, 0) : \begin{cases} \cos\frac{\theta}{2}\psi_1(0) + \mathrm{e}^{-i\phi}\sin\frac{\theta}{2}\psi_2(0) = 0, \\ \sin\frac{\theta}{2}\psi_1'(0) - \mathrm{e}^{-i\phi}\cos\frac{\theta}{2}\psi_2'(0) = 0, \end{cases} \tag{3.30a}$$

$$(\alpha_1^*, \alpha_2^*) = (0, \pi) : \begin{cases} \cos\frac{\theta}{2}\psi_1'(0) + \mathrm{e}^{-i\phi}\sin\frac{\theta}{2}\psi_2'(0) = 0, \\ \sin\frac{\theta}{2}\psi_1(0) - \mathrm{e}^{-i\phi}\cos\frac{\theta}{2}\psi_2(0) = 0. \end{cases} \tag{3.30b}$$

These are boundary conditions first discovered by Fülöp and Tsutsui [18]. Notice that when $\theta = \pi$ Eq.(3.30a) boils down to the Neumann-Dirichlet boundary conditions $\psi_1'(0) = 0 = \psi_2(0)$, whereas when $\theta = 0$ it becomes the Dirichlet-Neumann boundary conditions $\psi_1(0) = 0 = \psi_2'(0)$ $(\psi_1'(0) = 0 = \psi_2(0))$. The case $\theta = \pi/2$ and $\phi = \pi$ corresponds to the "free theory", $\psi_1(0) - \psi_2(0) = 0$ and $\psi_1'(0) + \psi_2'(0) = 0$, and the case $\phi = \pi$ corresponds to the system described by the $\delta'$ potential $V(x) = 2\frac{1+\tan(\theta/2)}{1-\tan(\theta/2)}\delta'(x)$.

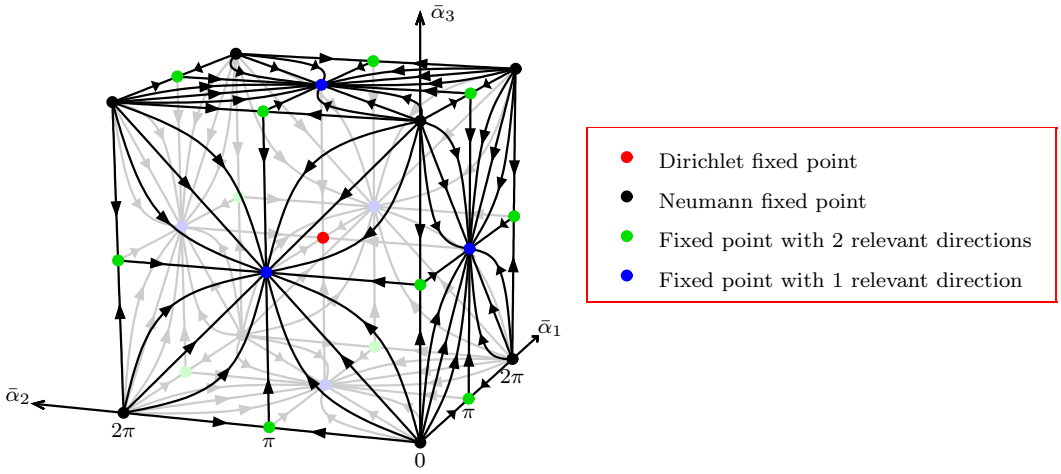


Figure 3.4: Exact RG flow of $(\alpha_1, \alpha_2, \alpha_3)$. Arrows denote the directions toward infrared.

### 3.3.2 Y-junction

As a next example let us consider the case $N = 3$, i.e. the Y-junction of three quantum wires at the origin (see Figure 2.5). The Y-junction of three quantum wires has been vastly studied in the literature [43–45] as the simplest topological space which is not manifold. The vertex of Y-junction is known to admit the $U(3)$ family of point interactions and there exist the following $2^3 = 8$ distinct fixed points:

$$(\alpha_1^*, \alpha_2^*, \alpha_3^*) = \begin{cases} (0,0,0): & S = U = \mathbb{1}_3, \\ (\pi,0,0): & S = U = -P_1 + P_2 + P_3 = \mathbb{1}_3 - 2P_1, \\ (0,\pi,0): & S = U = P_1 - P_2 + P_3 = \mathbb{1}_3 - 2P_2, \\ (0,0,\pi): & S = U = P_1 + P_2 - P_3 = \mathbb{1}_3 - 2P_3, \\ (0,\pi,\pi): & S = U = P_1 - P_2 - P_3 = -\mathbb{1}_3 + 2P_1, \\ (\pi,0,\pi): & S = U = -P_1 + P_2 - P_3 = -\mathbb{1}_3 + 2P_2, \\ (\pi,\pi,0): & S = U = -P_1 - P_2 + P_3 = -\mathbb{1}_3 + 2P_3, \\ (\pi,\pi,\pi): & S = U = -\mathbb{1}_3. \end{cases} \tag{3.31}$$

The exact RG flow of Y-junction is depicted in Figure 3.4, which is consistent with those obtained in [45]. According to the discussion given in section 2.3, there exist the following four distinct phases:

(i) zero bound state phase: $(\pi,\pi,\pi) < (\alpha_1,\alpha_2,\alpha_3) < (2\pi,2\pi,2\pi)$,

(ii) single bound state phase: $(\pi,\pi,0) < (\alpha_1,\alpha_2,\alpha_3) < (2\pi,2\pi,0)$,
$(\pi,0,\pi) < (\alpha_1,\alpha_2,\alpha_3) < (2\pi,\pi,2\pi)$,
$(0,\pi,\pi) < (\alpha_1,\alpha_2,\alpha_3) < (\pi,2\pi,2\pi)$,

(iii) two bound states phase: $(\pi,0,0) < (\alpha_1,\alpha_2,\alpha_3) < (2\pi,\pi,\pi)$,
$(0,\pi,0) < (\alpha_1,\alpha_2,\alpha_3) < (\pi,2\pi,\pi)$,
$(0,0,\pi) < (\alpha_1,\alpha_2,\alpha_3) < (\pi,\pi,2\pi)$,

(iv) three bound states phase: $(0,0,0) < (\alpha_1,\alpha_2,\alpha_3) < (\pi,\pi,\pi)$,

where we have assumed $L_0 > 0$.

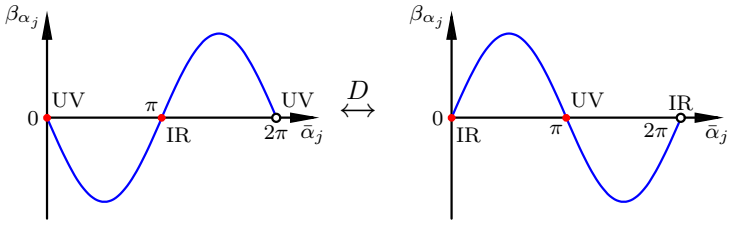


Figure 3.5: $\beta$-function flip. UV and IR fixed points are interchanged.

## 3.4 Duality

In this section we briefly discuss the UV/IR duality transformation which interchanges the UV and IR fixed points as depicted in Figure 3.5. As discussed in section 2.3, such a transformation can be expressed as

$$D : \bar{\alpha}_j \mapsto \begin{cases} \bar{\alpha}_j + \pi, & \text{for } 0 \leq \alpha_j < \pi, \\ \bar{\alpha}_j - \pi, & \text{for } \pi \leq \alpha_j < 2\pi, \end{cases} \tag{3.32}$$

which acts on $\cot(\bar{\alpha}_j/2)$ as

$$\cot \frac{\bar{\alpha}_j}{2} \overset{D}{\mapsto} \cot\left(\frac{\bar{\alpha}_j}{2} \pm \frac{\pi}{2}\right) = -\tan \frac{\bar{\alpha}_j}{2}, \tag{3.33}$$

and on the S-matrix as

$$S(kL_0; \alpha_j, e_j^a) \overset{D}{\mapsto} -S((kL_0)^{-1}; \alpha_j, e_j^a). \tag{3.34}$$

In summary, the duality consists of the following:

- *High energy/low energy scattering duality.*
  Scattering process in high energy regime ($|kL_j| > 1$) of the system characterized by the parameters $\{\alpha_j, e_j\}$ is dual to low energy regime ($|kL_j| < 1$) of that characterized by $\{\alpha_j \pm \pi, e_j\}$.

- *Bound state/antibound state duality.*
  Under the duality transformation a simple pole of $S(kL_0)$ lying on the imaginary $k$-axis changes its sign, which means that it exchanges a normalizable bound state and a non-normalizable antibound state.

## 3.5 Conclusions and discussions

In this chapter we have studied the renormalization group flow of $U(N)$ family of point interactions at the vertex of star graph. We have found that in a star graph with $N$ bonds there exist $2^N$ distinct fixed points, where the scale-independent point interactions are realized. We believe that this result strongly suggests that there exist $2^N$ types of universality classes of short ranged scatters in one spatial dimension: any short ranged interaction must flow to one of these $2^N$ fixed points in the long-wavelength limit.

# Chapter 4

# Path integral with point interaction

In this chapter we study a particle propagation on an $N$-petal rose in the presence of a point interaction at the vertex. We show that the one-particle Feynman kernel can be written into the sum of reflected and transmitted trajectories which are weighted by the elements of the $n$th power of a certain $2N \times 2N$ unitary matrix composed of the S-matrix $S(kL_0)$ evaluated on a star graph with $2N$ bonds and the so-called bond propagation matrix.

## 4.1 Introduction

Mathematically, the correct framework to treat the boundary conditions in quantum theory is by means of the analysis of von Neumann's self-adjoint extension of Hamiltonian operator [46]. The analysis of self-adjoint extension of the Hamiltonian operator, as the name suggests, is essentially based on the Hamiltonian operator approach. However, in the Feynman's path integral approach, we do not know *a priori* how to incorporate the boundary conditions into the integration measure nor into the path integral weight. As discussed in many textbooks (see for example [47, 48]), the naive path integral representation for a system on a bounded domain leads to a wrong boundary behavior and hence requires modification. The most rigorous way to incorporate the boundary conditions into the Feynman kernel is to evaluate it by the operator formalism. However, the kernel evaluated by the operator formalism becomes the summation over the energy spectrum. In order to switch to the path integral description, we have to perform resummation of the energy spectrum to the paths of the space. In general, this resummation is accomplished by *trace formulae*. Trace formulae provide a direct connection between quantum energy spectrum and classical length spectrum (periodic orbits). However, this connection is in general an asymptotic relation valid for large wave numbers, just as in the case of the Gutzwiller trace formula [49]. There are only few cases where the trace formulae become identities. Noteworthy among these are the Poisson summation formula and the Selberg trace formula [50], the former is the trace formula for the Laplace operator on flat tori and the latter on Riemannian manifolds with constant negative curvature.

Although in the operator formalism point interactions have been extensively discussed in the literature, the path-integral description of point interactions has not yet been fully understood. The aim of this chapter is to fulfill a gap of the description for boundary conditions between the operator formalism and the path integral formalism: we would like

to propose a physically transparent prescription how to incorporate the boundary conditions obtained in the operator formalism into the path integral description. To illustrate our idea in a simple setting, in this introductory section let us first consider a quantum particle on a circle of circumference $\ell$ in the presence of a $\delta'$-interaction described by the Hamiltonian $H = -\mathrm{d}^2/\mathrm{d}x^2 + 2c\delta'(x)$, where $c \in \mathbb{R}$ is the dimensionless coupling constant and prime ($\prime$) indicates the derivative with respect to $x$. It is known that the $\delta'$-interaction belongs to the so-called scale-independent subfamily of point interactions [16] and is verified by the boundary conditions $\psi(\ell) = [(1-c)/(1+c)]\psi(0)$ and $\psi'(\ell) = [(1+c)/(1-c)]\psi'(0)$ [51,52], where $\psi$ is the square integrable wave function on an interval $(0,\ell)$. Although the Feynman kernel of this system has been analyzed in the literature [15,18], the physical interpretation for the weight factors (see below) remains open. We would like to first address this issue.

As ubiquitous in the scale-independent point interactions, in this $\delta'$-interaction case the wave numbers are quantized in an integer step so that it is easy to rewrite the Feynman kernel $\langle x'|\mathrm{e}^{-iHT}|x\rangle$ evaluated in the operator formalism into the path integral description with the help of the Poisson summation formula. The resultant kernel takes the form

$$\langle x'|\mathrm{e}^{-iHT}|x\rangle = \frac{1}{\sqrt{4\pi iT}}\sum_{n\in\mathbb{Z}}\left\{\cos(n\theta)\mathrm{e}^{i\frac{T}{4}\left(\frac{n\ell+x'-x}{T}\right)^2} \mp \sin(n\theta)\mathrm{e}^{i\frac{T}{4}\left(\frac{n\ell+(\ell-x')-x}{T}\right)^2}\right\}, \qquad (4.1)$$

where $0 \le \theta := \mathrm{Arccos}[(1-c^2)/(1+c^2)] < \pi$ and $-$ $(+)$ sign for $c > 0$ $(c < 0)$. Arccos is the principal value of the inverse cosine. Notice that the presence of a point interaction breaks the global translational invariance. As a consequence the kernel (4.1) is the sum of partial amplitudes for the translational invariant and variant classes of trajectories, which are weighted by the factors $\cos(n\theta)$ and $\sin(n\theta)$ respectively.

Before going to discuss the physical meaning of the weight factors, we have to reveal the particle propagations described by (4.1). To this end, it should first be noted that $c = 0$ leads to $\theta = 0$ so that Eq.(4.1) becomes the well-known form of the one-particle Feynman kernel on a circle with periodic boundary conditions. As discussed in many textbooks (see for example Ref. [47,48]), in this $c = 0$ case the kernel (4.1) is the sum of partial amplitudes for transitions via classical paths distinguished by the homotopy class of $S^1$, i.e., the winding number. For nonzero $c$, however, the classical trajectories of a particle are not so trivial due to the presence of $\delta'$-potential, which acts as a point scatterer. When a particle reaches to the position of the point scatterer, there must be in general two possibilities: reflection or transmission. Thus the paths for a particle interacting $n$-times to the point interaction must consist of $2\times 2^n$ distinct paths, where the first factor 2 is due to the initial particle's momentum directions, i.e. clockwise or counterclockwise directions. Notice that the clockwise direction corresponds to $n > 0$ in (4.1) and the counterclockwise $n < 0$. As an example the classical world lines for $n = 2$ and $-2$ in (4.1) are depicted in Figure 4.1. As we will see below, the half of these $2\times 2^n$ paths belongs to the translational invariant class and the other half of them to the translational variant class.

Now it is time to discuss the physical meaning of the weight factors. It is intuitively clear that reflected trajectory should be weighted with a reflection coefficient $R_2$ ($R_1$) for every time when a particle is reflected by the point scatterer from left to left (right to right), where $R_2$ ($R_1$) is the reflection coefficient for a particle propagating the 2nd half-line $x_2 \in \mathbb{R}_+$ (1st half-line $x_1 \in \mathbb{R}_+$) in the system of I-junction of two half-lines (see Figure 2.4). Similarly, transmitted trajectory should be weighted with a transmission coefficient $T_{12}$ ($T_{21}$) for every time when a particle is transmitted by the point scatterer from left to right (right to left), where $T_{12}$ ($T_{21}$) is the transmission coefficient for a particle propagating

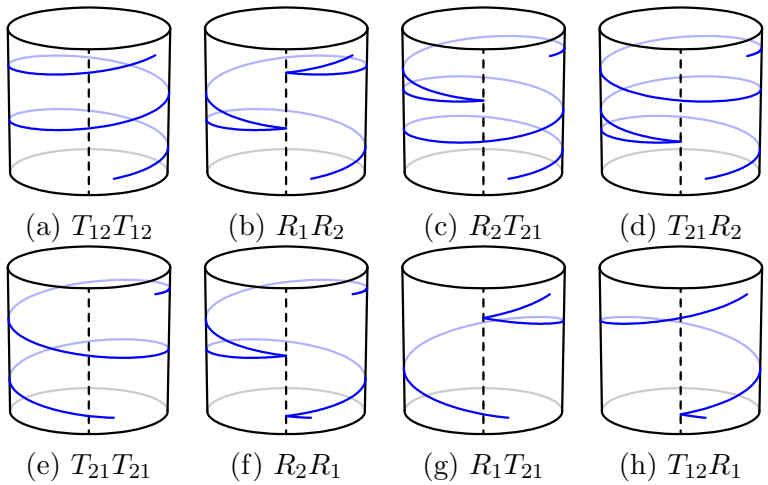

(a) $T_{12}T_{12}$ (b) $R_1R_2$ (c) $R_2T_{21}$ (d) $T_{21}R_2$

(e) $T_{21}T_{21}$ (f) $R_2R_1$ (g) $R_1T_{21}$ (h) $T_{12}R_1$

Figure 4.1: Classical worldlines for a particle scattered twice by the point interaction. Time is flowing along the vertical direction. Dashed lines represent the worldlines for the point interaction.

from the 2nd half-line to the 1st half-line and vice versa. The physical meaning of the weight factors is now obvious: these must be elements of the $n$th power of the matrix $\left(\begin{smallmatrix} R_1 & T_{12} \\ T_{21} & R_2 \end{smallmatrix}\right)$, which is given by $S\sigma_1$ with $S$ being the (scale-independent) S-matrix for a system on a I-junction of two half-lines introduced in chapter 2. In the case of $\delta'$-interaction, it is easy to compute the one-particle S-matrix with the result

$$S\sigma_1 = \begin{pmatrix} T_{12} & R_1 \\ R_2 & T_{21} \end{pmatrix} = \begin{cases} \begin{pmatrix} \cos\theta & \sin\theta \\ -\sin\theta & \cos\theta \end{pmatrix}, & \text{for } c > 0, \\ \begin{pmatrix} \cos\theta & -\sin\theta \\ \sin\theta & \cos\theta \end{pmatrix}, & \text{for } c < 0, \end{cases} \tag{4.2}$$

which is just the rotational matrix. The $n$th power of $S\sigma_1$ is thus given by just replacing the argument $\theta$ in (4.2) to $n\theta$. These matrix elements are nothing but the weight factors in (4.1). In this sense the identity $\cos^2(n\theta) + \sin^2(n\theta) = 1$ is a consequence of the unitarity of the S-matrix.

So far we have studied only the case of $\delta'$-interaction, in Ref. [53] we have shown that the above discussion is valid for any one-particle quantum mechanics on a circle even in the presence of a $U(2)$ family of point interaction and derived the most general formula for the one-particle Feynman kernel.

The purpose of this chapter is to extend the analysis given in [53] to a system on a rose graph as depicted in Figure 4.2. The reason why we consider a rose graph is due to its *topology change*, which will be discussed in great detail at the end of this chapter.

Similarly to the star graph with $N$ bonds, on a rose graph with $N$ petals the boundary conditions at the vertex consistent with the Kirchhoff's law of the probability current density, $\sum_{j=1}^{N} j_j(0_j) = \sum_{j=1}^{N} j_j(\ell_j)$, takes the following form

$$\vec{\Psi}(0) - iL_0\vec{\Psi}'(0) = U\big[\vec{\Psi}(0) + iL_0\vec{\Psi}'(0)\big], \quad U \in U(2N), \tag{4.3}$$

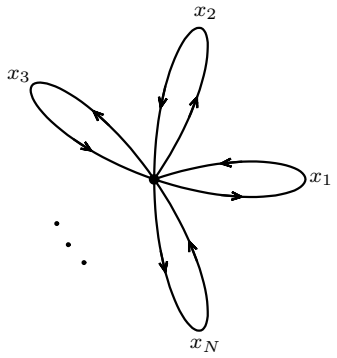


Figure 4.2: $N$-petal rose. Each petal is numbered counterclockwise and introduced a coordinate $x_j \in (0_j, \ell_j)$, $j = 1, 2, \cdots, N$. The vertex is located at $x_j = 0_j = \ell_j$, $j = 1, 2, \cdots, N$.

where $\vec{\Psi}$ and its derivative $\vec{\Psi}'$ are $2N$-component column vectors defined by

$$\vec{\Psi}(x_1, \cdots, x_N) := (\psi_1(x_1), \psi_1(\ell_1 - x_1), \cdots, \psi_N(x_N), \psi_N(\ell_N - x_N))^T, \tag{4.4a}$$

$$\vec{\Psi}'(x_1, \cdots, x_N) := (\psi_1'(x_1), -\psi_1'(\ell_1 - x_1), \cdots, \psi_N'(x_N), -\psi_N'(\ell_N - x_N))^T, \tag{4.4b}$$

and $\vec{\Psi}(0)$ and $\vec{\Psi}'(0)$ are shorthand notations for the boundary value vectors $\vec{\Psi}(0, \cdots, 0)$ and $\vec{\Psi}'(0, \cdots, 0)$. Making use of these boundary value vectors and the spectral decomposition of $U \in U(2N)$ given in (2.8a) (with the replacement $N \to 2N$), we immediately see that the boundary condition (4.3) boils down to the following form

$$P_j\big[\vec{\Psi}(0) + L_j\vec{\Psi}'(0)\big] = \vec{0}, \quad j = 1, 2, \cdots, 2N. \tag{4.5}$$

The rest of this chapter is organized as follows. In section 4.2 we define one-particle quantum mechanics on a rose graph with $N$ petals. Section 4.2.1 is devoted to detailed analysis of the spectral property for the free Hamiltonian (i.e. Laplace operator) on a rose graph. We also study exact trace formulae which provide a direct connection between quantum energy spectrum and classical length spectrum of rose graph with $U(2N)$ family of point interaction at the vertex. These can be regarded as generalizations of the Poisson summation formula. In section 4.3 we derive the general formulae for the path integral description of the Feynman kernel on a rose graph. In section 4.4 we present explicit examples of the Feynman kernels for several subfamilies of $U(2)$ and $U(4)$ family of point interactions. Section 4.5 is devoted to conclusions and discussions.

## 4.2 Quantum particle on a rose

In this section we analyze quantum dynamics of a free particle on a rose graph that consists of $N$ petals and a single vertex. Each petal is numbered counterclockwise and assigned a coordinate $x_j \in (0_j, \ell_j)$, where $\ell_j$ is a length of the $j$th petal (see Figure 4.2). $x_j = 0_j$ and $x_j = \ell_j$ ($j = 1, 2 \cdots, N$) are assumed to be the same vertex point. The purpose of this section is to illuminate the deep connection between scattering theory on the star graph with $2N$ bonds and the spectral property of the $N$-petal rose.

To this end let us first solve the Schrödinger equation $-(\mathrm{d}^2/\mathrm{d}x_j^2)\psi_j(x_j) = E\psi_j(x_j)$ ($j = 1, 2, \cdots, N$), where $\psi_j$ is a square integrable function on the $j$th petal. The general

solution to this equation for positive energy $E > 0$ is given by the linear combination of the plain waves

$$\psi_j(x_j;k) = A_j^+(k)\mathrm{e}^{ikx_j} + A_j^-(k)\mathrm{e}^{ik(\ell_j - x_j)}, \quad j = 1, 2, \cdots, N, \tag{4.6}$$

where $k = \sqrt{E} > 0$. Notice that the coefficients $A_j^+(k)$ and $A_j^-(k)$ may depend on $k$. The phase factor $\mathrm{e}^{ik\ell_j}$ in the second term is introduced for later convenience. By substituting (4.6) into (4.4a) and (4.4b) we find that the boundary value vectors take the forms

$$\vec{\Psi}(0) = \vec{A}(k) + \Sigma_1 \mathrm{e}^{ikL}\vec{A}(k), \tag{4.7a}$$

$$\vec{\Psi}'(0) = ik\big[\vec{A}(k) - \Sigma_1 \mathrm{e}^{ikL}\vec{A}(k)\big], \tag{4.7b}$$

where $\vec{A}(k)$ is a $2N$-component coefficient column vector defined by

$$\vec{A}(k) := \big(A_1^+(k), A_1^-(k), A_2^+(k), A_2^-(k), \cdots, A_N^+(k), A_N^-(k)\big)^T, \tag{4.8}$$

and $\Sigma_1$ and $L$ are $2N \times 2N$ matrices given by

$$\Sigma_1 := \begin{pmatrix} \sigma_1 & 0 & \cdots & 0 \\ 0 & \sigma_1 & \cdots & 0 \\ \vdots & \vdots & \ddots & \vdots \\ 0 & 0 & \cdots & \sigma_1 \end{pmatrix}, \quad L := \begin{pmatrix} \ell_1 \mathbb{1}_2 & 0 & \cdots & 0 \\ 0 & \ell_2 \mathbb{1}_2 & \cdots & 0 \\ \vdots & \vdots & \ddots & \vdots \\ 0 & 0 & \cdots & \ell_N \mathbb{1}_2 \end{pmatrix}. \tag{4.9}$$

In the literature [2], the diagonal unitary matrix $\mathrm{e}^{ikL} = \mathrm{diag}(\mathrm{e}^{ik\ell_1}\mathbb{1}_2, \mathrm{e}^{ik\ell_2}\mathbb{1}_2, \cdots, \mathrm{e}^{ik\ell_N}\mathbb{1}_2)$ is referred to as the *bond propagation matrix*. Substituting (4.7a) and (4.7b) into the boundary condition (4.5) we get

$$P_j\left(\mathbb{1}_{2N} - \frac{ikL_j - 1}{ikL_j + 1}\Sigma_1 \mathrm{e}^{ikL}\right)\vec{A}(k) = \vec{0}, \quad j = 1, 2, \cdots, 2N. \tag{4.10}$$

Since Eq.(4.10) for different $j$ is orthogonal to each other, it can be combined into the following compact form

$$\mathcal{U}(k)\vec{A}(k) = \vec{A}(k) \quad \text{with} \quad \mathcal{U}(k) := S(kL_0)\Sigma_1 \mathrm{e}^{ikL}, \tag{4.11}$$

which follows from $\sum_{j=1}^{2N} P_j = \mathbb{1}_{2N}$. $S(kL_0)$ is the S-matrix for a free particle on a star graph with $2N$ bonds given in Eq.(2.20). The eigenvalue equation (4.11) suggests that the energy spectrum and energy eigenfunctions on a rose is completely determined by the S-matrix $S(kL_0)$ and the bond propagation matrix $\mathrm{e}^{ikL}$, the former determines the local interaction at the vertex and the latter the global structure of the graph.

Before closing this section we here note that the unitary matrix $\mathcal{U}(k)$ satisfies the identity

$$\mathcal{U}^{-1}(k) = \mathrm{e}^{-ikL}\Sigma_1 \mathcal{U}(-k)\Sigma_1 \mathrm{e}^{ikL}, \tag{4.12}$$

which follows from $S^\dagger(kL_0) = S(-kL_0)$. As we will see in section 4.2.1 and 4.3 the identity (4.12) plays an important role for the analysis of spectrum and path integral description of the Feynman kernel.

In the subsequent sections, we will analyze the eigenvalue equation (4.11) in detail.

### 4.2.1 Spectrum and exact trace formula

Let us first study the positive energy spectrum on a rose. The positive energy spectrum is determined as the positive roots of the following secular equation

$$\zeta(k) = 0, \quad k > 0, \tag{4.13}$$

where

$$\zeta(k) := \det[\mathbb{1}_{2N} - \mathcal{U}(k)]. \tag{4.14}$$

Since the matrix $\mathcal{U}(k)$ is unitary, it can be written into the following spectral decomposition form:

$$\mathcal{U}(k) = \sum_{a=1}^{2N} \mathrm{e}^{i\vartheta_a(k)} \mathcal{P}_a(k), \tag{4.15}$$

where $\mathrm{e}^{i\vartheta_a(k)}$ is the $a$th eigenvalue and $\mathcal{P}_a(k)$ is the corresponding hermitian projection operator fulfilling $\sum_{a=1}^{2N} \mathcal{P}_a(k) = \mathbb{1}_{2N}$, $\mathcal{P}_a(k)\mathcal{P}_b(k) = \delta_{ab}\mathcal{P}_b(k)$ and $\mathcal{P}_a^\dagger(k) = \mathcal{P}_a(k)$. Then, the secular equation (4.13) reduces to the following quantization conditions

$$\mathrm{e}^{i\vartheta_a(k)} = 1, \quad a = 1, 2, \cdots, 2N. \tag{4.16}$$

In the following we denote the positive roots of (4.16) as $0 < k_{a,1} < k_{a,2} < \cdots < k_{a,m} < \cdots$. We here emphasize that Eq.(4.16) implies there exists a one-to-one correspondence between the spectral multiplicity (degeneracy) for positive energy eigenvalues of the free Hamiltonian on a rose and the eigenvalue multiplicity (degeneracy) of the unitary matrix $\mathcal{U}(k)$: If two eigenvalues $\mathrm{e}^{i\vartheta_a(k)}$ and $\mathrm{e}^{i\vartheta_b(k)}$ are degenerate, then two sets of roots $\{k_{a,m}\}_{m=1}^\infty$ and $\{k_{b,m}\}_{m=1}^\infty$ are happened to be the same. It should also be emphasized that the following relation holds

$$\zeta(-k) = \det[\mathbb{1}_{2N} - \mathcal{U}^\dagger(k)] = \prod_{a=1}^{2N} \left[1 - \mathrm{e}^{-i\vartheta_a(k)}\right], \tag{4.17}$$

which follows from the identity (4.12). Note that Eq.(4.17) implies real roots of the equation $\zeta(k) = 0$ ($k \in \mathbb{R} \setminus \{0\}$) are symmetrically distributed on the real $k$-axis, although $\mathrm{e}^{i\vartheta_a(-k)}$ does not coincide with $\mathrm{e}^{-i\vartheta_a(k)}$ in general.

Next investigate the trace formula for a rose graph with general point interaction at the vertex, first given by Bolte and Endres [10]. To this end we start with the following contour integral

$$I = \oint_{C_\epsilon} \frac{\mathrm{d}k}{2\pi i}\, h(k) \frac{\mathrm{d}}{\mathrm{d}k} \log \zeta(k), \tag{4.18}$$

where $h(k)$ is a smooth test function that satisfies $h(-k) = h(k)$ and appropriately converges at infinity. The integration contour $C_\epsilon$ is depicted in Figure 4.3, where we have rearranged the numbering of the positive roots of the secular equation (4.13) as $\{0 < k_1 < k_2 < \cdots < k_m < \cdots\}$.

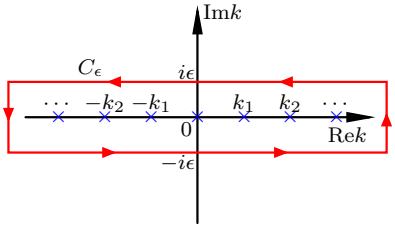


Figure 4.3: Integration contour $C_\epsilon$ and distribution of non-negative spectrum.

Note that with this notation $k_m$ may be multiply degenerate with multiplicity $g_m$ when the corresponding eigenvalue of $\mathcal{U}(k)$ is multiply degenerate with multiplicity $g_m$.

Let us next evaluate the integral (4.18). When $h(k-i\epsilon) = h(k+i\epsilon)$, i.e. the test function does not exhibit any discontinuity across the real $k$-axis, the integral (4.18) can then be written as follows:

$$I = \lim_{\epsilon\to 0_+} \int_{-\infty}^{\infty} \frac{\mathrm{d}k}{2\pi i}\, h(k) \left\{ \left(\frac{\mathrm{d}}{\mathrm{d}k}\log\zeta\right)(k-i\epsilon) - \left(\frac{\mathrm{d}}{\mathrm{d}k}\log\zeta\right)(k+i\epsilon) \right\}. \tag{4.19}$$

In order to compute this integral correctly, we have to carefully evaluate the discontinuity of $(\mathrm{d}\log\zeta/\mathrm{d}k)$ across the real $k$-axis. To this end, we first note that since $\mathcal{U}(k)$ is a meromorphic function of $k$, it can be analytically continued to the entire complex $k$-plain such that $\zeta(k)$ is also meromorphic on the entire complex $k$-plain. Thus in the neighborhood of the root $k = k_m$, whose multiplicity is $g_m$, we can expand $\zeta(k)$ into the following power series:

$$\zeta(k) = (k-k_m)^{g_m}[c_0 + c_1(k-k_m) + c_2(k-k_m)^2 + \cdots], \tag{4.20}$$

from which we obtain

$$\frac{\mathrm{d}}{\mathrm{d}k}\log\zeta(k) = \frac{\zeta'(k)}{\zeta(k)} = \frac{g_m}{k-k_m} + (\text{regular}). \tag{4.21}$$

Hence in the neighborhood of $k = k_m$, we find the following discontinuity

$$\left(\frac{\mathrm{d}}{\mathrm{d}k}\log\zeta\right)(k-i\epsilon) - \left(\frac{\mathrm{d}}{\mathrm{d}k}\log\zeta\right)(k+i\epsilon) = i2\pi g_m \delta(k-k_m), \tag{4.22}$$

which follows from the identity $1/(x\pm i\epsilon) = \mathcal{P}/x \mp i\pi\delta(x)$ with $\mathcal{P}$ standing for the principal value. Thus, except for the zero-mode, the integral (4.19) over the whole real $k$-axis picks up every positive energy eigenvalue correctly with *twice* of the spectral multiplicity (twice because the real roots of $\zeta(k) = 0$ is symmetrically distributed on the real $k$-axis):

$$I = \tilde{g}_0 h(0) + 2\sum_{m>0} g_m h(k_m), \tag{4.23}$$

where we have used $g_{-m} = g_m$, $k_{-m} = -k_m$ and $h(-k_m) = h(k_m)$. $\tilde{g}_0$ is the multiplicity for the vanishing root $k = 0$ of the secular equation (4.13) (known as the *algebraic multiplicity*) and given by the number of eigenvalue $+1$ of the unitary matrix $\mathcal{U}(0) = S(0)\Sigma_1$. It should be emphasized that $\tilde{g}_0$ does not coincide in general with the true spectral multiplicity for the zero energy eigenvalue solutions [10, 54].

Next re-evaluate the integral (4.19) in another way in terms of the eigenvalue of $\mathcal{U}(k)$. Since $\zeta(k) = \prod_{a=1}^{2N}[1 - \mathrm{e}^{i\vartheta_a(k)}]$ we have

$$\begin{aligned}
&\left(\frac{\mathrm{d}}{\mathrm{d}k}\log\zeta\right)(k-i\epsilon) - \left(\frac{\mathrm{d}}{\mathrm{d}k}\log\zeta\right)(k+i\epsilon) \\
&= -i\sum_{a=1}^{2N}\left(\frac{\mathrm{d}\vartheta_a}{\mathrm{d}k}\frac{\mathrm{e}^{i\vartheta_a}}{1-\mathrm{e}^{i\vartheta_a}}\right)(k-i\epsilon) + i\sum_{a=1}^{2N}\left(\frac{\mathrm{d}\vartheta_a}{\mathrm{d}k}\frac{\mathrm{e}^{i\vartheta_a}}{1-\mathrm{e}^{i\vartheta_a}}\right)(k+i\epsilon).
\end{aligned} \tag{4.24}$$

Again we have to carefully evaluate the discontinuity of (4.24) across the real $k$-axis. To this end we first note that $\mathrm{e}^{i\vartheta_a}/(1-\mathrm{e}^{i\vartheta_a}) = -1/(1-\mathrm{e}^{-i\vartheta_a})$ and further

$$\left|\exp\left[i\vartheta_a(k\pm i\epsilon)\right]\right| = \left|\exp\left[i\vartheta_a(k) \mp \epsilon\frac{\mathrm{d}\vartheta_a}{\mathrm{d}k}(k)\right] + O(\epsilon^2)\right| < 1, \tag{4.25a}$$

for $k+i\epsilon$ with $(\mathrm{d}\vartheta_a/\mathrm{d}k)(k)>0$ or $k-i\epsilon$ with $(\mathrm{d}\vartheta_a/\mathrm{d}k)(k)<0$, and

$$\left|\exp\left[-i\vartheta_a(k\pm i\epsilon)\right]\right| = \left|\exp\left[-i\vartheta_a(k)\pm\epsilon\frac{\mathrm{d}\vartheta_a}{\mathrm{d}k}(k)\right]+O(\epsilon^2)\right|<1, \tag{4.25b}$$

for $k-i\epsilon$ with $(\mathrm{d}\vartheta_a/\mathrm{d}k)(k)>0$ or $k+i\epsilon$ with $(\mathrm{d}\vartheta_a/\mathrm{d}k)(k)<0$. By taking these facts into account we can express the discontinuity (4.24) in terms of power series of the eigenvalue $\mathrm{e}^{i\vartheta_a}$. For example, for the case of $(\mathrm{d}\vartheta_a/\mathrm{d}k)(k)>0$, we have

$$\begin{aligned}(4.24) &= i\sum_{a=1}^{2N}\left(\frac{\mathrm{d}\vartheta_a}{\mathrm{d}k}\frac{1}{1-\mathrm{e}^{-i\vartheta_a}}\right)(k-i\epsilon) - i\sum_{a=1}^{2N}\left(\frac{\mathrm{d}\vartheta_a}{\mathrm{d}k}\frac{\mathrm{e}^{i\vartheta_a}}{1-\mathrm{e}^{i\vartheta_a}}\right)(k+i\epsilon)\\ &= i\sum_{a=1}^{2N}\left(\frac{\mathrm{d}\vartheta_a}{\mathrm{d}k}\sum_{n=0}^{\infty}\mathrm{e}^{-in\vartheta_a}\right)(k-i\epsilon) + i\sum_{a=1}^{2N}\left(\frac{\mathrm{d}\vartheta_a}{\mathrm{d}k}\sum_{n=1}^{\infty}\mathrm{e}^{in\vartheta_a}\right)(k+i\epsilon)\\ &= i\sum_{a=1}^{2N}\frac{\mathrm{d}\vartheta_a}{\mathrm{d}k}(k)\sum_{n\in\mathbb{Z}}\mathrm{e}^{in\vartheta_a}.\end{aligned} \tag{4.26a}$$

Similar analysis shows that for the case of $(\mathrm{d}\vartheta_a/\mathrm{d}k)(k)<0$ the discontinuity (4.24) across the real $k$-axis can be expressed as follows:

$$(4.24) = i\sum_{a=1}^{2N}\left[-\frac{\mathrm{d}\vartheta_a}{\mathrm{d}k}(k)\right]\sum_{n\in\mathbb{Z}}\mathrm{e}^{in\vartheta_a(k)}, \tag{4.26b}$$

from which we conclude that irrespective of the sign of the derivative $\mathrm{d}\vartheta_a/\mathrm{d}k$, the integral (4.19) can be written as follows:

$$I = \sum_{a=1}^{2N}\sum_{n\in\mathbb{Z}}\int_{-\infty}^{\infty}\frac{\mathrm{d}k}{2\pi}\left|\frac{\mathrm{d}\vartheta_a}{\mathrm{d}k}(k)\right|h(k)\mathrm{e}^{in\vartheta_a(k)}. \tag{4.27}$$

Combining the results (4.23) and (4.27) we finally obtain the following summation formulae

$$\sum_{m>0}g_m h(k_m) = -\frac{\tilde{g}_0}{2}h(0)+\frac{1}{2}\sum_{a=1}^{2N}\sum_{n\in\mathbb{Z}}\int_{-\infty}^{\infty}\frac{\mathrm{d}k}{2\pi}\left|\frac{\mathrm{d}\vartheta_a}{\mathrm{d}k}(k)\right|h(k)\mathrm{e}^{in\vartheta_a(k)}, \tag{4.28}$$

which is the *exact trace formulae* on a rose graph with $U(N)$ family of point interaction at the vertex.

Before closing this section let us take another (yet equivalent) look to the trace formulae by focusing on the periodicity of the eigenphases and give a shortcut derivation of the result (4.28). To this end let us consider a delta function $\sum_{q\in\mathbb{Z}}\delta(\vartheta_a(k)-2\pi q)$. This is a periodic function of $\vartheta_a(k)$ with period $2\pi$ so that it can be expanded into the Fourier series

$$\sum_{q\in\mathbb{Z}}\delta(\vartheta_a(k)-2\pi q) = \frac{1}{2\pi}\sum_{n\in\mathbb{Z}}\mathrm{e}^{in\vartheta_a(k)}, \tag{4.29}$$

from which we find

$$\left|\frac{\mathrm{d}\vartheta_a}{\mathrm{d}k}(k)\right|^{-1}\sum_{m\in\mathbb{Z}}\delta(k-k_{a,m}) = \frac{1}{2\pi}\sum_{n\in\mathbb{Z}}\mathrm{e}^{in\vartheta_a(k)}, \tag{4.30}$$

where $k_{a,m}$ for $m < 0$ is a negative root of the condition (4.16). Multiplying $|(\mathrm{d}\vartheta_a/\mathrm{d}k)(k)|$ and an appropriate test even function $h(k)$ on the both hand sides and then integrating over the range $-\infty < k < \infty$, we get the following summation formula

$$\sum_{m\in\mathbb{Z}} h(k_{a,m}) = \sum_{n\in\mathbb{Z}} \int_{-\infty}^{\infty} \frac{\mathrm{d}k}{2\pi} \left|\frac{\mathrm{d}\vartheta_a}{\mathrm{d}k}(k)\right| h(k)\mathrm{e}^{in\vartheta_a(k)}. \tag{4.31}$$

Notice that $k_{a,-m}$ does not necessarily coincide with $-k_{a,m}$ such that $h(k_{a,-m}) \neq h(k_{a,m})$ in general. However, by taking the summation over the index $a$ and noting the relation $\sum_{a=1}^{2N}\sum_{m\in\mathbb{Z}} h(k_{a,m}) = \sum_{a=1}^{2N}\sum_{m\in\mathbb{Z}} g_m h(k_m)$ we immediately recover the formula (4.28).

### 4.2.2 Normalization condition

In this subsection we study the normalization condition of an energy eigenfunction on an $N$-petal rose. As noted in section 4.2, the energy eigenfunction is completely determined by the eigenvalue and the eigenvector of the unitary matrix $\mathcal{U}(k)$. To see this, let $\vec{A}_a(k) = (A^+_{1,a}(k), A^-_{1,a}(k), \cdots, A^+_{N,a}(k), A^-_{N,a}(k))^T$ be an (unnormalized) orthogonal eigenvector of $\mathcal{U}(k)$ corresponding to the eigenvalue $\mathrm{e}^{i\vartheta_a(k)}$. Then the (unnormalized) energy eigenfunction (4.6) corresponding to the root $k = k_{a,m} > 0$ of (4.16) is given by

$$\psi_{j,a}(x_j; k_{a,m}) = A^+_{j,a}(k_{a,m})\mathrm{e}^{ik_{a,m}x_j} + A^-_{j,a}(k_{a,m})\mathrm{e}^{ik_{a,m}(l_j - xj)}. \tag{4.32}$$

With this eigenfunction let us next study the normalization condition $1 = \|\psi_{a,m}\|^2$ on an $N$-petal rose, where $\|\psi_{a,m}\|^2 = \sum_{j=1}^N \int_{0_j}^{\ell_j} \mathrm{d}x_j |\psi_{j,a}(x_j; k_{a,m})|^2$. To this end, let us compute the squared norm $\|\psi_{a,m}\|^2$. A straightforward calculation yields

$$\begin{aligned}
\|\psi_{a,m}\|^2 = \sum_{j=1}^{N} \Bigg[ & \Big(|A^+_{j,a}(k_{a,m})|^2 + |A^-_{j,a}(k_{a,m})|^2\Big)\ell_j \\
& + \Big([A^+_{j,a}(k_{a,m})]^* A^-_{j,a}(k_{a,m}) + [A^-_{j,a}(k_{a,m})]^* A^+_{j,a}(k_{a,m})\Big) \frac{\mathrm{e}^{ik_{a,m}\ell_j} - \mathrm{e}^{-ik_{a,m}\ell_j}}{2ik_{a,m}} \Bigg] \\
= \vec{A}^\dagger_a(k_{a,m}) & \left[ L + \Sigma_1 \frac{\mathrm{e}^{ik_{a,m}L} - \mathrm{e}^{-ik_{a,m}L}}{2ik_{a,m}} \right] \vec{A}_a(k_{a,m}).
\end{aligned} \tag{4.33}$$

Noting that the on-shell ($k = k_{a,m}$) identities $\Sigma_1 \mathrm{e}^{ik_{a,m}L}\vec{A}_a(k_{a,m}) = S^\dagger(k_{a,m}L_0)\vec{A}_a(k_{a,m})$ and $\vec{A}^\dagger_a(k_{a,m})\Sigma_1 \mathrm{e}^{-ik_{a,m}L} = \vec{A}^\dagger_a(k_{a,m})S(k_{a,m}L_0)$, which follow from $S^{-1}(kL_0) = S^\dagger(kL_0)$, $\mathrm{e}^{-ikL}\Sigma_1 = \Sigma_1\mathrm{e}^{-ikL}$ and $\mathrm{e}^{i\vartheta_a(k_{a,m})} = 1$, we get

$$\begin{aligned}
\|\psi_{a,m}\|^2 &= \vec{A}^\dagger_a(k_{a,m}) \left[ L + \frac{S^\dagger(k_{a,m}L_0) - S(k_{a,m}L_0)}{2ik_{a,m}} \right] \vec{A}_a(k_{a,m}) \\
&= \vec{A}^\dagger_a(k_{a,m}) \left[ \frac{1}{i}\frac{\mathrm{d}\mathcal{U}}{\mathrm{d}k}(k_{a,m}) \right] \vec{A}_a(k_{a,m}),
\end{aligned} \tag{4.34}$$

where in the last equality we have used the off-sell identity

$$\frac{1}{i}\frac{\mathrm{d}\mathcal{U}}{\mathrm{d}k}(k) = \mathcal{U}(k)L + \frac{S^\dagger(kL_0) - S(kL_0)}{2ik}\mathcal{U}(k), \tag{4.35}$$

which follows from Eq.(2.28), and the hermitian conjugate of the eigenvalue equation $\vec{A}^\dagger(k)\mathcal{U}(k) = \mathrm{e}^{i\vartheta_a(k)}\vec{A}^\dagger(k)$ together with the on-shell condition $\mathrm{e}^{i\vartheta_a(k_{a,m})} = 1$.

Let us next compute the derivative of $\mathcal{U}(k)$ using the spectral decomposition (4.15):

$$\frac{1}{i}\frac{\mathrm{d}\mathcal{U}}{\mathrm{d}k}(k) = \sum_{a=1}^{2N}\left[\frac{\mathrm{d}\vartheta_a}{\mathrm{d}k}(k)\mathrm{e}^{i\vartheta_a(k)}\mathcal{P}_a(k) + \mathrm{e}^{i\vartheta_a(k)}\frac{\mathrm{d}\mathcal{P}_a}{\mathrm{d}k}(k)\right]. \tag{4.36}$$

Noting that the identity

$$\frac{\mathrm{d}\mathcal{P}_a}{\mathrm{d}k}(k)\mathcal{P}_a(k) + \mathcal{P}_a(k)\frac{\mathrm{d}\mathcal{P}_a}{\mathrm{d}k}(k) = \frac{\mathrm{d}\mathcal{P}_a}{\mathrm{d}k}(k), \tag{4.37}$$

which follows from the relation $\mathcal{P}_a(k)\mathcal{P}_a(k) = \mathcal{P}_a(k)$, we obtain the off-shell identity

$$\vec{A}_a^\dagger(k)\frac{\mathrm{d}\mathcal{P}_a}{\mathrm{d}k}(k)\vec{A}_a(k) = 0, \tag{4.38}$$

where we have used the off-shell identities $\mathcal{P}_a(k)\vec{A}_a(k) = \vec{A}_a(k)$ and $\vec{A}_a^\dagger(k)\mathcal{P}_a(k) = \vec{A}_a^\dagger(k)$. Thus, by using the off-shell relations (4.36) and (4.38) as well as the on-shell condition $\mathrm{e}^{i\vartheta_a(k_{a,m})} = 1$ we get the on-shell identity

$$\vec{A}_a^\dagger(k_{a,m})\left[\frac{1}{i}\frac{\mathrm{d}\mathcal{U}}{\mathrm{d}k}(k_{a,m})\right]\vec{A}_a(k_{a,m}) = \frac{\mathrm{d}\vartheta_a}{\mathrm{d}k}(k_{a,m})\left|\vec{A}_a(k_{a,m})\right|^2. \tag{4.39}$$

Combining the results (4.34) and (4.39) we see that the normalization condition $\|\psi_{a,m}\| = 1$ boils down to $(\mathrm{d}\vartheta_a/\mathrm{d}k)(k_{a,m})|\vec{A}_a(k_{a,m})|^2 = 1$, or, equivalently,

$$\left|\vec{A}_a(k_{a,m})\right|^{-2} = \frac{\mathrm{d}\vartheta_a}{\mathrm{d}k}(k_{a,m}). \tag{4.40}$$

In summary, the energy eigenfunction (4.32) can be normalized by using a coefficient vector $\vec{A}_a(k_{a,m})$ subject to the condition (4.40).

### 4.2.3 Reconstruction of $\mathcal{U}(k)$

Once given eigenvalues and corresponding orthonormal eigenvectors one can easily reconstruct a unitary matrix in terms of them. In this section we will reconstruct the unitary matrix $\mathcal{U}(k)$ in terms of the eigenvalue $\mathrm{e}^{i\vartheta_a(k)}$ and the coefficient vector $\vec{A}_a(k)$, $a = 1, 2, \cdots, 2N$.

To this end we first note that the projection operator $\mathcal{P}_a(k)$ can be reconstructed, in terms of the eigenvector $\vec{A}_a(k)$, as

$$\mathcal{P}_a(k) = \frac{1}{\left|\vec{A}_a(k)\right|^2}\vec{A}_a(k)\vec{A}_a^\dagger(k), \tag{4.41}$$

which satisfies the desired relation $\sum_{a=1}^{2N}\mathcal{P}_a(k) = \mathbb{1}_{2N}$, $\mathcal{P}_a(k)\mathcal{P}_b = \delta_{ab}\mathcal{P}_b(k)$ and $\mathcal{P}_a^\dagger(k) = \mathcal{P}_a(k)$ thanks to the completeness and orthogonality of each eigenvector. It should be noted that the normalization factor $\left|\vec{A}_a(k)\right|^{-2}$ becomes $(\mathrm{d}\vartheta_a/\mathrm{d}k)(k)$ on-shell.

Now it is easy to rewrite the unitary matrix $\mathcal{U}(k)$ as well as its $n$th power in terms of $\mathrm{e}^{i\vartheta_a(k)}$ and $\vec{A}_a(k)$. Using (4.41) $\mathcal{U}^n(k)$ is reconstructed as follows:

$$\mathcal{U}^n(k) = \sum_{a=1}^{2N}\frac{\mathrm{e}^{in\vartheta_a(k)}}{\left|\vec{A}_a(k)\right|^2}\vec{A}_a(k)\vec{A}_a^\dagger(k), \quad n \in \mathbb{Z}. \tag{4.42}$$

As we will see in the next section, the $n$th power of $\mathcal{U}(k)$ plays an important role for the path integral description of the Feynman kernel. Although we will discuss this point in detail in the subsequent sections, the reason for the significance of $\mathcal{U}^n(k)$ could be schematically understood even at this stage as follows; that is, since $\mathcal{U}(k)$ is composed of the S-matrix, which describes the local interaction at the vertex, and the bond propagation matrix, which describes how a particle freely propagate on a petal (bond), $\mathcal{U}^n(k)$ might admit the following schematic representation

$$\begin{aligned}\mathcal{U}^n = &\text{(local interaction)(bond propagation)} \times \text{(local interaction)(bond propagation)} \\ &\times \cdots \times \text{(local interaction)(bond propagation)},\end{aligned} \tag{4.43}$$

from which we could conclude that $\mathcal{U}^n(k)$ would have sufficiently enough information how a particle interacts with the vertex $n$-times and how a particle winds around petals $n$-times for the duration of its propagation.

Next move on to an analysis of the property of $\mathcal{U}^n(k)$. To this end, it is convenient to introduce $2 \times 2$ submatrix $u_{ij}^{(n)}(k)$ $(i, j = 1, 2, \cdots, N)$ as

$$\mathcal{U}^n(k) =: \begin{pmatrix} u_{11}^{(n)}(k) & \cdots & u_{1N}^{(n)}(k) \\ \vdots & \ddots & \vdots \\ u_{N1}^{(n)}(k) & \cdots & u_{NN}^{(n)}(k) \end{pmatrix}, \quad u_{ij}^{(n)}(k) =: \begin{pmatrix} \left[u_{ij}^{(n)}(k)\right]_{++} & \left[u_{ij}^{(n)}(k)\right]_{+-} \\ \left[u_{ij}^{(n)}(k)\right]_{-+} & \left[u_{ij}^{(n)}(k)\right]_{--} \end{pmatrix}. \tag{4.44}$$

Then, in terms of a submatrix $u_{ij}^{(n)}(k)$, Eq.(4.42) can be rewritten as the following form:

$$u_{ij}^{(n)}(k) = \sum_{a=1}^{2N} \frac{\mathrm{e}^{in\vartheta_a(k)}}{\left|\vec{A}_a(k)\right|^2} \begin{pmatrix} A_{i,a}^{+}(k)[A_{j,a}^{+}(k)]^* & A_{i,a}^{+}(k)[A_{j,a}^{-}(k)]^* \\ A_{i,a}^{-}(k)[A_{j,a}^{+}(k)]^* & A_{i,a}^{-}(k)[A_{j,a}^{-}(k)]^* \end{pmatrix}, \quad n \in \mathbb{Z}. \tag{4.45}$$

As we will see soon in the next section, $u_{ij}^{(n)}$ is closely related to the transition amplitude (Feynman kernel) for a particle traveling from the $j$th petal to the $i$th petal and interacting with a point interaction at the vertex $n$-times.

Let us finally study a property of matrix elements of $\mathcal{U}^n(k)$ under the momentum flip $k \to -k$. To this end we first note that the $n$th power of the unitary matrix $\mathcal{U}(k)$ satisfies the following identity

$$\mathcal{U}^n(k) = \mathrm{e}^{-ikL}\Sigma_1\mathcal{U}^{-n}(-k)\Sigma_1\mathrm{e}^{ikL}, \quad n \in \mathbb{Z}, \tag{4.46}$$

which follows from (4.12). In terms of the submatrix $u_{ij}^{(n)}(k)$, the identity (4.46) is then rewritten as $u_{ij}^{(n)}(k) = \mathrm{e}^{-ik\ell_i}\sigma_1 u_{ij}^{(-n)}(-k)\sigma_1\mathrm{e}^{ik\ell_j}$, or, in components,

$$\left[u_{ij}^{(n)}(k)\right]_{+-} = \mathrm{e}^{-ik(\ell_i-\ell_j)}\left[u_{ij}^{(-n)}(-k)\right]_{-+}, \tag{4.47a}$$

$$\left[u_{ij}^{(n)}(k)\right]_{--} = \mathrm{e}^{-ik(\ell_i-\ell_j)}\left[u_{ij}^{(-n)}(-k)\right]_{++}, \quad n \in \mathbb{Z}. \tag{4.47b}$$

In the next section these identities will play important roles for the derivation of path integral description for the Feynman kernel.

## 4.3 Path integral on a rose

In this section we derive the path integral description of the Feynman kernel for a free particle on an $N$-petal rose. Although over the past decade quantum graph has been vastly studied by many authors, path integral treatment of quantum graph is quite few. This is due to the fact that we do not know *a priori* neither how classical action or Lagrangian we should adopt as a weight of the path integration on a rose nor what trajectories on a rose we should integrate over. The most mathematically reliable way is to first write down the Feynmen kernel in terms of the energy eigenfunctions and then switch the summation over the energy spectrum to that of classical trajectories (periodic orbits) by using the trace formulae.

In terms of the energy eigenfunction (4.32) subject to the normalization condition (4.40), the Feynman kernel is given by

$$\begin{aligned}\langle x_i'|\mathrm{e}^{-iHT}|x_j\rangle = &\sum_{a=1}^{2N}\sum_{m>0}\mathrm{e}^{-i(k_{a,m})^2T}\psi_{i,a}(x_i';k_{a,m})\psi_{j,a}^*(x_j;k_{a,m})\\ &+(\text{zero energy modes})+(\text{negative energy modes}),\end{aligned}\tag{4.48}$$

where we have separated the contributions of the possible zero energy as well as negative energy eigenfunctions from those of positive energy ones because non-positive modes are out of the scope of our trace formula.

Making use of the trick $\psi_{i,a}(x_i';k)=\begin{pmatrix}\mathrm{e}^{-ikx_i'}\\ \mathrm{e}^{-ik(\ell_i-x_i')}\end{pmatrix}^\dagger\begin{pmatrix}A_{i,a}^+(k)\\ A_{i,a}^-(k)\end{pmatrix}$, we see that (4.48) can be cast into the following form

$$\begin{aligned}\langle x_i'|\mathrm{e}^{-iHT}|x_j\rangle = &\sum_{a=1}^{2N}\sum_{m>0}\mathrm{e}^{-ik^2T}\\ &\times\begin{pmatrix}\mathrm{e}^{-ikx_i'}\\ \mathrm{e}^{-ik(\ell_i-x_i')}\end{pmatrix}^\dagger\begin{pmatrix}A_{i,a}^+(k)[A_{j,a}^+(k)]^* & A_{i,a}^+(k)[A_{j,a}^-(k)]^*\\ A_{i,a}^-(k)[A_{j,a}^+(k)]^* & A_{i,a}^-(k)[A_{j,a}^-(k)]^*\end{pmatrix}\begin{pmatrix}\mathrm{e}^{-ikx_j}\\ \mathrm{e}^{-ik(\ell_j-x_j)}\end{pmatrix}\Bigg|_{k=k_{a,m}}\\ &+(\text{zero energy modes})+(\text{negative energy modes}).\end{aligned}\tag{4.49}$$

Inserting the unity $1=|\vec{A}_a(k_{a,m})|^2\cdot|\vec{A}_a(k_{a,m})|^{-2}$ into the summation $\sum_a\sum_m$ and using the on-shell identity (4.40) and then the trace formula (4.28) we get

$$\begin{aligned}\langle x_i'|\mathrm{e}^{-iHT}|x_j\rangle = &\frac{1}{2}\sum_{n\in\mathbb{Z}}\int_{-\infty}^{\infty}\frac{\mathrm{d}k}{2\pi}\,\mathrm{e}^{-ik^2T}\begin{pmatrix}\mathrm{e}^{-ikx_i'}\\ \mathrm{e}^{-ik(\ell_i-x_i')}\end{pmatrix}^\dagger u_{ij}^{(n)}(k)\begin{pmatrix}\mathrm{e}^{-ikx_j}\\ \mathrm{e}^{-ik(\ell_j-x_j)}\end{pmatrix}\\ &+(\text{zero energy modes})'+(\text{negative energy modes}),\end{aligned}\tag{4.50}$$

where

$$(\text{zero energy modes})'=(\text{zero energy modes})-\sum_{a=1}^{2N}\psi_{i,a}(x_i;0)\psi_{j,a}^*(x_j;0).\tag{4.51}$$

It follows from the identities (4.47a) (4.47b) that the Feynman kernel can also be written

as follows:

$$\begin{aligned}\langle x_i'|\mathrm{e}^{-iHT}|x_j\rangle &= \sum_{n\in\mathbb{Z}}\int_{-\infty}^{\infty}\frac{\mathrm{d}k}{2\pi}\left[u_{ij}^{(n)}(k)\right]_{++}\exp\left(iT\left[k\left(\frac{x_i'-x_j}{T}\right)-k^2\right]\right)\\ &+\sum_{n\in\mathbb{Z}}\int_{-\infty}^{\infty}\frac{\mathrm{d}k}{2\pi}\left[u_{ij}^{(n)}(k)\right]_{-+}\exp\left(iT\left[k\left(\frac{\ell_i-x_i'-x_j}{T}\right)-k^2\right]\right)\\ &+(\text{zero energy modes})'+(\text{negative energy modes}).\end{aligned}\tag{4.52}$$

This is the final expression for our path integral representation of the Feynman kernel.

## 4.4 Examples

### 4.4.1 Circle

In this section we present explicit examples of the Feynman kernels on a circle of circumference $\ell$ for several subfamilies of point interactions, which are completely classified in the literature [15,18] and summarized in Table 2.1. Since the time-reversal invariant subfamily and the $\mathscr{P}\mathscr{T}$-symmetric subfamily are quite involved, in what follows we will only consider the cases of the reflectionless subfamily (smooth subfamily), the scale-independent subfamily, the transmissionless subfamily (separated subfamily) and the parity invariant subfamily. As we will see below, our formalism recover all known results.

#### 4.4.1.1 Smooth subfamily

Let us first consider the reflectionless point interaction as the simplest example because in this case the $2\times 2$ unitary matrix $\mathcal{U}(k)$ becomes diagonal. Since $\mathcal{U}(k)=S(kL_0)\sigma_1\mathrm{e}^{ik\ell}$, the diagonal $\mathcal{U}(k)$ is obtained by the off-diagonal $S(kL_0)$, which is given by $e_z=0$ and $(\alpha_1,\alpha_2)=(0,\pi)$ or $(\pi,0)$ in (2.9a) and (2.9b). Since the difference between the two cases $(\alpha_1,\alpha_2)=(0,\pi)$ and $(\pi,0)$ is just the overall sign of the S-matrix, without any loss of generality we can restrict ourselves to the case $(\alpha_1,\alpha_2)=(0,\pi)$ by using the parameterization $\vec{e}=(\cos\theta,\sin\theta,0)$, $0\le\theta<2\pi$. With this parameterization the $n$th power of $\mathcal{U}(k)$ becomes

$$\mathcal{U}^n(k)=\begin{pmatrix}\mathrm{e}^{-in\theta} & 0\\ 0 & \mathrm{e}^{in\theta}\end{pmatrix}\mathrm{e}^{ikn\ell}.\tag{4.53}$$

The Feynman kernel (4.52) is cast into the well-known form [47]

$$\langle x'|\mathrm{e}^{-iHT}|x\rangle=\sum_{n\in\mathbb{Z}}\mathrm{e}^{-in\theta}\int_{-\infty}^{\infty}\frac{\mathrm{d}p}{2\pi}\mathrm{e}^{iT\left[p\left(\frac{n\ell+x'-x}{T}\right)-p^2\right]}.\tag{4.54}$$

It should be mentioned here the connection between the Laidlaw-DeWitt theorem [55] and our formalism. The theorem states that the path-integral in a multiply-connected space has to be taken the sum over the homotopy class of the space with a weight factor which forms a scalar unitary representation of the fundamental group of the space. In this well-known example, the weight factor is just a phase $\mathrm{e}^{-in\theta}$. In the viewpoint of the Laidlaw-DeWitt theorem, this weight factor is a scalar unitary representation of $\pi_1(S^1)\cong\mathbb{Z}$, while in our viewpoint it is just the element of diagonal $(S\sigma_1)^n$, which is essentially unitary thanks to the unitarity of the S-matrix.

#### 4.4.1.2 Scale-independent subfamily

As a next example let us consider the scale-independent point interactions, which include the above reflectionless point interaction and the $\delta'$-interaction discussed in section 4.1. As shown in section 2.4.1.4 the scale-independent point interactions are characterized by the matrices $U$ whose two eigenphases are $(\alpha_1, \alpha_2) = (0,0), (\pi,\pi), (0,\pi), (\pi,0)$ [15,18]. The first two cases also belong to the transmissionless point interactions and will be considered in the next example. The latter two cases, however, are different only for the overall sign of the S-matrix, without any loss of generality we can restrict ourselves to the case $(\alpha_1, \alpha_2) = (0,\pi)$ by using the parameterization $\vec{e} = (\cos\theta, \sin\theta\cos\phi, \sin\theta\sin\phi)$ with $0 \le \theta \le \pi$ and $0 \le \phi < 2\pi$. With this choice of the parameters, the matrix $\mathcal{U}(k)$ has the form $\mathcal{U}(k) = (\vec{e}\cdot\vec{\sigma})\sigma_1 \mathrm{e}^{ik\ell}$.

The matrix $\mathcal{U}(k)$ has the spectral decomposition $\mathcal{U}(k) = \big(\mathrm{e}^{i\theta}\mathcal{P}_1 + \mathrm{e}^{-i\theta}\mathcal{P}_2\big)\mathrm{e}^{ik\ell}$ with $\mathcal{P}_{1,2} = (\mathbb{1} \mp \sin\phi\sigma_2 \pm \cos\phi\sigma_3)/2$. Then its $n$th power is cast into the following form

$$\mathcal{U}^{(n)}(k) = \begin{pmatrix} \cos(n\theta) - i\cos\phi\sin(n\theta) & \sin\phi\sin(n\theta) \\ -\sin\phi\sin(n\theta) & \cos(n\theta) + i\cos\phi\sin(n\theta) \end{pmatrix} \mathrm{e}^{ikn\ell}. \tag{4.55}$$

Thus the Feynman kernel (4.52) becomes

$$\begin{aligned} \langle x'|\mathrm{e}^{-iHT}|x\rangle = {} & \sum_{n\in\mathbb{Z}} [\cos(n\theta) - i\cos\phi\sin(n\theta)] \int_{-\infty}^{\infty} \frac{\mathrm{d}p}{2\pi} \mathrm{e}^{iT\left[p\left(\frac{n\ell+x'-x}{T}\right)-p^2\right]} \\ & - \sum_{n\in\mathbb{Z}} \sin\phi\sin(n\theta) \int_{-\infty}^{\infty} \frac{\mathrm{d}p}{2\pi} \mathrm{e}^{iT\left[p\left(\frac{n\ell+(\ell-x')-x}{T}\right)-p^2\right]}. \end{aligned} \tag{4.56}$$

Observe that $\phi = 0$ ($\phi = \pi$) reduces to the previous results (4.54) for $0 \le \theta \le \pi$ ($\pi \le \theta < 2\pi$). The case $\phi = \pi/2$ ($\phi = 3\pi/2$) becomes the kernel (4.1) for $c > 0$ ($c < 0$).

The kernel (4.56) coincides with the results given in [15, 18] with suitable redefinitions of the parameters.

#### 4.4.1.3 Separated subfamily

Next consider the transmissionless point interactions, i.e. the separated subfamily of $U(2)$ family of point interactions. These point interactions are obtained from the diagonal $S(kL_0)$, which is realized by $e_x = e_y = 0$ in (2.9a) and (2.9b). With this choice the transmission coefficients identically vanish and the reflection coefficients become $R_{1/2}(k) = \frac{ikL_{2/1}-1}{ikL_{2/1}+1}$ for $e_z = 1$ and $R_{1/2}(k) = \frac{ikL_{1/2}-1}{ikL_{1/2}+1}$ for $e_z = -1$. In the following we will consider the case $e_z = 1$. The result for $e_z = -1$ will be obtained by replacing the index '1' to '2' and vice versa. In the $e_z = 1$ case the $n$th power of $\mathcal{U}(k)$ has the form

$$\begin{aligned} &\mathcal{U}^n(k) \\ &= \begin{cases} \begin{pmatrix} \left(\frac{ikL_1-1}{ikL_1+1}\right)^{\frac{n}{2}} \left(\frac{ikL_2-1}{ikL_2+1}\right)^{\frac{n}{2}} & 0 \\ 0 & \left(\frac{ikL_1-1}{ikL_1+1}\right)^{\frac{n}{2}} \left(\frac{ikL_2-1}{ikL_2+1}\right)^{\frac{n}{2}} \end{pmatrix} \mathrm{e}^{ikn\ell}, & \text{for } n \text{ even}, \\ \begin{pmatrix} 0 & \left(\frac{ikL_1-1}{ikL_1+1}\right)^{\frac{n+1}{2}} \left(\frac{ikL_2-1}{ikL_2+1}\right)^{\frac{n-1}{2}} \\ \left(\frac{ikL_1-1}{ikL_1+1}\right)^{\frac{n-1}{2}} \left(\frac{ikL_2-1}{ikL_2+1}\right)^{\frac{n+1}{2}} & 0 \end{pmatrix} \mathrm{e}^{ikn\ell}, & \text{for } n \text{ odd}. \end{cases} \end{aligned} \tag{4.57}$$

In this case of the separated subfamily, the physical meanings of the eigenphases are clear: $\frac{ikL_2-1}{ikL_2+1}$ ($\frac{ikL_1-1}{ikL_1+1}$) is nothing but the *phase shift* which occurs every time when a particle hits the reflecting wall at $x=\ell$ ($x=0$) from the left (right).

Now we can rewrite the kernel (4.52) into the following form

$$\begin{aligned}\langle x'|\mathrm{e}^{-iHT}|x\rangle &= \sum_{n\in\mathbb{Z}}\int_{-\infty}^{\infty}\frac{\mathrm{d}p}{2\pi}\left(\frac{ipL_1-1}{ipL_1+1}\right)^n\left(\frac{ipL_2-1}{ipL_2+1}\right)^n \mathrm{e}^{iT\left[p\left(\frac{2n\ell+x'-x}{T}\right)-p^2\right]}\\ &+\sum_{n\in\mathbb{Z}}\int_{-\infty}^{\infty}\frac{\mathrm{d}p}{2\pi}\left(\frac{ipL_1-1}{ipL_1+1}\right)^{n-1}\left(\frac{ipL_2-1}{ipL_2+1}\right)^n \mathrm{e}^{iT\left[p\left(\frac{2n\ell-x'-x}{T}\right)-p^2\right]}\\ &+(\text{negative energy mode}).\end{aligned}\tag{4.58}$$

Observe that by tuning the parameters $\alpha_{1,2}$ to be 0 or $\pi$, the kernel becomes the simpler form because in these spacial cases the phase shifts become independent of momentum. Thus there are $2\times 2=4$ simpler cases, $(\alpha_1,\alpha_2)=(0,0)$, $(\pi,\pi)$, $(0,\pi)$ and $(\pi,0)$, which correspond to the Neumann-Neumann, Dirichlet-Dirichlet, Neumann-Dirichlet and Dirichlet-Neumann boundary conditions at $x=0$ and $\ell$. These cases belong to the scale-independent subfamily of the $U(2)$ family of point interactions and the corresponding kernels are vastly studied in the literature [15, 18, 56], whose results coincide with (4.58) as the above special cases.

It should also be pointed out here that the partial amplitude for $n=0$ in (4.58) is nothing but the one-particle Feynman kernel evaluated on a half-line in the presence of a reflecting wall characterized by the boundary condition $\psi(0)+L_1\psi'(0)=0$ [57, 58].

#### 4.4.1.4 $\mathscr{P}$-symmetric subfamily

Next consider the parity invariant point interactions, which include the famous $\delta$- and $\epsilon$-interactions. The parity transformation on a circle is defined as $\mathscr{P}: x\mapsto \ell-x$. As shown in section 2.4 the parity invariant point interactions are characterized by the matrix $U$ satisfying $U=\sigma_1 U\sigma_1$ [15, 18]. Such a matrix is obtained by choosing $e_y=e_z=0$ so that the matrix $\mathcal{U}(k)$ becomes $\mathcal{U}(k)=\left(\frac{ikL_1-1}{ikL_1+1}\mathcal{P}_1-\frac{ikL_2-1}{ikL_2+1}\mathcal{P}_2\right)\mathrm{e}^{ik\ell}$ for $e_x=1$ and $\mathcal{U}(k)=\left(\frac{ikL_2-1}{ikL_2+1}\mathcal{P}_1-\frac{ikL_1-1}{ikL_1+1}\mathcal{P}_2\right)\mathrm{e}^{ik\ell}$ for $e_x=-1$, where $\mathcal{P}_{1,2}$ are the projection operators given by $\mathcal{P}_{1,2}=(\mathbb{1}\pm\sigma_1)/2$. In what follows we will consider the case $e_x=1$. The result for $e_x=-1$ can be obtained by changing the index '1' and '2'. The $n$the power of $\mathcal{U}(k)$ is easily computed with the result

$$\mathcal{U}^n(k)=\frac{1}{2}\begin{pmatrix}\left(\frac{ikL_1-1}{ikL_1+1}\right)^n+\left(-\frac{ikL_2-1}{ikL_2+1}\right)^n & \left(\frac{ikL_1-1}{ikL_1+1}\right)^n-\left(-\frac{ikL_2-1}{ikL_2+1}\right)^n\\ \left(\frac{ikL_1-1}{ikL_1+1}\right)^n-\left(-\frac{ikL_2-1}{ikL_2+1}\right)^n & \left(\frac{ikL_1-1}{ikL_1+1}\right)^n+\left(-\frac{ikL_2-1}{ikL_2+1}\right)^n\end{pmatrix}\mathrm{e}^{ikn\ell}.\tag{4.59}$$

The Feynman kernel (4.52) is therefore

$$\begin{aligned}\langle x'|\mathrm{e}^{-iHT}|x\rangle &= \sum_{n\in\mathbb{Z}}\frac{1}{2}\int_{-\infty}^{\infty}\frac{\mathrm{d}p}{2\pi}\left(\frac{ipL_1-1}{ipL_1+1}\right)^n\left\{\mathrm{e}^{iT\left[p\left(\frac{n\ell+x'-x}{T}\right)-p^2\right]}+\mathrm{e}^{iT\left[p\left(\frac{n\ell+(\ell-x')-x}{T}\right)-p^2\right]}\right\}\\ &+\sum_{n\in\mathbb{Z}}\frac{1}{2}\int_{-\infty}^{\infty}\frac{\mathrm{d}p}{2\pi}\left(-\frac{ipL_2-1}{ipL_2+1}\right)^n\left\{\mathrm{e}^{iT\left[p\left(\frac{n\ell+x'-x}{T}\right)-p^2\right]}-\mathrm{e}^{iT\left[p\left(\frac{n\ell+(\ell-x')-x}{T}\right)-p^2\right]}\right\}\\ &+(\text{negative energy mode}).\end{aligned}\tag{4.60}$$

Notice that the first and second lines are parity-even and -odd contributions respectively: the former is invariant under the parity transformation $\mathscr{P}: x\mapsto\ell-x$, while the latter changes the sign.

### 4.4.2 Figure eight

Let us next consider particle propagation on a figure eight (see Figure 4.4). As opposed to the previous circle case, to the best of my knowledge, no work has been made on the path integral representation of the Feynman kernel on a figure eight. Furthermore, possible symmetries and invariant subfamilies of $U(4)$ family of point interactions on a figure eight has not yet been fully understood. So in this section we will concentrate ourselves upon a "free theory" on a figure eight as the simplest example. "Free theory" on a figure eight is defined as the perfectly connected vertex, which, as we will see immediately, is described by the following unitary matrix:

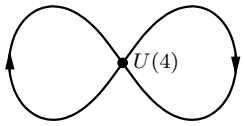


Figure 4.4: Figure eight.

$$\begin{aligned} U &= \frac{1}{2}\begin{pmatrix} -1 & 1 & 1 & 1 \\ 1 & -1 & 1 & 1 \\ 1 & 1 & -1 & 1 \\ 1 & 1 & 1 & -1 \end{pmatrix} = \begin{pmatrix} -\sigma_1^- & \sigma_1^+ \\ \sigma_1^+ & -\sigma_1^- \end{pmatrix} \\ &= P_1 - P_2 - P_3 - P_4 = -\mathbb{1}_4 + 2P_1, \end{aligned} \tag{4.61}$$

where $\sigma_1^\pm = (\mathbb{1}_2 \pm \sigma_1)/2$. $P_j$ $(j = 1, 2, 3, 4)$ is a hermitian projection operator given by

$$P_1 = \frac{1}{2}\begin{pmatrix} \sigma_1^+ & \sigma_1^+ \\ \sigma_1^+ & \sigma_1^+ \end{pmatrix} = \sigma_1^+ \otimes \sigma_1^+, \tag{4.62a}$$

$$P_2 = \frac{1}{2}\begin{pmatrix} \sigma_1^+ & -\sigma_1^+ \\ -\sigma_1^+ & \sigma_1^+ \end{pmatrix} = \sigma_1^- \otimes \sigma_1^+, \tag{4.62b}$$

$$P_3 = \frac{1}{2}\begin{pmatrix} \sigma_1^- & \sigma_1^- \\ \sigma_1^- & \sigma_1^- \end{pmatrix} = \sigma_1^+ \otimes \sigma_1^-, \tag{4.62c}$$

$$P_4 = \frac{1}{2}\begin{pmatrix} \sigma_1^- & -\sigma_1^- \\ -\sigma_1^- & \sigma_1^- \end{pmatrix} = \sigma_1^- \otimes \sigma_1^-, \tag{4.62d}$$

those satisfying $\sum_{j=1}^4 P_j = \mathbb{1}_4$, $P_i P_j = \delta_{ij} P_j$ and $P_j^\dagger = P_j$. Note that the tensor product notation will be useful for computation: For example, $P_2 P_2 = (\sigma_1^- \otimes \sigma_1^+)(\sigma_1^- \otimes \sigma_1^+) = \sigma_1^-\sigma_1^- \otimes \sigma_1^+\sigma_1^+ = \sigma_1^- \otimes \sigma_1^+ = P_2$, $P_2 P_3 = (\sigma_1^- \otimes \sigma_1^+)(\sigma_1^+ \otimes \sigma_1^-) = \sigma_1^-\sigma_1^+ \otimes \sigma_1^+\sigma_1^- = 0$ and so on.

Since the eigenvalues of $U$ corresponding to $P_1$, $P_2$, $P_3$ and $P_4$ are, respectively, $+1$, $-1$, $-1$ and $-1$, the boundary conditions at the vertex are simply given by $P_{2,3,4}\vec{\Psi}(0) = \vec{0}$ and $P_1\vec{\Psi}'(0) = \vec{0}$, or, more explicitly,

$$\psi_1(0_1) = \psi_1(\ell_1) = \psi_2(0_2) = \psi_2(\ell_2), \tag{4.63a}$$

$$\psi_1'(0_1) + \psi_2'(0_2) = \psi_1'(\ell_1) + \psi_2'(\ell_2). \tag{4.63b}$$

This is the boundary conditions that describe a perfectly connected vertex. It should be noted that $S(kL_0) = U$, $\Sigma_1 = \mathbb{1}_2 \otimes \sigma_1$ and $\mathrm{e}^{ikL} = \begin{pmatrix} \mathrm{e}^{ik\ell_1} & 0 \\ 0 & \mathrm{e}^{ik\ell_2} \end{pmatrix} \otimes \mathbb{1}_2$. Thus, the matrix $\mathcal{U}(k)$ can be written as follows

$$\mathcal{U}(k) = S\Sigma_1 \mathrm{e}^{ikL} = \begin{pmatrix} \mathrm{e}^{ik\ell_1} & 0 \\ 0 & \mathrm{e}^{ik\ell_2} \end{pmatrix} \otimes \sigma_1^- + \begin{pmatrix} 0 & \mathrm{e}^{ik\ell_2} \\ \mathrm{e}^{ik\ell_1} & 0 \end{pmatrix} \otimes \sigma_1^+. \tag{4.64}$$

Since $\sigma_1^+$ and $\sigma_1^-$ are orthogonal to each other, the spectral decomposition of $\mathcal{U}(k)$ is reduced to the problem of that of two $2\times 2$ unitary matrices, $\left(\begin{smallmatrix} \mathrm{e}^{ik\ell_1} & 0 \\ 0 & \mathrm{e}^{ik\ell_2} \end{smallmatrix}\right)$ and $\left(\begin{smallmatrix} 0 & \mathrm{e}^{ik\ell_2} \\ \mathrm{e}^{ik\ell_1} & 0 \end{smallmatrix}\right)$. Following this procedure, one can immediately see that the $n$th power of $\mathcal{U}(k)$ is given as follows:

$$\mathcal{U}^n(k) = \mathrm{e}^{ikn\ell_1}\mathcal{P}_1(k) + \mathrm{e}^{ikn\ell_2}\mathcal{P}_2(k) + \mathrm{e}^{ikn(\ell_1+\ell_2)/2}\mathcal{P}_3(k) + (-1)^n\mathrm{e}^{ikn(\ell_1+\ell_2)/2}\mathcal{P}_4(k). \quad (4.65)$$

where $\mathcal{P}_j(k)$ $(j=1,2,3,4)$ is a hermitian projection operator given by

$$\mathcal{P}_1(k) = \begin{pmatrix} 1 & 0 \\ 0 & 0 \end{pmatrix} \otimes \sigma_1^-, \quad (4.66a)$$

$$\mathcal{P}_2(k) = \begin{pmatrix} 0 & 0 \\ 0 & 1 \end{pmatrix} \otimes \sigma_1^-, \quad (4.66b)$$

$$\mathcal{P}_3(k) = \frac{1}{2}\begin{pmatrix} 1 & \mathrm{e}^{-ik(\ell_1-\ell_2)/2} \\ \mathrm{e}^{ik(\ell_1-\ell_2)} & 1 \end{pmatrix} \otimes \sigma_1^+, \quad (4.66c)$$

$$\mathcal{P}_4(k) = \frac{1}{2}\begin{pmatrix} 1 & -\mathrm{e}^{-ik(\ell_1-\ell_2)/2} \\ -\mathrm{e}^{ik(\ell_1-\ell_2)/2} & 1 \end{pmatrix} \otimes \sigma_1^+. \quad (4.66d)$$

The submatrices $u_{ab}^{(n)}(k)$ $(a,b=1,2)$ are:

$$u_{11}^{(n)}(k) = \mathrm{e}^{ikn\ell_1}\sigma_1^- + \frac{1+(-1)^n}{2}\mathrm{e}^{ikn(\ell_1+\ell_2)/2}\sigma_1^+, \quad (4.67a)$$

$$u_{21}^{(n)}(k) = \frac{1-(-1)^n}{2}\mathrm{e}^{ik(n(\ell_1+\ell_2)+(\ell_1-\ell_2))/2}\sigma_1^+. \quad (4.67b)$$

The transition amplitude for a particle traveling from the position $x_1$ to $x_1'$ (both are lying on the 1st petal) is thus given by

$$\begin{aligned}
&\langle x_1'|\mathrm{e}^{-iHT}|x_1\rangle \\
&= \sum_{n\in\mathbb{Z}}\frac{1}{2}\int_{-\infty}^{\infty}\frac{\mathrm{d}p}{2\pi}\left\{\mathrm{e}^{iT\left[p\left(\frac{n\ell_1+x_1'-x_1}{T}\right)-p^2\right]} - \mathrm{e}^{iT\left[p\left(\frac{n\ell_1+(\ell_1-x_1')-x_1}{T}\right)-p^2\right]}\right\} \\
&+ \sum_{n\in\mathbb{Z}}\frac{1}{2}\int_{-\infty}^{\infty}\frac{\mathrm{d}p}{2\pi}\left\{\mathrm{e}^{iT\left[p\left(\frac{n(\ell_1+\ell_2)+x_1'-x_1}{T}\right)-p^2\right]} + \mathrm{e}^{iT\left[p\left(\frac{n(\ell_1+\ell_2)+(\ell_1-x_1')-x_1}{T}\right)-p^2\right]}\right\}. \quad (4.68a)
\end{aligned}$$

Similarly, the transition amplitude for a particle traveling from the position $x_1$ to $x_2'$ (the former lies on the 1st petal and the latter the 2nd petal) is given by

$$\begin{aligned}
&\langle x_2'|\mathrm{e}^{-iHT}|x_1\rangle \\
&= \sum_{n\in\mathbb{Z}}\frac{1}{2}\int_{-\infty}^{\infty}\frac{\mathrm{d}p}{2\pi}\left\{\mathrm{e}^{iT\left[p\left(\frac{n(\ell_1+\ell_2)-(\ell_2-x_2')-x_1}{T}\right)-p^2\right]} + \mathrm{e}^{iT\left[p\left(\frac{n(\ell_1+\ell_2)-x_2'-x_1}{T}\right)-p^2\right]}\right\}. \quad (4.68b)
\end{aligned}$$

Classical worldlines for a particle scattered twice at the vertex that corresponds to the kernel (4.68a) is depicted in Figure 4.5.

**Spectrum of figure eight**.

Before closing this section it should be mentioned about the spectrum of figure eight with a perfectly connected vertex. The positive energy spectrum is determined by the conditions $\mathrm{e}^{ik\ell_1}=1$, $\mathrm{e}^{ik\ell_2}=1$, $\mathrm{e}^{ik(\ell_1+\ell_2)/2}=1$ and $-\mathrm{e}^{ik(\ell_1+\ell_2)/2}=1$. The solutions to these conditions are:

$$k_{1,n} = \frac{2n\pi}{\ell_1}, \quad k_{2,n} = \frac{2n\pi}{\ell_2}, \quad k_{3,n} = \frac{2n\pi}{(\ell_1+\ell_2)/2}, \quad k_{4,n} = \frac{(2n-1)\pi}{(\ell_1+\ell_2)/2}, \quad (4.69)$$

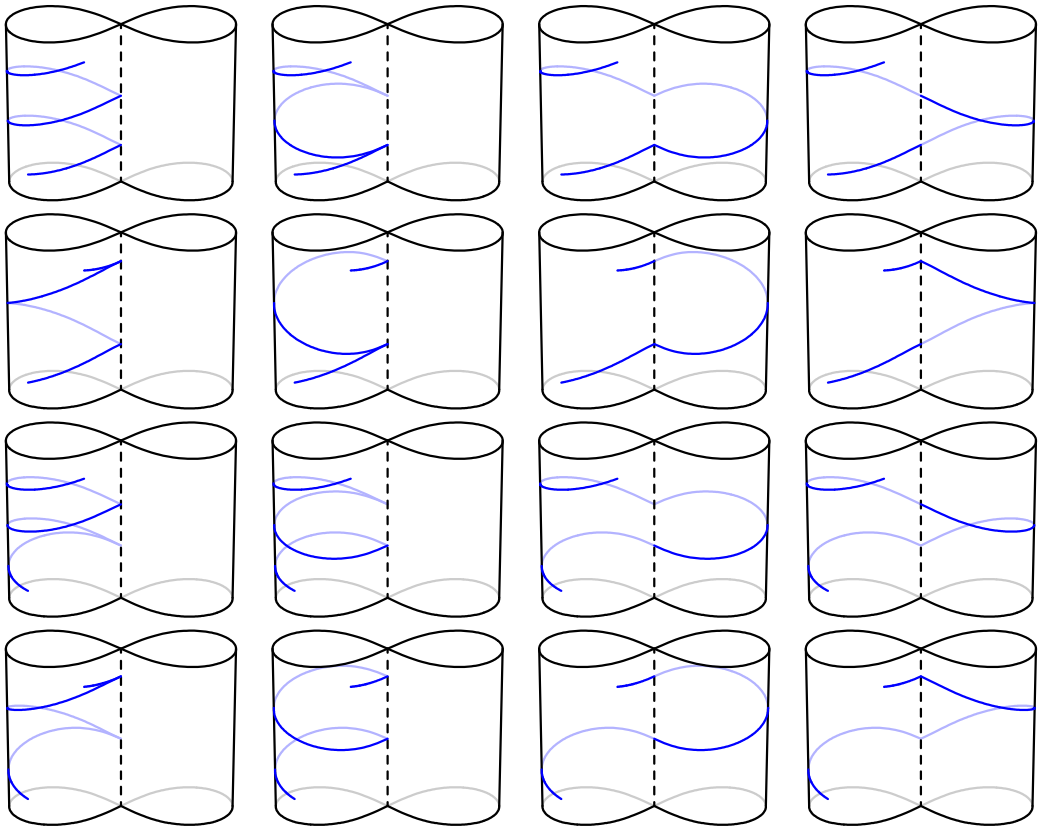

Figure 4.5: Classical worldlines for a particle on a figure eight scattered twice by the vertex. There are 16 distinct worldlines. Time is flowing along the vertical direction. Dashed lines represent the worldlines of the vertex and arrows represent the directions of momentum flow.

where $n = 1, 2, 3, \cdots$.

Next move on to the analysis of zero energy solution. The zero energy solution $\psi_j(x_j) = A_j + B_j x_j$ $(j = 1, 2)$ consistent with the boundary conditions exist only when $B_1 = B_2 = 0$ and $A_1 = A_2$. Thus there exits a single zero mode in the spectrum.

It should be noted here that if $\ell_1 = \ell_2$, i.e. figure eight becomes symmetric under the exchange of two petals, the spectrum of figure eight exhibits the *three-fold degeneracy* except for the zero-energy ground state, which strongly implies a hidden (extended) supersymmetry structure of the system. We would like to report this issue elsewhere.

## 4.5 Conclusions and discussions

In this chapter we have studied the path integral description of the Feynman kernel on an $N$-petal rose in the presence of a single point interaction compatible with the conservation of the probability current at the vertex, or the self-adjoint extension of the Laplace operator $-\mathrm{d}^2/\mathrm{d}x^2$ on a wedge sum (or one-point union) of $N$ circles $S^1 \vee S^1 \vee \cdots \vee S^1$. We uncovered the classical trajectories for a quantum particle on an $N$-petal rose, which consist of $2 \times (N^{n-1} \times 2) = 4N^{n-1}$ distinct paths for a particle scattered $n$-times from the point interaction

(point scatterer). We also illuminated deep connection between the scattering theory on a star graph with $2N$ bonds and the spectral property of an $N$-petal rose, which, in roughly speaking, is summarized as the following correspondences:

$$\begin{array}{lcl} \text{eigenvalues of } \mathcal{U}(k) = S(kL_0)\Sigma_1 \mathrm{e}^{ikL} & \Leftrightarrow & \text{energy spectrum on a rose;} \\ \text{eigenvectors of } \mathcal{U}(k) = S(kL_0)\Sigma_1 \mathrm{e}^{ikL} & \Leftrightarrow & \text{energy eigenfunctions on a rose.} \end{array}$$

The main success of this work is the systematic description for a one-particle Feynman kernel on a rose with a point interaction. The point is that we do not need any knowledge of the spectrum nor the complete set of energy eigenfunctions of the system (except for the non-positive energy eigenstates). What we have to know is the one-particle scattering matrix $S(kL_0)$ on a star graph and the bond propagation matrix $\mathrm{e}^{ikL}$ on a rose graph.

We are left with a number of questions, however. Let us close with a few comments on these issues:

1. *Algebraic construction of trajectories.*
   We showed that the particle propagation scattered $n$-times from the point interaction should be weighted by the elements of $\mathcal{U}^n(k)$. As briefly discussed in section 4.4, in the case of reflectionless subfamily of point interactions unitarity of S-matrix and the Laidlaw-DeWitt theorem seem to be the same thing. However, the theorem is essentially based on the homotopy theory so that it could not be applied in general to the other subfamily of point interactions. We thought that the unitarity of $\mathcal{U}^n(k)$ would provide a wider notion than the Laidraw-DeWitt theorem and should be derived from some fundamental properties of the Feynman kernel such as the unitarity $K(x_i', T; x_j, 0) = \sum_{k=1}^{N} \int_0^{\ell_k} \mathrm{d}x_k K(x_i', T; x_k, t) K(x_k, t; x_j, 0)$.
   Another related issue is an algebraic structure for the construction of classical trajectories for a particle on a rose. As mentioned before, the classical trajectories for a particle interacting $n$-times to the point interaction consist of $4N^{n-1}$ distinct paths. These trajectories are constructed from the more fundamental trajectories by gluing them under the multiplication rule of the matrix $\mathcal{U}(k)$. For example, twice-scattered trajectories for a particle on a circle in the presence of a single point interaction is algebraically constructed as follows:

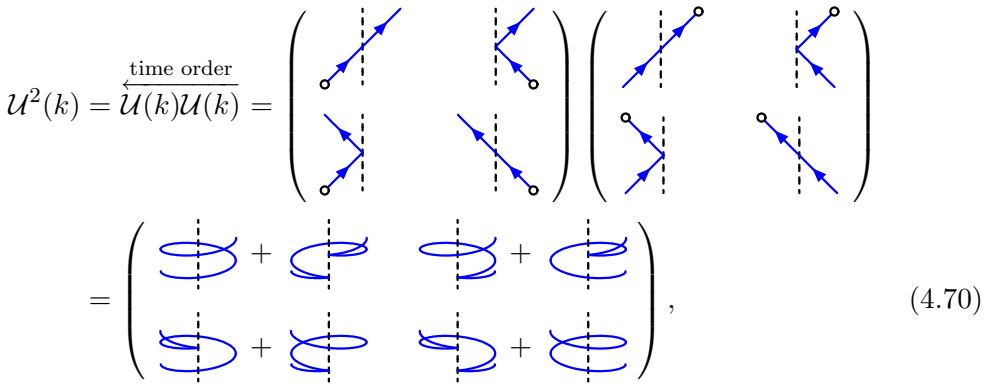


   (4.70)

   where the last equality follows from the computation method that connects $\circ$ and $\circ$ in time order: For example,

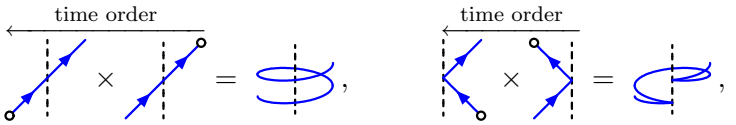


   (4.71)

and so on. This algebraic construction of trajectories implies that, in spite of the presence of a point singularity, it might be possible to introduce some kind of notion analogous to the fundamental group. We would like to report this issue elsewhere.

2. *Path-integral representation for the kernels.*
The Feynman kernels derived in this chapter have the forms which will be obtained after performing the path-integration. It is very interesting to investigate its path integral representation. As mentioned in the Introduction, boundary conditions are treated unambiguously in operator formalism by von Neumann's theory of self-adjoint extension. However, in path integral formalism we do not know *a priori* what kind of trajectories we should integrate over and what kind of "classical action" we should adopt as a weight. Indeed, even in the system of a free particle confined on an interval with an infinitely deep well potential, the "classical action" we should adopt as a path integral weight includes the so-called *topological term* that localizes at the boundaries [48]. Furthermore, this topological term is proportional to the Planck constant so that it is no longer classical.

A system on a circle in the presence of a single point interaction may provide one of the simplest theoretical laboratory for the study of path integral representation of the Feynman kernel. In such a system we have to consider the limit $N \to \infty$ of the equation:

$$\langle x'|\mathrm{e}^{-iHT}|x\rangle = \left[\prod_{n=1}^{N-1}\int_0^\ell \mathrm{d}x_n\right]\langle x'|\mathrm{e}^{-iH\delta t}|x_{N-1}\rangle\cdots\langle x_1|\mathrm{e}^{-iH\delta t}|x\rangle, \tag{4.72}$$

where $\delta t := T/N$. We already know the exact form of each partial amplitude $\langle x_{i+1}|\mathrm{e}^{-iH\delta t}|x_i\rangle$. In order to evaluate the right hand side we have to tackle with the $N-1$ products of both translational invariant and variant classes of infinite sums. For the case of a system on a circle in the presence of a scale-independent subfamily of point interactions studied in section 4.4.1.2, this procedure is easily performed. The resultant kernel takes the form[1]

$$\begin{aligned}
&\langle x'|\mathrm{e}^{-iHT}|x\rangle \\
&= \sum_{n\in\mathbb{Z}} W_{++}^{(n)}\left[\left(\frac{1}{\sqrt{4\pi i\delta t}}\right)^N\prod_{n=1}^{N-1}\int_{-\infty}^{\infty}\mathrm{d}x_n\right]\exp\left[i\sum_{j=1}^{N}\delta t\,\frac{1}{4}\left(\frac{x_j-x_{j-1}}{\delta t}\right)^2\right]_{x_0=x}^{x_N=n\ell+x'} \\
&+ \sum_{n\in\mathbb{Z}} W_{-+}^{(n)}\left[\left(\frac{1}{\sqrt{4\pi i\delta t}}\right)^N\prod_{n=1}^{N-1}\int_{-\infty}^{\infty}\mathrm{d}x_n\right]\exp\left[i\sum_{j=1}^{N}\delta t\,\frac{1}{4}\left(\frac{x_j-x_{j-1}}{\delta t}\right)^2\right]_{x_0=x}^{x_N=n\ell+(\ell-x')},
\end{aligned} \tag{4.73}$$

[1] In order to derive (4.73) we have only used the relations $W_{++}^{(-n)} = W_{--}^{(n)}$, $W_{-+}^{(-n)} = W_{+-}^{(n)}$, $W_{++}^{(n)}W_{++}^{(m)} + W_{+-}^{(n)}W_{-+}^{(m)} = W_{++}^{(n+m)}$ and $W_{-+}^{(n)}W_{++}^{(m)} + W_{--}^{(n)}W_{-+}^{(m)} = W_{-+}^{(n+m)}$ $(n, m \in \mathbb{Z})$ as well as the simple identity $\sum_{n\in\mathbb{Z}}\int_{n\ell}^{(n+1)\ell} = \int_{-\infty}^{\infty}$.

or, more symbolically (by taking the limit $N \to \infty$)[2],

$$\langle x'|\mathrm{e}^{-iHT}|x\rangle = \sum_{n\in\mathbb{Z}} W^{(n)}_{++} \int_{x(0)=x}^{x(T)=n\ell+x'} \mathcal{D}x(\tau)\, \exp\left[i\int_0^T \mathrm{d}\tau\, \frac{1}{4}\dot{x}^2(\tau)\right] + \sum_{n\in\mathbb{Z}} W^{(n)}_{-+} \int_{x(0)=x}^{x(T)=n\ell+(\ell-x')} \mathcal{D}x(\tau)\, \exp\left[i\int_0^T \mathrm{d}\tau\, \frac{1}{4}\dot{x}^2(\tau)\right], \tag{4.74}$$

where $W^{(n)}_{\pm\pm}$ is a weight factor given as the matrix element of the unitary matrix $W^{(n)} := (S\sigma_1)^n$ with $S$ being the S-matrix given in 4.4.1.2:

$$W^{(n)} = \begin{pmatrix} W^{(n)}_{++} & W^{(n)}_{+-} \\ W^{(n)}_{-+} & W^{(n)}_{--} \end{pmatrix} = \begin{pmatrix} \cos(n\theta) - i\cos\phi\sin(n\theta) & \sin\phi\sin(n\theta) \\ -\sin\phi\sin(n\theta) & \cos(n\theta) + i\cos\phi\sin(n\theta) \end{pmatrix}. \tag{4.75}$$

Although in Eq.(4.74) it is clear that the weight factors are given by the S-matrix elements, it is far from obvious what kind of "classical action" we should adopt as a path integral weight. Furthermore, for the case of weight factors that depend on the particle's momentum it is very difficult to discern any simple formulae for position-space path integral such as (4.74).

3. *Topology change.*
In this chapter we have considered the path integral description on a rose graph. One may wonder why should we concern a rose graph? We believe that it is a quite general setting in a sense that rose graph may provide any compact graph via its topology change. One of the simplest example of topology change is a transition from a circle to an interval. As we have seen, quantum systems on a circle with a single point interaction contains the separated subfamily, which is nothing but the system on an interval. From the perspective of the conservation of probability current density, $j(0) = j(\ell)$, it is obvious that the original requirement of the Kirchhoff's law clearly contains the weaker solution $j(0) = 0 = j(\ell)$, where no probability current flows at the origin. Then, resultant system is physically equivalent to that on an interval and admits $U(1) \times U(1)$ family of point interactions, where each $U(1)$ corresponds to the two ends of the interval.

A less trivial example is a topology change of a figure eight, which admits a $U(4)$ family of point interactions at the vertex. In group theoretical language, any topology change of a figure eight corresponds to the following reductions to its subgroups:

$$U(4) \to \begin{cases} U(1)\times U(1)\times U(1)\times U(1), \\ U(1)\times U(1)\times U(2), \\ U(1)\times U(3), \\ U(2)\times U(2). \end{cases} \tag{4.76}$$

Let us take a closer look at these four "symmetry breakdowns" in terms of the Kirchhoff's law and the S-matrix.

[2] It should be noted that in our units ($\hbar = 2m = 1$) the kinetic term $\frac{m}{2}\dot{x}^2$ becomes $\frac{1}{4}\dot{x}^2$.

(a) *Case* $U(4) \to U(1) \times U(1) \times U(1) \times U(1)$.
In this case the original requirement for the Kirchhoff's law reduces to the weakest one $j_1(0_1) = j_1(\ell_1) = j_2(0_2) = j_2(\ell_2) = 0$. The corresponding S-matrix turns out to be of the form

$$S \to \begin{pmatrix} R_1 & 0 & 0 & 0 \\ 0 & R_2 & 0 & 0 \\ 0 & 0 & R_3 & 0 \\ 0 & 0 & 0 & R_4 \end{pmatrix}, \tag{4.77}$$

which corresponds to the situation where a figure eight has snapped at the vertex and then been reduced to two disconnected intervals; see below.

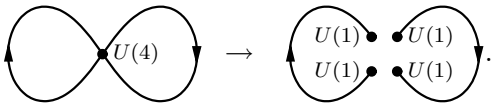


(b) *Case* $U(4) \to U(1) \times U(1) \times U(2)$.
In this case the original requirement for the Kirchhoff's law reduces to the less strong ones $j_1(0_1) = j_1(\ell_1) = 0 = j_2(0_2) - j_2(\ell_2)$, $j_1(0_1) - j_1(\ell_1) = 0 = j_2(0_2) = j_2(\ell_2)$, $j_1(0_1) = j_2(\ell_2) = 0 = j_1(\ell_1) - j_2(0_2)$. In terms of the S-matrix, these cases corresponds to the following three distinct reductions:

$$S \to \begin{pmatrix} R_1 & 0 & 0 & 0 \\ 0 & R_2 & 0 & 0 \\ 0 & 0 & R_3 & T_{34} \\ 0 & 0 & T_{43} & R_4 \end{pmatrix}, \begin{pmatrix} R_1 & T_{12} & 0 & 0 \\ T_{21} & R_2 & 0 & 0 \\ 0 & 0 & R_3 & 0 \\ 0 & 0 & 0 & R_4 \end{pmatrix}, \begin{pmatrix} R_1 & 0 & 0 & 0 \\ 0 & R_2 & T_{23} & 0 \\ 0 & T_{32} & R_3 & 0 \\ 0 & 0 & 0 & R_4 \end{pmatrix}, \tag{4.78}$$

which are, respectively, graphically depicted as follows:

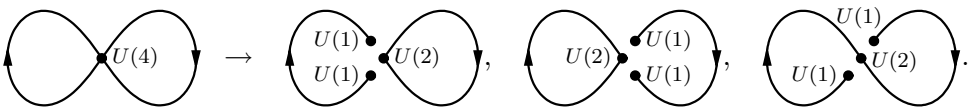


Thus in this case a figure eight breaks down to the system of two disconnected interval and circle, and a single interval.

(c) *Case* $U(4) \to U(1) \times U(3)$.
In this case the original requirement for the Kirchhoff's law reduces to the less strong conditions $j_1(0_1) = 0 = j_2(0_2) - j_1(\ell_1) - j_2(\ell_2)$ and $j_2(\ell_2) = 0 = j_1(0_1) + j_2(0_2) - j_1(\ell_1)$. Correspondingly, the S-matrix reduces to the following forms:

$$S \to \begin{pmatrix} R_1 & 0 & 0 & 0 \\ 0 & R_2 & T_{23} & T_{24} \\ 0 & T_{32} & R_3 & T_{34} \\ 0 & T_{42} & T_{43} & R_4 \end{pmatrix}, \begin{pmatrix} R_1 & T_{12} & T_{13} & 0 \\ T_{21} & R_2 & T_{23} & 0 \\ T_{31} & T_{32} & R_3 & 0 \\ 0 & 0 & 0 & R_4 \end{pmatrix}. \tag{4.79}$$

These situations are depicted below:

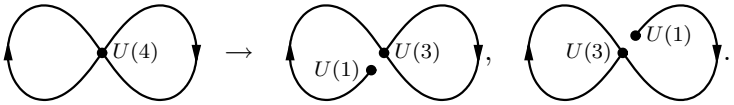


Thus in this case a figure eight breaks down to the system of tadpole.

(d) *Case* $U(4) \to U(2) \times U(2)$.
In this case the original requirement of the Kirchhoff's law is reduced to $j_1(0_1) - j_1(\ell_1) = 0 = j_2(0_2) - j_2(\ell_2)$ and $j_1(0_1) = j_2(\ell_2) = 0 = j_2(0_2) - j_1(\ell_1)$, where the S-matrix takes the forms

$$S \to \begin{pmatrix} R_1 & T_{12} & 0 & 0 \\ T_{21} & R_2 & 0 & 0 \\ 0 & 0 & R_3 & T_{34} \\ 0 & 0 & T_{43} & R_4 \end{pmatrix}, \begin{pmatrix} R_1 & 0 & 0 & T_{14} \\ 0 & R_2 & T_{23} & 0 \\ 0 & T_{32} & R_3 & 0 \\ T_{41} & 0 & 0 & R_4 \end{pmatrix}, \tag{4.80}$$

which are graphically depicted as follows:

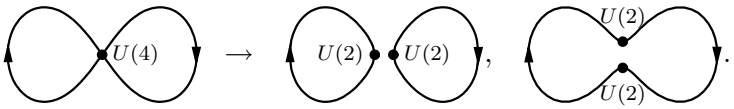


Thus in this case a figure eight breaks down to the system of two disconnected circles and a single circle (or oval).

As we have seen, quantum system on a figure eight contains as its subgroups the systems on two disconnected intervals, tadpoles, two circles, and so on. Along this thought, it is quite natural to expect that any compact graph can be generated by the topology change of corresponding rose graph. For example, six-petal rose must contain a tetrahedron and a hexagon (see below):

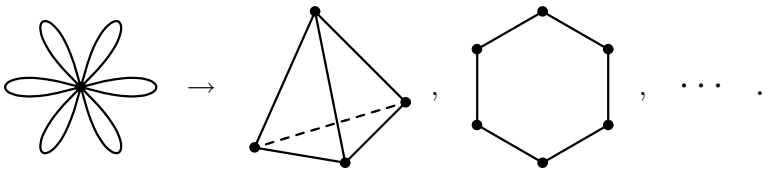

| 6-petal rose | tetrahedron | hexagon |
|---|---|---|
| $U(12)$ | $U(3)^4$ | $U(2)^6$ |

However, a systematic classification of topology change of rose graph in a general setting is quite involved so that we will not concern this issue anymore in this dissertation. We would like to report these issues elsewhere.

# Chapter 5

# Worldline formalism with extra dimension

In this chapter we derive the master formulae for scalar one-loop amplitude with arbitrary number of external gauge bosons in Abelian gauge theory in $D$-dimensional spacetime with a single extra dimension compactified on a circle.

## 5.1 Introduction

A bit surprisingly, quantum mechanics on a graph we have studied so far is also applicable to perturbative quantum field theory. The reason is twofold. The first is so simple; because Feynman graphs are indeed graphs. In the first-quantization approach to quantum field theory, nowadays dubbed as the worldline or "string-inspired" formalism (see for review [59]), a virtual particle circulating along internal lines of a given Feynman diagram is identified as a single relativistic quantum mechanical particle traveling along its spacetime trajectory (i.e. worldline) in the presence of some background fields. In such an approach, first introduced by Feynman in his seminal paper [60], S-matrix elements are obtained by single-particle path integrals over all possible worldlines of given topology, or graph, corresponding to a given Feynman diagrams. There, worldline Green's functions on one-dimensional arbitrary graphs are needed for computations of arbitrary Feynman diagrams [61–63]. It is now known that worldline approach to perturbative quantum field theory generally provides a powerful alternative method for the computation of S-matrix elements and effective action [14, 59, 64–67], whereas from the perspective of Lagrangians or off-shell Feynman rules it is very difficult to discern any simple formulae for field theory amplitudes.

The second reason arises when one considers perturbative quantum field theory with a single extra compact dimension in the presence of defects, or boundaries, where extra dimensional space can be viewed as a one-dimensional system with point interactions. Worldline formulation on such a spacetime requires a knowledge for the path integral representation of a quantum mechanical particle in a one-dimensional space with point interactions, which we already addressed and solved in general in the previous chapter 4.

An important point to note is that, thanks to its nature of path integral, in the worldline formalism it is much clear how many times a virtual particle winds around the direction of an extra dimension, on account of winding number. Winding number plays an important role in extra dimensional models because any non-zero winding contributions are essentially

UV finite thanks to its long-distance natures: If one computes a radiative correction of a quantity that naively diverges in UV as $\sim \Lambda^D$ with $\Lambda$ being a cutoff scale, then such a loop induced correction from non-zero winding contributions must be of the form $\sim \sum_{w\in\mathbb{Z}} C^{(w)}(wL)^{-D}$, where $w$ is the winding number, $L$ is a circumference of extra dimension and $C^{(w)}$ is a possible ($w$-dependent) dimensionless coefficient. This estimation follows from the dimensional analysis and the fact that internal line winding around the extra dimension $w$ times cannot be shorter than $wL$ and hence it plays a role of a cutoff length scale for $w$-winding sector. The sum $\sum_{w\in\mathbb{Z}}$ ensures the summation of all possible physically distinct closed loops, which goes quite well with the philosophy of path integral. Thus, determination of whether given S-matrix elements are those from the contributions of zero- or non-zero winding is an essentially significant problem especially for the perturbative renormalization procedures and/or classification of UV finite quantities such as the Higgs mass in the gauge-Higgs unification scenario in a quantitative level.

Concerning these facts, in this chapter we attempt to construct a worldline formalism for perturbative quantum field theory with a single extra dimension. For the sake of simplicity, in this chapter we consider a massive scalar field theory in the presence of a background Abelian gauge field with a single extra dimension compactified on a circle. As shown in the rest of this chapter, scalar one-loop amplitude of $N$ external gauge bosons with definite momentum $k_j^\mu$ ($j = 1, \cdots, N$), Kaluza-Klein mode $k_j^y = \frac{2\pi n_j}{L}$ ($n_j$: integer) and polarization $\epsilon_j^M = (\epsilon_j^\mu, \epsilon_j^y)$ is given by the following Gaussian path-integral

$$i\Gamma_N[k_1,\epsilon_1;\cdots;k_N,\epsilon_N] = \sum_{w\in\mathbb{Z}}\int_0^\infty \frac{\mathrm{d}T}{T}\,\mathrm{e}^{-im^2T}\int_{x(T)=x(0)}\mathcal{D}x\int_{y(T)=y(0)+wL}\mathcal{D}y \times V_1[k_1,\epsilon_1]\cdots V_N[k_N,\epsilon_N]\exp\left[i\int_0^T \mathrm{d}\tau\,\frac{1}{4}\dot{X}^2(\tau)\right], \tag{5.1}$$

where $V_j[k_j,\epsilon_j]$ is the *vertex operator* given by

$$V_j[k_j,\epsilon_j] = ig\int_0^T \mathrm{d}\tau_j\,\epsilon_j\cdot\dot{X}(\tau_j)\mathrm{e}^{ik_j\cdot X(\tau_j)}, \tag{5.2}$$

with $g$ being the gauge coupling. As mentioned before, the path-integral (5.1) corresponds to first quantization of perturbative quantum field theory in a sense that it describes a *single* point particle propagating in a given spacetime in the presence of a given background gauge field. The parameter $\tau \in (0,T)$ parameterizes the worldline of a particle, where $T$ is the so-called Schwinger's propertime and integrated over the range $(0,\infty)$. Larger value of $T$ corresponds to the larger extent of worldline in the spacetime so that $T$ also provides a smooth regulator scale [68]. In section 5.2.1, it turns out that any contributions from $w$-winding sector are suppressed by the factor $\exp[-(wL)^2/T_E]$ for small $T_E$, as they should in a respect that classically there are no short-distance UV fluctuations shorter than the scale $wL$. The coordinate field $X^M(\tau) = (x^\mu(\tau), y(\tau))$ is defined on the worldline (target space) and describes the position of a scalar particle in a background spacetime. The integral $\int\mathcal{D}x\int\mathcal{D}y$ is performed over the space of all closed trajectories swept by the point particle with a definite winding number $w$, which described by the boundary conditions $(x^\mu(T), y(T)) = (x^\mu(0), y(0)+wL)$. The sum $\sum_{w\in\mathbb{Z}}$ ensures the path-integration over all topologically (or physically) distinct closed trajectories winding around the extra spatial dimension $S^1$.

The rest of this chapter is organized as follows. In section 5.2 we derive the master formulae for scalar one-loop amplitudes in Abelian gauge theory with a single extra dimension

$S^1$. In section 5.3 we demonstrate an explicit example of vacuum polarization. We conclude in section 5.4.

## 5.2 One-loop master formula for gauge theory amplitudes

Let us consider a scalar field theory with a background Abelian gauge field $A_M = (A_\mu, A_y)$ in $D = d + 1$-dimensional spacetime with a single extra dimension conpactified on a circle of circumference $L$. The action we consider is

$$\begin{aligned} S[\phi, \phi^*, A] &= \int \mathrm{d}^d x \int_0^L \mathrm{d}y \, \left[ -\eta^{MN} (D_M \phi)^* (D_N \phi) - m^2 \phi^* \phi \right] \\ &= - \int \mathrm{d}^d x \int_0^L \mathrm{d}y \, \phi^* \left( -D^2 + m^2 \right) \phi, \end{aligned} \tag{5.3}$$

where $\eta_{MN} = \eta^{MN} = \mathrm{diag}(-1, +1, \ldots, +1)$ and $D_M = \partial_M - igA_M$. The partition function is therefore

$$Z[A] = \frac{\int \mathcal{D}\phi \mathcal{D}\phi^* \exp(iS[\phi, \phi^*, A])}{\int \mathcal{D}\phi \mathcal{D}\phi^* \exp(iS[\phi, \phi^*, A = 0])} = \exp\left[ -\mathrm{Tr} \log \frac{-D^2 + m^2}{-\partial^2 + m^2} \right]. \tag{5.4}$$

The one-loop effective action is thus given by

$$i\Gamma[A] = -\mathrm{Tr} \log \frac{-(\partial_M - igA_M)^2 + m^2}{-\partial^2 + m^2}. \tag{5.5}$$

Noting that the elementary identity[1]

$$-\mathrm{Tr} \log \frac{\hat{H}}{\hat{H}_0} = \int_0^\infty \frac{\mathrm{d}T}{T} \, \mathrm{Tr}(\mathrm{e}^{-i\hat{H}T} - \mathrm{e}^{-i\hat{H}_0 T}), \tag{5.6}$$

where $\hat{H}$ and $\hat{H}_0$ are assumed to be positive definite, and taking the functional trace over the coordinate space, $\mathrm{Tr}\, \hat{O} = \int \mathrm{d}^d x \int_0^L \mathrm{d}y \, \langle x, y | \hat{O} | x, y \rangle$, we get

$$\begin{aligned} i\Gamma[A] = &\int_0^\infty \frac{\mathrm{d}T}{T} \int \mathrm{d}^d x \int_0^L \mathrm{d}y \, \left\langle x, y \middle| \exp\left( -i \left[ -(\partial_M - igA_M)^2 + m^2 \right] T \right) \middle| x, y \right\rangle \\ &- (A \to 0). \end{aligned} \tag{5.7}$$

[1] To derive this, consider the arithmetic

$$\log x = \int_1^x \frac{\mathrm{d}y}{y} = i \int_1^x \mathrm{d}y \int_0^\infty \mathrm{d}t \, \mathrm{e}^{-iyt} = - \int_0^\infty \frac{\mathrm{d}t}{t} \left( \mathrm{e}^{-ixt} - \mathrm{e}^{-it} \right), \quad x > 0. \tag{f5.1}$$

Next, the matrix element of $\exp\left(-i\left[-(\partial_M - igA_M)^2 + m^2\right]T\right)$ on $\mathbb{R}^{d-1,1} \times S^1$ has the following path-integral representation[2]

$$\begin{aligned}&\left\langle x', y'\middle|\exp\left(-i\left[-(\partial_M - igA_M)^2 + m^2\right]T\right)\middle|x, y\right\rangle \\ &= \mathrm{e}^{-im^2T}\sum_{w\in\mathbb{Z}}\int_{x(0)=x}^{x(T)=x'}\mathcal{D}x\int_{y(0)=y}^{y(T)=y'+wL}\mathcal{D}y\,\exp\left[i\int_0^T\mathrm{d}\tau\left(\frac{1}{4}\dot{X}^2(\tau) + gA(X(\tau))\cdot\dot{X}(\tau)\right)\right],\end{aligned} \tag{5.8}$$

where $w$ is the *winding number*, $w \in \pi_1(S^1) \simeq \mathbb{Z}$. Taking into account that

$$\int\mathrm{d}^dx\int_0^L\mathrm{d}y\int_{x(0)=x}^{x(T)=x}\mathcal{D}x\int_{y(0)=y}^{y(T)=y+wL}\mathcal{D}y = \int_{x(T)=x(0)}\mathcal{D}x\int_{y(T)=y(0)+wL}\mathcal{D}y, \tag{5.9}$$

we get

$$\begin{aligned}i\Gamma[A] = \sum_{w\in\mathbb{Z}}\int_0^\infty\frac{\mathrm{d}T}{T}\,\mathrm{e}^{-im^2T}\int_{x(T)=x(0)}\mathcal{D}x\int_{y(T)=y(0)+wL}\mathcal{D}y \\ \times\exp\left[i\int_0^T\mathrm{d}\tau\left(\frac{1}{4}\dot{X}^2(\tau) + gA(X(\tau))\cdot\dot{X}(\tau)\right)\right] - (A\to 0).\end{aligned} \tag{5.10}$$

Next we expand the exponential in the following perturbative series

$$\exp\left[i\int_0^T\mathrm{d}\tau\, gA(X(\tau))\cdot\dot{X}(\tau)\right] = 1 + \sum_{N=1}^\infty\frac{(ig)^N}{N!}\prod_{j=1}^N\left[\int_0^T\mathrm{d}\tau_j\, A(X(\tau_j))\cdot\dot{X}(\tau_j)\right]. \tag{5.11}$$

Notice that the first term correctly eliminates the vacuum bubble diagram, or $A_M$-independent contribution $(A \to 0)$, as it should.

Now specializing to the incoming plane wave background with definite momentum $k_j^M = (k_j^\mu, k_j^y = \frac{2\pi n_j}{L})$ and polarization $\epsilon_j^M$

$$A_M(X(\tau)) = \sum_{j=1}^N\epsilon_{jM}\mathrm{e}^{ik_j\cdot X(\tau)}, \tag{5.12}$$

and picking out a term including each mode $j$ once, which eliminates the combinatorics factor $1/N!$, we arrive at the $N$-point gauge boson amplitude

$$\begin{aligned}i\Gamma_N[k_1,\epsilon_1;\cdots;k_N,\epsilon_N] = (ig)^N\sum_{w\in\mathbb{Z}}\int_0^\infty\frac{\mathrm{d}T}{T}\,\mathrm{e}^{-im^2T}\int_{x(T)=x(0)}\mathcal{D}x\int_{y(T)=y(0)+wL}\mathcal{D}y \\ \times\prod_{j=1}^N\left[\int_0^T\mathrm{d}\tau_j\,\epsilon_j\cdot\dot{X}(\tau_j)\mathrm{e}^{ik_j\cdot X(\tau_j)}\right]\exp\left[i\int_0^T\mathrm{d}\tau\,\frac{1}{4}\dot{X}^2(\tau)\right].\end{aligned} \tag{5.13}$$

This is the expression advertised in section 5.1. In the subsequent three sections we will evaluate Eq.(5.13) step by step.

[2] A Feynman kernel for a nonrelativistic particle in the presence of a background vector potential described by the Hamiltonian $H = \frac{1}{2m}\left(-i\hbar\vec{\nabla} - \frac{e}{c}\vec{A}(\vec{x})\right)^2 + V(\vec{x})$ is given by

$$\langle\vec{x}|\exp\left(-\frac{i}{\hbar}\hat{H}T\right)|\vec{y}\rangle = \int_{\vec{x}(0)=\vec{y}}^{\vec{x}(T)=\vec{x}}\mathcal{D}x\exp\left[\frac{i}{\hbar}\int_0^T\mathrm{d}\tau\left(\frac{m}{2}\left(\frac{\mathrm{d}\vec{x}(\tau)}{\mathrm{d}\tau}\right)^2 + \frac{e}{c}\vec{A}(\vec{x}(\tau))\cdot\frac{\mathrm{d}\vec{x}(\tau)}{\mathrm{d}\tau} - V(\vec{x}(\tau))\right)\right]. \tag{f5.2}$$

### 5.2.1 Separation of zero-mode

Observe that both $\int \mathcal{D}x$ and $\int \mathcal{D}y$ contain the integration over the constant loop, i.e. the zero-mode of the Laplace operator on a loop. The presence of the zero-mode is due to the translational invariance on a loop and, as we will see soon, the path-integration over this zero-mode just reduces to the total momentum conservation. It should also be pointed out that we must get rid of the zero-mode to obtain the well-defined inverse of the Laplace operator, or Green's function. To this end, we first note that the bosonic free coordinate field $X^M(\tau) = (x^\mu(\tau), y(\tau))$ subject to the boundary conditions $x^\mu(T) = x^\mu(0)$ and $y(T) = y(0) + wL$ can be decomposed into the following mode-expansions

$$x^\mu(\tau) = x_0^\mu + \frac{1}{\sqrt{T}} \sum_{n=1}^{\infty} \left( \alpha_n^\mu \mathrm{e}^{i\frac{2\pi n}{T}\tau} + (\alpha_n^\mu)^* \mathrm{e}^{-i\frac{2\pi n}{T}\tau} \right), \tag{5.14a}$$

$$y(\tau) = y_0 + \frac{wL}{T}\tau + \frac{1}{\sqrt{T}} \sum_{n=1}^{\infty} \left( \alpha_n^y \mathrm{e}^{i\frac{2\pi n}{T}\tau} + (\alpha_n^y)^* \mathrm{e}^{-i\frac{2\pi n}{T}\tau} \right). \tag{5.14b}$$

We separate these dangerous zero-modes by introducing new coordinate field $\tilde{X}^M(\tau) = (\tilde{x}^\mu(\tau), \tilde{y}(\tau))$:

$$\tilde{x}^\mu(\tau) := x^\mu(\tau) - x_0^\mu, \tag{5.15a}$$

$$\tilde{y}(\tau) := y(\tau) - \left( y_0 + \frac{wL}{T}\tau \right). \tag{5.15b}$$

There are three important issues with this separation of zero-modes:

1. *Integration measure.*
   By substituting the new coordinate field, the integration measure becomes

$$\begin{aligned} \int_{x(T)=x(0)} \mathcal{D}x \int_{y(T)=y(0)+wL} \mathcal{D}y &= \int \mathrm{d}^d x_0 \int_{\tilde{x}(T)=\tilde{x}(0)} \mathcal{D}\tilde{x} \int_0^L \mathrm{d}y_0 \int_{\tilde{y}(T)=\tilde{y}(0)} \mathcal{D}\tilde{y} \\ &= \int \mathrm{d}^d x_0 \int_0^L \mathrm{d}y_0 \int_{\tilde{X}(T)=\tilde{X}(0)} \mathcal{D}\tilde{X}, \end{aligned} \tag{5.16a}$$

   where $\tilde{X}^M(\tau) = (\tilde{x}^\mu(\tau), \tilde{y}(\tau))$.

2. *Free worldline action.*
   The free worldline action becomes

$$\int_0^T \mathrm{d}\tau \, \frac{1}{4}\dot{X}^2(\tau) = \frac{(wL)^2}{4T} + \int_0^T \mathrm{d}\tau \, \frac{1}{4}\dot{\tilde{X}}^2(\tau). \tag{5.17}$$

   Notice that the first term after the Wick rotation $T \to -iT_E$ ensures the total convergence (or UV cutoff independence) of amplitude for nonzero winding sector thanks to the exponential suppression factor $\exp[-(wL)^2/4T_E] \overset{T_E \to 0}{\to} 0$ for $w \neq 0$.

3. *Vertex operator.*
   The vertex operator becomes

$$\begin{aligned} &\prod_{j=1}^N \left[ \int_0^T \mathrm{d}\tau_j \, \epsilon_j \cdot \dot{X}(\tau_j) \mathrm{e}^{ik_j \cdot X(\tau_j)} \right] \\ &= \mathrm{e}^{i(k_1 + \cdots + k_N)\cdot X_0} \prod_{j=1}^N \left[ \int_0^T \mathrm{d}\tau_j \, \epsilon_j \cdot \left( V + \dot{\tilde{X}}(\tau_j) \right) \mathrm{e}^{ik_j \cdot (V\tau + \tilde{X}(\tau_j))} \right], \end{aligned} \tag{5.18}$$

where $X_0^M := (x_0^\mu, y_0)$, $V^M := (0^\mu, wL/T)$ and $\tilde{X}^M(\tau) := (\tilde{x}^\mu(\tau), \tilde{y}(\tau))$. Notice that the factor $\mathrm{e}^{i(k_1+\cdots+k_N)\cdot X_0}$ with the integral $\int \mathrm{d}^d x_0 \int_0^L \mathrm{d}y_0$ just produces the total momentum conservation:

$$\int \mathrm{d}^d x_0 \int_0^L \mathrm{d}y_0 \, \mathrm{e}^{i(k_1+\cdots+k_N)\cdot X_0} = (2\pi)^d \delta^{(d)}(k_1^\mu + \cdots + k_N^\mu) \cdot L\delta_{n_1+\cdots+n_N,0}. \tag{5.19}$$

### 5.2.2 Completing the square and performing the path-integration

Note that the vertex operators can be rewritten as follows

$$\begin{aligned}\prod_{j=1}^N \left[\int_0^T \mathrm{d}\tau_j \, \epsilon_j \cdot \left(V + \dot{\tilde{X}}(\tau_j)\right) \mathrm{e}^{ik_j\cdot(V\tau + \tilde{X}(\tau_j))}\right] &= \left[\prod_{j=1}^N \int_0^T \mathrm{d}\tau_j\right] \\ \times \exp\left[\sum_{j=1}^N (\epsilon_j + i\tau_j k_j)\cdot V + i\int_0^T \mathrm{d}\tau \, J(\tau; \{\tau_j, k_j, \epsilon_j\}_{j=1}^N)\cdot \tilde{X}(\tau)\right]&\Bigg|_{\text{linear in each } \epsilon_j}\end{aligned} \tag{5.20}$$

where the source field $J^M$ is defined by

$$J^M(\tau; \{\tau_j, k_j, \epsilon_j\}_{j=1}^N) := \sum_{j=1}^N \delta(\tau - \tau_j)\left(-i\epsilon_j^M \frac{\mathrm{d}}{\mathrm{d}\tau} + k_j^M\right). \tag{5.21}$$

$J^M$ represents the point sources localized on the positions of vertex operators $\tau = \tau_j$. Then, the $N$ gauge boson amplitude becomes

$$\begin{aligned}i\Gamma_N[k_1, \epsilon_1; \cdots; k_N, \epsilon_N] &= (ig)^N (2\pi)^d L\delta^{(d)}(k_1^\mu + \cdots + k_2^\mu)\delta_{n_1+\cdots+n_N,0} \\ \times \sum_{w\in\mathbb{Z}} \int_0^\infty \frac{\mathrm{d}T}{T} \mathrm{e}^{-im^2T + i(wL)^2/4T} &\left[\prod_{j=1}^N \int_0^T \mathrm{d}\tau_j\right] \exp\left[\sum_{j=1}^N (\epsilon_j + i\tau_j k_j)\cdot V\right] \\ \times \int_{\tilde{X}(T)=\tilde{X}(0)} \mathcal{D}\tilde{X} \exp\left[i\int_0^T \mathrm{d}\tau \left(\frac{1}{4}\dot{\tilde{X}}^2(\tau) + J(\tau)\cdot\tilde{X}(\tau)\right)\right]&\Bigg|_{\text{linear in each } \epsilon_j}.\end{aligned} \tag{5.22}$$

Let us next perform the path-integration over the coordinate field $\tilde{X}$. To this end, we first integrate the worldline action by parts:

$$\int_0^T \mathrm{d}\tau \left[\frac{1}{4}\dot{\tilde{X}}^2(\tau) + J(\tau)\cdot\tilde{X}(\tau)\right] = \int_0^T \mathrm{d}\tau \left[\frac{1}{2}\tilde{X}(\tau)\cdot\left(-\frac{1}{2}\frac{\mathrm{d}^2}{\mathrm{d}\tau^2}\tilde{X}(\tau)\right) + J(\tau)\cdot\tilde{X}(\tau)\right]. \tag{5.23}$$

By shifting the variable

$$\tilde{X}^M(\tau) \to \tilde{X}^M(\tau) - \int_0^T \mathrm{d}\tau' J^{M*}(\tau') G_B(\tau - \tau'), \tag{5.24}$$

where $G_B(\tau - \tau')$ is the bosonic worldline Green's function defined by

$$-\frac{1}{2}\frac{\mathrm{d}^2}{\mathrm{d}\tau^2} G_B(\tau - \tau') = \delta(\tau - \tau'), \tag{5.25}$$

the worldline action becomes

$$\int_0^T \mathrm{d}\tau\, \frac{1}{2}\tilde{X}(\tau)\cdot\left(-\frac{1}{2}\frac{\mathrm{d}^2}{\mathrm{d}\tau^2}\tilde{X}(\tau)\right) - \frac{1}{2}\int_0^T \mathrm{d}\tau \int_0^T \mathrm{d}\tau' J(\tau)\cdot J^*(\tau')G_B(\tau-\tau'). \tag{5.26}$$

The Gaussian path integral that correspond to the first term is now easily performed with the result

$$\int_{\tilde{X}(T)=\tilde{X}(0)} \mathcal{D}\tilde{X}\exp\left[i\int_0^T \mathrm{d}\tau\, \frac{1}{4}\dot{\tilde{X}}^2(\tau)\right] = (4\pi i T)^{-D/2}. \tag{5.27}$$

Let us next evaluate the second term of the integral

$$\begin{aligned}
&\int_0^T \mathrm{d}\tau \int_0^T \mathrm{d}\tau' J(\tau)\cdot J^*(\tau')G_B(\tau-\tau') \\
&= \sum_{i,j=1}^N \int_0^T \mathrm{d}\tau \int_0^T \mathrm{d}\tau' \delta(\tau-\tau_i)\delta(\tau'-\tau_j)\left(-i\epsilon_i\frac{\mathrm{d}}{\mathrm{d}\tau}+k_i\right)\cdot\left(+i\epsilon_j\frac{\mathrm{d}}{\mathrm{d}\tau'}+k_j\right)G_B(\tau-\tau') \\
&= \sum_{i,j=1}^N \left[k_i\cdot k_j G_B(\tau_i-\tau_j) - 2i\epsilon_i\cdot k_j\dot{G}_B(\tau_i-\tau_j) - \epsilon_i\cdot\epsilon_j\ddot{G}_B(\tau_i-\tau_j)\right].
\end{aligned} \tag{5.28}$$

As we will see below, the worldline Green's function is a symmetric function, $G_B(\tau_i-\tau_j)=G_B(\tau_j-\tau_i)$, so that its first and second derivatives are antisymmetric and symmetric functions, respectively: $\dot{G}_B(\tau_i-\tau_j)=-\dot{G}_B(\tau_j-\tau_i)$ and $\ddot{G}_B(\tau_i-\tau_j)=\ddot{G}_B(\tau_j-\tau_i)$. Taking into account these facts, Eq.(5.28) becomes

$$2\sum_{i>j=1}^N \left[k_i\cdot k_j G_B(\tau_i-\tau_j) - i(\epsilon_i\cdot k_j-\epsilon_j\cdot k_i)\dot{G}_B(\tau_i-\tau_j) - \epsilon_i\cdot\epsilon_j\ddot{G}_B(\tau_i-\tau_j)\right]. \tag{5.29}$$

Substituting these into Eq.(5.22) we obtain the following parameter integral representation of the $N$ gauge boson amplitude

$$\begin{aligned}
&i\Gamma_N[k_1,\epsilon_1;\cdots;k_N,\epsilon_N] \\
&= (ig)^N(2\pi)^d L\delta^{(d)}(k_1^\mu+\cdots+k_2^\mu)\delta_{n_1+\cdots+n_N,0}\sum_{w\in\mathbb{Z}}\int_0^\infty \frac{\mathrm{d}T}{T}(4\pi i T)^{-D/2}\mathrm{e}^{-im^2T+i(wL)^2/4T} \\
&\times\left[\prod_{j=1}^N\int_0^T \mathrm{d}\tau_j\right]\exp\left[\sum_{j=1}^N i\tau_j k_j\cdot V - i\sum_{i>j=1}^N k_i\cdot k_j G_B(\tau_i-\tau_j)\right] \\
&\times\exp\left[\sum_{j=1}^N \epsilon_j\cdot V + \sum_{i>j=1}^N\left(-(\epsilon_i\cdot k_j-\epsilon_j\cdot k_i)\dot{G}_B(\tau_i-\tau_j)+i\epsilon_i\cdot\epsilon_j\ddot{G}_B(\tau_i-\tau_j)\right)\right]\Bigg|_{\text{linear in each }\epsilon_j}.
\end{aligned} \tag{5.30}$$

### 5.2.3 Worldline Green's function

Let us consider the inverse of the Hamiltonian operator $H = -\frac{1}{2}\frac{\mathrm{d}^2}{\mathrm{d}\tau^2}$ on the reduced Hilbert space spanned by the (incomplete) orthonormal basis $\left\{ \frac{1}{\sqrt{T}} \mathrm{e}^{i2\pi n\tau/T} \,\middle|\, n \in \mathbb{Z} \setminus \{0\} \right\}$.

$$\begin{aligned}\langle \tau_1 | \hat{H}^{-1} | \tau_2 \rangle &= \frac{T}{\pi^2} \sum_{n=1}^{\infty} \frac{\cos(2\pi n(\tau_1 - \tau_2)/T)}{n^2} \\ &= T \left[ \left( \frac{\tau_1 - \tau_2}{T} \right)^2 - \left| \frac{\tau_1 - \tau_2}{T} \right| + \frac{1}{6} \right], \quad -T \le \tau_1 - \tau_2 \le T, \end{aligned} \tag{5.31}$$

where the second equality follows from the formula

$$\sum_{n=1}^{\infty} \frac{\cos(nx)}{n^2} = \frac{1}{4}(x^2 - 2\pi|x|) + \frac{\pi^2}{6}, \quad -2\pi \le x \le 2\pi. \tag{5.32}$$

It should be noted that the $\tau$-independent term $T/6$ in Eq.(5.31) does not affect to the amplitude because it appears only in the exponent $\sum_{i,j=1}^{N} k_i \cdot k_j G_B(\tau_i - \tau_j)$ and the term $(\text{const}) \times \sum_{i,j=1}^{N} k_i \cdot k_j = (\text{const}) \times (k_1 + \cdots + k_N)^2$ always vanishes thanks to the total momentum conservation $\delta^{(d)}(k_1^\mu + \cdots + k_N^\mu)\delta_{n_1+\cdots+n_N,0}$. Thus without any loss of generality we can omit any constant term in Eq.(5.31) and thus obtain the following *primed* Green's function

$$G'_B(\tau_1 - \tau_2) = T \left[ \left( \frac{\tau_1 - \tau_2}{T} \right)^2 - \left| \frac{\tau_1 - \tau_2}{T} \right| \right], \tag{5.33}$$

where prime ($\prime$) indicates the exclusion of the zero-mode contribution. Its first and second derivatives are

$$\dot{G}'_B(\tau_1 - \tau_2) = \frac{2(\tau_1 - \tau_2)}{T} - \mathrm{sign}(\tau_1 - \tau_2), \tag{5.34a}$$

$$\ddot{G}'_B(\tau_1 - \tau_2) = 2\left[ \frac{1}{T} - \delta(\tau_1 - \tau_2) \right]. \tag{5.34b}$$

Notice that the primed Green's function satisfies the differential equation

$$-\frac{1}{2}\frac{\mathrm{d}^2}{\mathrm{d}\tau_1^2} G'_B(\tau_1 - \tau_2) = \delta(\tau_1 - \tau_2) - \frac{1}{T} = \sum_{n \in \mathbb{Z}\setminus\{0\}} \frac{\mathrm{e}^{i2\pi n(\tau_1 - \tau_2)/T}}{T}, \tag{5.35}$$

which is consistent with the exclusion of the zero-mode contribution.

## 5.3 Example: vacuum polarization

As a demonstration of the power of the formula, in this Section we compute the vacuum polarization $\Pi_{MN}$ defined as

$$i\Gamma_2[k_1, \epsilon_1; k_2, \epsilon_2] = (2\pi)^d L \delta^{(d)}(k_1^\mu + k_2^\mu)\delta_{n_1+n_2,0} \epsilon_1^M \epsilon_2^N i\Pi_{MN}[k_1, k_2]. \tag{5.36}$$

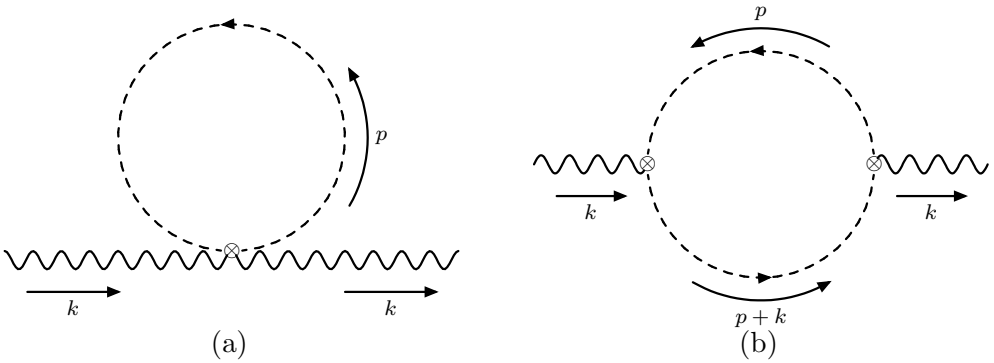


Figure 5.1: Vacuum polarization. $k^M = (k^\mu, \frac{2\pi n}{L})$ and $p^M = (p^\mu, \frac{2\pi l}{L})$.

To this end we first extract the multilinear terms of $\epsilon_j$ from the exponential.

$$\exp\left[\sum_{j=1}^{2}\epsilon_j\cdot V+\sum_{i>j=1}^{2}\Big(-(\epsilon_i\cdot k_j-\epsilon_j\cdot k_i)\dot{G}_B(\tau_i-\tau_j)+i\epsilon_i\cdot\epsilon_j\ddot{G}_B(\tau_i-\tau_j)\Big)\right]\Bigg|_{\text{linear in each }\epsilon_j}$$
$$=\epsilon_1^M\epsilon_2^N\left[\Big(-k_2\dot{G}_B(\tau_1-\tau_2)+V\Big)_M\Big(k_1\dot{G}_B(\tau_1-\tau_2)+V\Big)_N+i\eta_{MN}\ddot{G}_B(\tau_1-\tau_2)\right]. \quad (5.37)$$

Thus, taking the total momentum conservation $k_1 = -k_2(=: k)$ into account, we obtain the following parameter integral representation of the vacuum polarization

$$\begin{aligned}i\Pi_{MN}[k] = (ig)^2\sum_{w\in\mathbb{Z}}\int_0^\infty\frac{\mathrm{d}T}{T}(4\pi iT)^{-D/2}\mathrm{e}^{-im^2T+i(wL)^2/4T}\\ \times\int_0^T\mathrm{d}\tau_1\int_0^T\mathrm{d}\tau_2\,\mathrm{e}^{i(\tau_1-\tau_2)k\cdot V+ik^2G_B(\tau_1-\tau_2)}\\ \times\left[\Big(k\dot{G}_B(\tau_1-\tau_2)+V\Big)_M\Big(k\dot{G}_B(\tau_1-\tau_2)+V\Big)_N+i\eta_{MN}\ddot{G}_B(\tau_1-\tau_2)\right]. \quad (5.38)\end{aligned}$$

As a check let us compute the vacuum polarization using the Feynman rules. At one-loop order there are two Feynman diagrams that contribute to the vacuum polarization.

$$\text{(a)} = -i2g^2\eta_{MN}\sum_{w\in\mathbb{Z}}\int\frac{\mathrm{d}^Dp}{(2\pi)^D}\frac{i\mathrm{e}^{ip_ywL}}{-p^2-m^2+i\epsilon}, \quad (5.39)$$

where we have used the Poisson summation formula

$$\frac{1}{L}\sum_{l\in\mathbb{Z}}\delta(p_y-\tfrac{2\pi l}{L}) = \frac{1}{2\pi}\sum_{w\in\mathbb{Z}}\mathrm{e}^{ip_ywL}. \quad (5.40)$$

Using the Schwinger's parameterization and shifting the variable $p_y \to p_y + wL/2T$, we get

$$\text{(a)} = -2ig^2\eta_{MN}\sum_{w\in\mathbb{Z}}\int_0^\infty\mathrm{d}T\,\mathrm{e}^{-iT(m^2-i\epsilon)+i(wL)^2/4T}\int\frac{\mathrm{d}^Dp}{(2\pi)^D}\,\mathrm{e}^{-iTp^2} \quad (5.41)$$

The momentum integral is now Gaussian and is easily performed with the result

$$\text{(a)} = -2g^2\eta_{MN}\sum_{w\in\mathbb{Z}}\int_0^\infty \mathrm{d}T\,(4\pi iT)^{-D/2}\mathrm{e}^{-iT(m^2-i\epsilon)+i(wL)^2/4T}. \tag{5.42}$$

Next evaluate the second diagram (b):

$$\text{(b)} = (ig)^2\sum_{w\in\mathbb{Z}}\int\frac{\mathrm{d}^Dp}{(2\pi)^D}\frac{i^2(2p+k)_M(2p+k)_N\mathrm{e}^{ip_ywL}}{(-p^2-m^2+i\epsilon)(-(p+k)^2-m^2+i\epsilon)}, \tag{5.43}$$

where we have again used the Poisson summation formula. Successive use of the Feynman's parameter formula and the Schwinger's parameterization yields

$$\begin{aligned}\text{(b)} = (ig)^2\sum_{w\in\mathbb{Z}}\int_0^1\mathrm{d}x\int_0^\infty\mathrm{d}T T\int\frac{\mathrm{d}^Dp}{(2\pi)^D}(-2i\partial_v+k)_M(-2i\partial_v+k)_N\\ \times\mathrm{e}^{ip\cdot v+iT[-p^2-m^2+i\epsilon-x(k^2+2p\cdot k)]}\Big|_{v^M=(0^\mu,wL)}.\end{aligned} \tag{5.44}$$

Completing the square with respect to $p$ and shifting the variable $p\to p-xk+v/2T$, we get

$$\begin{aligned}\text{(b)} = (ig)^2\sum_{w\in\mathbb{Z}}\int_0^1\mathrm{d}x\int_0^\infty\mathrm{d}T T\,\mathrm{e}^{-iT[m^2-i\epsilon+x(1-x)k^2]}\\ \times(-2i\partial_v+k)_M(-2i\partial_v+k)_N\mathrm{e}^{-ixk\cdot v+iv^2/4T}\Big|_{v^M=(0^\mu,wL)}\\ \times\int\frac{\mathrm{d}^Dp}{(2\pi)^D}\mathrm{e}^{-iTp^2}.\end{aligned} \tag{5.45}$$

Performing the $p$-integration and computing the $v$-derivatives we get

$$\begin{aligned}\text{(b)} = -i(ig)^2\sum_{w\in\mathbb{Z}}\int_0^1\mathrm{d}x\int_0^\infty\mathrm{d}T T(4\pi iT)^{-D/2}\mathrm{e}^{-iT[m^2-i\epsilon+x(1-x)k^2]}\\ \times\left\{\left[(1-2x)k+\frac{v}{T}\right]_M\left[(1-2x)k+\frac{v}{T}\right]_N-i\eta_{MN}\frac{2}{T}\right\}\mathrm{e}^{-ixk\cdot v+iv^2/4T}\Big|_{v^M=(0^\mu,wl)}.\end{aligned} \tag{5.46}$$

Sum of these two contributions (a) and (b) recovers the result given by the formula (5.38).

## 5.4 Conclusions and discussions

In this chapter we have studied worldline formulation of gauge theory with a single extra dimension compactified on a circle. By carefully separating out the dangerous zero-mode contribution, we have successfully derived the master formulae for scalar one-loop amplitudes with arbitrary number of gauge bosons in Abelian gauge theory.

For the sake of simplicity, we have restricted ourselves to a smooth circle with no point interaction as a single extra dimension. As discussed at the end of chapter 4, we already know the path integral representation at least for scale-independent point interactions characterized by two parameters $\theta$ and $\phi$. Thus, as the possible simplest extension, it is interesting to investigate the worldline formalism for an extra dimensional model in the presence of

scale-independent point interaction and then study the effects of two parameters to gauge theory amplitudes and effective potential. Since the presence of scale-independent point interaction breaks the translational invariance along the direction of extra dimension, it is also interesting to study what boundary localized operators are radiatively induced by the violation of translational invariance.

Another possible extension of this work is to include fermion loop. In four dimensional worldline formalism, it has been known that when one considers a worldline fermion, the worldline action exhibits worldline supersymmetry as a consequence of separation of spin and orbital degrees of freedom. However, this worldline supersymmetry is violated in general due to the discrepancy in boundary conditions for worldline boson and fermion: the former obeys the periodic and the latter antiperiodic boundary conditions. It is interesting to investigate how worldline supersymmetry is affected due to the presence of point interaction. Further investigations are required.

# Chapter 6

# Summary and outlook

In this dissertation we have studied theoretical aspects of point interactions in quantum theory on a graph (quantum graph). We are mainly motivated by the following two different fields of quantum physics. The first is mesoscopic or nanoscale systems. Recent development of nanotechnology such as an electron-beam lithography enables us to fabricate mesoscopic networks of one-dimensional wires, whose simplest model is quantum graph. The second is perturbative quantum field theory with a single extra dimension in the presence of defects or boundaries, which can be viewed as point interactions along the direction of extra dimension. Apparently, these two fields of quantum physics have nothing in common. However, they actually have a single common point in respect that boundary condition plays a crucial role in their quantum dynamics.

Whatever the motivation, studies of point interactions all end up with the study of boundary conditions. The essential ingredient to treat boundary conditions in quantum system is the Kirchhoff's law of probability current at the vertex. In mathematical language, it is von Neumann's theory of self-adjoint extension of symmetric operator. These two methods are equivalent and reveal a much rich structure of point interaction available in quantum theory. More specifically, in a star graph with $N$ bonds a point interaction at the vertex is specified by an $N \times N$ unitary matrix $U \in U(N)$. Therefore there exist in principle much variety of point interactions characterized by $N^2$ parameters. In other words, in such a system theory space spanned by all possible point interactions is just equivalent to the parameter space of unitary group $U(N)$.

As naively expected, any short ranged interaction, which may be a defect or impurity or brane, could be approximated by a point interaction in the long-wavelength limit. In this sense point interaction is essentially for low energy physics. According to the idea of renormalization group theory, such a low energy system will be well described by symmetries and relevant interactions regardless of microscopic details of a system. In this respect, after the introductory chapter we have investigated symmetries and invariant subfamilies of point interactions and renormalization group flow in the parameter space of unitary group $U(N)$ in chapter 2 and 3, respectively.

In chapter 2, after the precise definition of point interaction on a star graph we reviewed symmetry classes of $U(2)$ family of point interactions and then proceed to extend the analysis to $U(3)$ family of point interactions on a Y-junction of three half-lines. We have revealed that the set of eight discrete transformations generated by the counterclockwise rotation through an angle $2\pi/3$ and $\mathbb{Z}_3$-reflection spans the Lie algebra $\mathfrak{su}(3)$ of the special unitary group $SU(3)$. One of the remarkable point to note is that these eight discrete

transformations commute with the free Hamiltonian. Hence, under any elements of $\mathfrak{su}(3)$ spectrum of an original system is preserved. We further extend to a general star graph with $N$ bonds and find that the set of $N^2-1$ discrete transformations, which is generated by the counterclockwise rotation through an angle $2\pi/N$ and $\mathbb{Z}_N$-reflection, consists of spectrum-preserving $\mathfrak{su}(N)$ algebra.

In chapter 3 we have derived exact renormalization group flow of point interactions and found $2^N$ distinct fixed points in the parameter space spanned by eigenphases of unitary matrix $U \in U(N)$. In general the most infrared (IR) stable fixed point is the Dirichlet fixed point where the Dirichlet boundary conditions are realized. On the other hand, the most ultraviolet (UV) stable fixed point is the Neumann fixed point where the Neumann boundary conditions are realized. The other $2^N-2$ fixed points have in general IR unstable directions. Because, in naively speaking, any short ranged interactions can be approximated by a point interaction in the long-wavelength limit, it is natural to expect that our analysis shows that there exists $2^N$ distinct universality classes of short ranged interactions that must flow into one of the fixed points in the IR limit.

Quantum theory on a graph is also responsible to perturbative quantum field theory. It becomes obvious when one considers a worldline formalism of perturbative quantum field theory, where internal lines of a given position-space Feynman diagram are identified as a single particle's worldline in configuration space. Then field theoretical S-matrix elements are obtained by one-particle quantum mechanical path integral with some background fields. There, Green's functions on a worldline such as a circle (for one-loop amplitudes) or an figure eight (for two-loop amplitudes of $\phi^4$ theory) are needed for computations. Nowadays it is known that worldline formalism generally provides a powerful alternative method to compute effective action and/or S-matrix elements at least to one-loop order. Thanks to its nature of position-space oriented descriptions for quantum field theory, worldline formalism is also powerful enough to perturbative quantum field theory with an extra compact dimension for another reason: that is, for the clarity of winding number, that counts how many times an internal line winds around the direction of extra dimension. It plays an important role in extra dimensional models because any non-zero winding contributions are essentially UV finite thanks to its long-distance nature: If one computes a radiative correction of a quantity that naively diverges in UV as $\sim \Lambda^D$ with $\Lambda$ being a cutoff scale, then such a loop induced correction from non-zero winding contributions must be of the form $\sim \sum_{w\in\mathbb{Z}} C^{(w)}(wL)^{-D}$, where $w$ is the winding number, $L$ is a circumference of extra dimension and $C^{(w)}$ is a possible ($w$-dependent) dimensionless coefficient[1]. This estimation follows from the dimensional analysis and the fact that internal line winding around the extra dimension $w$ times cannot be shorter than $wL$ and hence it plays a role of a cutoff length scale for $w$-winding sector. The sum $\sum_{w\in\mathbb{Z}}$ ensures the summation of all possible physically distinct closed loops, which goes quite well with the philosophy of path integral. Thus, determination of whether given S-matrix elements are those from the contributions of zero- or non-zero winding is an essentially significant problem especially for the perturbative renormalization procedures and/or classification of UV finite quantities such as the Higgs mass in the gauge-Higgs unification scenario in a quantitative level. However, it has been a longstanding problem and not yet fully understood how to incorporate boundary conditions (which describes zero-thick branes in the context of extra dimension) into path integration

[1]In fact, $C^{(w)}$ is given by an matrix elements for the $w$th power of corresponding one-particle quantum mechanical S-matrix.

on a compact space, where the Poisson summation formula is no longer available[2].

In this respect, chapter 4 is devoted to the study of path integral formulation of one-particle quantum mechanics on a rose graph. We found the most general path integral description of the Feynman kernel valid for $U(N)$ family of point interactions at the vertex of $N$-petal rose. We also discussed the topology change of figure eight and speculated that any compact graphs can be generated via topology change of an appropriate rose graph. This is the reason why we have concerned a rose graph.

In chapter 5 we have studied the worldline formalism of Abelian gauge theory with a single extra dimension compactified on a circle. We successfully derived the master formula for scalar one-loop amplitudes with arbitrary number of external gauge bosons in Abelian gauge theory.

Let us close this concluding chapter on a more speculative level. Over the past decade, an intensive study has been made on domain wall networks, or junctions, realized as topological solitons of supersymmetric quantum field theory [69–71]. One of the motivations for those studies are field theoretical constructions of D-branes for models of brane-world scenario. A typical example of such a soliton is the Y-junction of domain walls. Just as in the case of kink configuration background, when one considers fermion fields in the background of such a Y-junction of domain walls, it is natural to expect that fermion's wavefunction would be localized to the Y-junction. If so, in the low-energy regime where thickness of domain walls will be ignored, fermions could be effectively described as those confined on the one-dimensional network of Y-junction of three half-lines. As we have seen in chapter 2, quantum system on Y-junction admits three distinct bound states, which might be used to address the generation problem of quarks and leptons: three generations of fermions in our world could be explained as the three distinct bound states of the lowest three Kaluza-Klein modes of a single fermion field residing on a higher-dimensional spacetime with an extra "Y-dimension". Furthermore, the wavefunctions of these three bound states are localized to the junction point $x_j = 0$ as $\sim \exp(-x_j/L_j)$, $j = 1, 2, 3$. Thus, it might be possible to address simultaneously the mass hierarchy of quarks and leptons, or the Yukawa couplings hierarchy, as overlapping integrals of three distinct wavefunctions without use of any large hierarchical assumptions of Yukawa couplings. However, all of these arguments are just speculations. Further investigations will be required.

[2]The Poisson summation formula is applicable only to the scale-independent point interactions.

# Bibliography


[1] V. Kostrykin and R. Schrader, "Kirchhoff's Rule for Quantum Wires," *J. Phys.* **A32** (1999) 595–630, arXiv:math-ph/9806013.

[2] S. Gnutzmann and U. Smilansky, "Quantum Graphs: Applications to Quantum Chaos and Universal Spectral Statistics," *Adv. Phys.* **55** (2006) 527–625, arXiv:nlin/0605028.

[3] V. V. Moshchalkov, V. Bruyndoncx, E. Rosseel, L. Van Look, M. Baert, M. J. Van Bael, T. Puig, C. Strunk, and Y. Bruynseraede, "Confinement and Quantization Effects in Mesoscopic Superconducting Structures," arXiv:cond-mat/9804267.

[4] V. V. Moshchalkov, L. Gielen, C. Strunk, R. Junckheere, X. Qiu, C. Van Haesendonck, and Y. Bruynseraede, "Effect of sample topology on the critical fields of mesoscopic superconductors," *Nature* **373** (1995) 319–322.

[5] V. Bruyndoncx, C. Strunk, V. V. Moshchalkov, C. Van Haesendonck, and Y. Bruynseraede, "Fluxoid quantization in mesoscopic Al multiloop structures ," *Czech. J. Phys.* **46** (1996) 2339–2340.

[6] M. Tinkham, *Introduction to Superconductivity*. McGraw-Hill, New York, 1975.

[7] W. A. Little and R. D. Parks, "Observation of Quantum Periodicity in the Transition Temperature of a Superconducting Cylinder," *Phys. Rev. Lett.* **9** (1962) 9–12.

[8] H. J. Fink, A. López, and R. Maynard, "Magnetic phase boundary of simple superconductive micronetworks," *Phys. Rev.* **B26** (1982) 5237–5240.

[9] V. M. Fomin, J. T. Devreese, V. Bruyndoncx, and V. V. Moshchalkov, "Superconductivity in a mesoscopic double square loop: Effects of imperfections," *Phys. Rev.* **B62** (2000) 9186–9190, arXiv:cond-mat/0001201.

[10] J. Bolte and S. Endres, "The trace formula for quantum graphs with general self adjoint boundary conditions," *Ann. H. Poincare* **10** (2009) 189–223, arXiv:0805.3111 [math-ph].

[11] H. Hatanaka, T. Inami, and C. S. Lim, "The gauge hierarchy problem and higher dimensional gauge theories," *Mod. Phys. Lett.* **A13** (1998) 2601–2612, arXiv:hep-th/9805067.

[12] F. Bastianelli, O. Corradini, and P. A. G. Pisani, "Worldline approach to quantum field theories on flat manifolds with boundaries," *JHEP* **02** (2007) 059, arXiv:hep-th/0612236.

[13] F. Bastianelli, O. Corradini, and P. A. G. Pisani, "Scalar Field with Robin Boundary Conditions in the Worldline Formalism," *J. Phys.* **A41** (2008) 164010, arXiv:0710.4026 [hep-th].

[14] F. Bastianelli, O. Corradini, P. A. G. Pisani, and C. Schubert, "Scalar heat kernel with boundary in the worldline formalism," *JHEP* **10** (2008) 095, arXiv:0809.0652 [hep-th].

[15] T. Fülöp, I. Tsutsui, and T. Cheon, "Spectral Properties on a Circle with a Singularity," *J. Phys. Soc. Jpn.* **72** (2003) 2737–2746, arXiv:quant-ph/0307002.

[16] S. Albeverio, L. Dąbrowski, and P. Kurasov, "Symmetries of Schrödinger Operators with Point Interactions," *Lett. Math. Phys.* **45** (1998) 33–47.

[17] T. Cheon, T. Fülöp, and I. Tsutsui, "Symmetry, Duality and Anholonomy of Point Interactions in One Dimension," *Annals Phys.* **294** (2001) 1–23, arXiv:quant-ph/0008123.

[18] T. Fülöp and I. Tsutsui, "A Free particle on a circle with point interaction," *Phys. Lett.* **A264** (2000) 366–374, arXiv:quant-ph/9910062.

[19] M. R. Kibler, "An angular momentum approach to quadratic Fourier transform, Hadamard matrices, Gauss sums, mutually unbiased bases, unitary group and Pauli group," *J. Phys.* **A42** (2009) 353001, arXiv:0907.2838 [quant-ph].

[20] C. B. Thorn, "Quark Confinement in the Infinite Momentum Frame," *Phys. Rev.* **D19** (1979) 639.

[21] M. A. B. Beg and R. C. Furlong, "$\lambda\phi^4$ theory in the nonrelativistic limit," *Phys. Rev.* **D31** (1985) 1370.

[22] L. R. Mead and J. Godines, "An analytical example of renormalization in two-dimensional quantum mechanics," *Am. J. Phys.* **59** (1991) 935–937.

[23] C. Manuel and R. Tarrach, "Perturbative renormalization in quantum mechanics," *Phys. Lett.* **B328** (1994) 113–118, arXiv:hep-th/9309013.

[24] L. J. Boya and A. Rivero, "Renormalization in 1-D quantum mechanics: Contact interactions," arXiv:hep-th/9411081.

[25] S. K. Adhikari and T. Frederico, "Renormalization group in potential scattering," *Phys. Rev. Lett.* **74** (1995) 4572–4575.

[26] S. K. Adhikari and A. Ghosh, "Renormalization in Nonrelativistic Quantum Mechanics," *J. Phys.* **A30** (1997) 6553–6564, arXiv:hep-th/9706193.

[27] M. C. Birse, J. A. McGovern, and K. G. Richardson, "A renormalization-group treatment of two-body scattering," *Phys. Lett.* **B464** (1999) 169–176, arXiv:hep-ph/9807302.

[28] H. E. Camblong, L. N. Epele, H. Fanchiotti, and C. A. Garcia Canal, "Dimensional transmutation and dimensional regularization in quantum mechanics. I: General theory," *Ann. Phys.* **287** (2001) 14–56, arXiv:hep-th/0003255.

[29] V. de Alfaro, S. Fubini, and G. Furlan, "Conformal Invariance in Quantum Mechanics," *Nuovo Cim.* **A34** (1976) 569.

[30] K. S. Gupta and S. G. Rajeev, "Renormalization in quantum mechanics," *Phys. Rev.* **D48** (1993) 5940–5945, arXiv:hep-th/9305052.

[31] S. R. Beane *et al.*, "Singular Potentials and Limit Cycles," *Phys. Rev.* **A64** (2001) 042103, arXiv:quant-ph/0010073.

[32] T. Barford and M. C. Birse, "A renormalisation group approach to two-body scattering in the presence of long-range forces," *Phys. Rev.* **C67** (2003) 064006, arXiv:hep-ph/0206146.

[33] M. Bawin and S. A. Coon, "The singular inverse square potential, limit cycles and self-adjoint extensions," *Phys. Rev.* **A67** (2003) 042712, arXiv:quant-ph/0302199.

[34] H. E. Camblong and C. R. Ordonez, "Renormalization in conformal quantum mechanics," *Phys. Lett.* **A345** (2005) 22–30, arXiv:hep-th/0305035.

[35] T. Barford and M. C. Birse, "Effective theories of scattering with an attractive inverse-square potential and the three-body problem," *J. Phys.* **A38** (2005) 697–720, arXiv:nucl-th/0406008.

[36] D. B. Kaplan, J.-W. Lee, D. T. Son, and M. A. Stephanov, "Conformality Lost," arXiv:0905.4752 [hep-th].

[37] S. Moroz and R. Schmidt, "Nonrelativistic inverse square potential, scale anomaly, and complex extension," arXiv:0909.3477 [hep-th].

[38] G. Amelino-Camelia, "T-duality for boundary-non-critical point-particle and string quantum mechanics," *Fortsch. Phys.* **47** (1999) 93–100, arXiv:hep-th/9808098.

[39] A. P. Balachandran, G. Bimonte, G. Marmo, and A. Simoni, "Topology change and quantum physics," *Nucl. Phys.* **B446** (1995) 299–314, arXiv:gr-qc/9503046.

[40] M. Asorey, A. Ibort, and G. Marmo, "Global theory of quantum boundary conditions and topology change," *Int. J. Mod. Phys.* **A20** (2005) 1001–1026, arXiv:hep-th/0403048.

[41] C. Bachas, J. de Boer, R. Dijkgraaf, and H. Ooguri, "Permeable conformal walls and holography," *JHEP* **06** (2002) 027, arXiv:hep-th/0111210.

[42] T. Quella, I. Runkel, and G. M. T. Watts, "Reflection and Transmission for Conformal Defects," *JHEP* **04** (2007) 095, arXiv:hep-th/0611296.

[43] M. Oshikawa, C. Chamon, and I. Affleck, "Junctions of three quantum wires," *J. Stat. Mech.* **0602** (2006) 008, arXiv:cond-mat/0509675.

[44] B. Bellazzini, M. Mintchev, and P. Sorba, "Bosonization and scale invariance on quantum wires," *J. Phys.* **A40** (2007) 2485–2508, arXiv:hep-th/0611090.

[45] B. Bellazzini, P. Calabrese, and M. Mintchev, "Junctions of anyonic Luttinger wires," *Phys. Rev.* **B79** (2009) 085122, arXiv:0808.2719 [cond-mat.str-el].

[46] M. Reed and B. Simon, *Methods of modern mathematical physics II: Fourier analysis, self-adjointness*. Academic Press, New York, 1975.

[47] L. S. Schulman, *Techniques and Applications of Path Integration*. Wiley, New York, 1981.

[48] M. Chaichian and A. Demichev, *Path Integrals in Physics Volume I: Stochastic Processes and Quantum Mechanics*. Institute of Physics, Bristol, 2001.

[49] M. C. Gutzwiller, "Periodic Orbits and Classical Quantization Conditions," *J. Math. Phys.* **12** (1971) 343–358.

[50] A. Selberg, "Harmonic analysis and discontinuous groups in weakly symmetric riemannian spaces with applications to dirichlet series," *J. Indian Math. Soc.* **20** (1956) 47–87.

[51] D. J. Griffiths, "Boundary conditions at the derivative of a delta function," *J. Math. Phys.* **A26** (1993) 2265–2267.

[52] P. B. Kurasov, A. Scrinzi, and N. Elander, "$\delta'$ potential arising in exterior complex scaling," *Phys. Rev.* **A49** (1994) 5095–5097.

[53] S. Ohya and M. Sakamoto, "Particle Propagation on a Circle with a Point Interaction," *J. Phys.* **A42** (2009) 275301, `arXiv:0902.0855 [quant-ph]`.

[54] S. A. Fulling, P. Kuchment, and J. H. Wilson, "Index theorems for quantum graphs," *J. Phys.* **A40** (2007) 14165–14180, `arXiv:0708.3456 [math.SP]`.

[55] M. G. G. Laidlaw and C. M. DeWitt, "Feynman functional integrals for systems of indistinguishable particles," *Phys. Rev.* **D3** (1971) 1375–1378.

[56] M. Asorey, J. M. Munoz-Castaneda, and J. Clemente-Gallardo, "Boundary conditions: The path integral approach," *J. Phys. Conf. Ser.* **87** (2007) 012004, `arXiv:0712.4353 [quant-ph]`.

[57] E. Farhi and S. Gutmann, "THE FUNCTIONAL INTEGRAL ON THE HALF LINE," *Int. J. Mod. Phys.* **A5** (1990) 3029–3052.

[58] T. Fülöp, I. Tsutsui, and T. Cheon, "Classical aspects of quantum walls in one dimension," *Phys. Rev.* **A66** (2002) 052102, `arXiv:quant-ph/0111057`.

[59] C. Schubert, "Perturbative quantum field theory in the string-inspired formalism," *Phys. Rept.* **355** (2001) 73–234, `arXiv:hep-th/0101036`.

[60] R. P. Feynman, "Mathematical formulation of the quantum theory of electromagnetic interaction," *Phys. Rev.* **80** (1950) 440–457.

[61] P. Dai and W. Siegel, "Worldline green functions for arbitrary Feynman diagrams," *Nucl. Phys.* **B770** (2007) 107–122, `arXiv:hep-th/0608062`.

[62] H. Holzler, "World Graph Formalism for Feynman Amplitudes," *JHEP* **09** (2008) 022, `arXiv:0704.3392 [hep-th]`.

[63] P. Dai, Y.-t. Huang, and W. Siegel, "Worldgraph Approach to Yang-Mills Amplitudes from N=2 Spinning Particle," *JHEP* **10** (2008) 027, arXiv:0807.0391 [hep-th].

[64] Z. Bern and D. A. Kosower, "Efficient calculation of one loop QCD amplitudes," *Phys. Rev. Lett.* **66** (1991) 1669–1672.

[65] Z. Bern and D. A. Kosower, "Color decomposition of one loop amplitudes in gauge theories," *Nucl. Phys.* **B362** (1991) 389–448.

[66] Z. Bern and D. A. Kosower, "The Computation of loop amplitudes in gauge theories," *Nucl. Phys.* **B379** (1992) 451–561.

[67] M. J. Strassler, "Field theory without Feynman diagrams: One loop effective actions," *Nucl. Phys.* **B385** (1992) 145–184, arXiv:hep-ph/9205205.

[68] H. Gies and K. Klingmuller, "Quantum energies with worldline numerics," *J. Phys.* **A39** (2006) 6415–6422, arXiv:hep-th/0511092.

[69] G. W. Gibbons and P. K. Townsend, "A Bogomolnyi equation for intersecting domain walls," *Phys. Rev. Lett.* **83** (1999) 1727–1730, arXiv:hep-th/9905196.

[70] H. Oda, K. Ito, M. Naganuma, and N. Sakai, "An exact solution of BPS domain wall junction," *Phys. Lett.* **B471** (1999) 140–148, arXiv:hep-th/9910095.

[71] M. Eto, Y. Isozumi, M. Nitta, K. Ohashi, and N. Sakai, "Solitons in the Higgs phase: The moduli matrix approach," *J. Phys.* **A39** (2006) R315–R392, arXiv:hep-th/0602170.